

การผลิตโมโนโคลนัลแอนติบอดีต่อต้านไทรอยด์สติมูเลติงฮอร์โมน
โดยใช้เครื่องปฏิกรณ์ชีวภาพชนิดฮอลโลว์ไฟเบอร์



นางสาวจารณี พึ่งโพธิ์สภ

สถาบันวิทยบริการ

จุฬาลงกรณ์มหาวิทยาลัย

วิทยานิพนธ์นี้เป็นส่วนหนึ่งของการศึกษาตามหลักสูตรปริญญาวิทยาศาสตรมหาบัณฑิต

สาขาเทคโนโลยีชีวภาพ

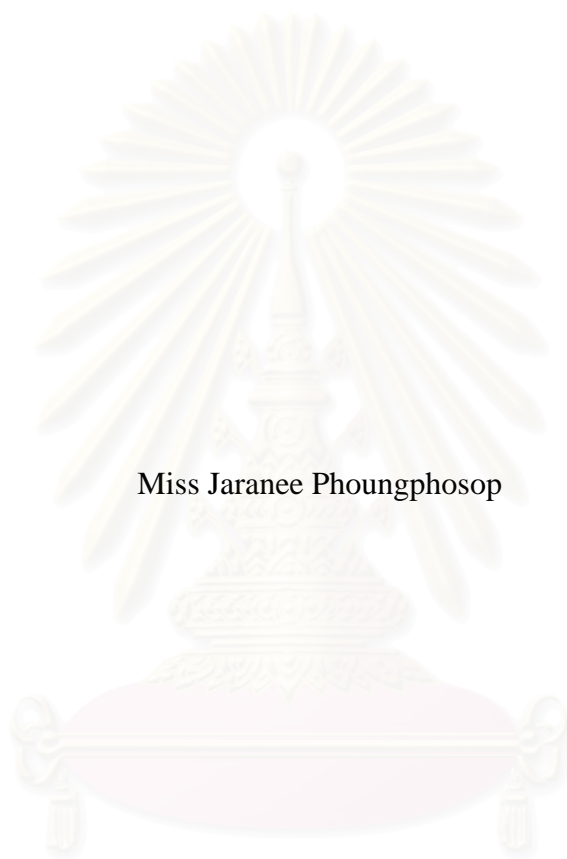
คณะวิทยาศาสตร์ จุฬาลงกรณ์มหาวิทยาลัย

ปีการศึกษา 2546

ISBN 974-17-4561-3

ลิขสิทธิ์ของ จุฬาลงกรณ์มหาวิทยาลัย

PRODUCTION OF MONOCLONAL ANTIBODY
AGAINST THYROID STIMULATING HORMONE USING
HOLLOW FIBER BIOREACTOR



Miss Jaranee Phoungphosop

สถาบันวิทยบริการ
จุฬาลงกรณ์มหาวิทยาลัย

A Thesis Submitted in Partial Fulfillment of the Requirements
for the Degree of Master of Science in Biotechnology

Faculty of Science

Chulalongkorn University

Academic Year 2003

ISBN 974-17-4561-3

Thesis title PRODUCTION OF MONOCLONAL ANTIBODY
AGAINST THYROID STIMULATING HORMONE USING
HOLLOW FIBER BIOREACTOR

By Miss Jaranee Phoungphosop

Field of study Biotechnology

Thesis Advisor Associate Professor Amorn Petsom, Ph.D.

Thesis Co-advisor Miss Wiyada Charoensiriwatana

Accepted by the Faculty of Science, Chulalongkorn University in Partial
Fulfillment of the Requirements for the Master's Degree

.....Dean of Faculty of Science
(Professor Piamsak Menasveta, Ph.D.)

THESIS COMMITTEE

.....Chairman
(Supat Chareonpornwattana, Ph.D.)

.....Thesis Advisor
(Associate Professor Amorn Petsom, Ph.D.)

.....Thesis Co-advisor
(Miss Wiyada Charoensiriwatana)

.....Member
(Associate Professor Sirirat Rengpipat, Ph.D.)

.....Member
(Assistant Professor Nattaya Ngamrojnavanich, Ph.D.)

จารณี พึ่งโพธิ์สม: การผลิตโมโนโคลนัลแอนติบอดีต่อต้านไทรอยด์สติมูเลติงฮอร์โมนโดยใช้
 เครื่องปฏิกรณ์ชีวภาพชนิดฮอลโลว์ไฟเบอร์ (PRODUCTION OF MONOCLONAL
 ANTIBODY AGAINST THYROID STIMULATING HORMONE USING HOLLOW
 FIBER BIOREACTOR) อ. ที่ปรึกษา : รศ.ดร. อมร เพชรสม, อ. ที่ปรึกษาร่วม นางสาว
 วิยะดา เจริญศิริวัฒน์, 117 หน้า ISBN 974-17-4561-3

ศึกษาการผลิตโมโนโคลนัลแอนติบอดีต่อไทรอยด์สติมูเลติงฮอร์โมน โดยใช้เครื่องปฏิกรณ์
 ชีวภาพชนิดฮอลโลว์ไฟเบอร์ที่ประกอบขึ้นเองโดยใช้หลอดไตเทียมราคาถูก ในการผลิตเพื่อให้ได้ปริมาณโมโน
 โคลนัลแอนติบอดีสูงสุด เครื่องปฏิกรณ์ชีวภาพชนิดฮอลโลว์ไฟเบอร์ต้องติดตั้งให้มีการเปลี่ยนทิศทางกรไหล
 ของอาหารเลี้ยงเซลล์ก่อนผ่านเข้าหลอดที่ทำการเลี้ยงเซลล์ ทั้งนี้เพื่อลดผลกระทบจากการเกิดแรงดันที่ลดลง
 ภายในระบบ ปริมาณเซลล์ที่มีชีวิตจำนวน 10^6 เซลล์ ฉีดเข้าไปในส่วนด้านนอกของไฟเบอร์ของหลอดที่ทำการ
 เลี้ยงเซลล์ ภายหลังจากฉีดเซลล์ทำการเลี้ยงแบบแบทช์เป็นเวลา 5 วัน โดยอาหารเลี้ยงเซลล์ไหลผ่าน
 ทิศทางเดียว จากนั้นจึงสลับทิศทางกรไหลของอาหารเลี้ยงเซลล์ทุกๆ 24 ชั่วโมง ในทิศทางตามเข็มนาฬิกา
 และทวนเข็มนาฬิกาตลอดระยะเวลาการเลี้ยง ในกรณีที่มีการมีชีวิตอยู่ของเซลล์ลดลงน้อยกว่า 10% การสลับ
 ทิศทางต้องเปลี่ยนจากทุก 24 ชั่วโมง เป็นทุก 12 ชั่วโมง เพื่อที่จะเพิ่มปริมาณโมโนโคลนัลแอนติบอดีจากการ
 เก็บผลผลิต ช่องที่ต่อกับส่วนด้านนอกของไฟเบอร์ของหลอดที่ทำการเลี้ยงเซลล์ต้องปรับให้อยู่ที่ตำแหน่งมุม 90
 องศา จากตำแหน่งในแนวตั้ง นอกจากนี้เมื่อการเลี้ยงเข้าสู่ภาวะคงที่แล้ว ปริมาณพีดีบีโวนีซีรัมสามารถ
 ลดลงทีละน้อยจนถึงศูนย์เปอร์เซ็นต์ โดยที่ไม่มีผลกระทบต่อการผลิตโมโนโคลนัลแอนติบอดีและเมแทบอลิซึม
 ของเซลล์ ตลอดระยะเวลาที่ทำการเลี้ยงอัตราการป้อนอาหารเลี้ยงเซลล์ การเปลี่ยนขวดบรรจุอาหารเลี้ยง
 เซลล์และการเก็บผลผลิต ขึ้นอยู่กับผลผลิตของเมแทบอลิซึมของเซลล์ ภายใต้วาดังกล่าวสามารถผลิตโมโน
 โคลนัลแอนติบอดีได้ปริมาณ 750 มิลลิกรัม ในระยะเวลา 67 วัน

สถาบันวิทยบริการ
 จุฬาลงกรณ์มหาวิทยาลัย

สาขาวิชา.....เทคโนโลยีชีวภาพ..... ลายมือชื่อนิสิต.....

ปีการศึกษา.....2546..... ลายมือชื่ออาจารย์ที่ปรึกษา.....

ลายมือชื่ออาจารย์ที่ปรึกษาร่วม.....

4372229723 : MAJOR BIOTECHNOLOGY

KEY WORD: MONOCLONAL ANTIBODY/HOLLOW FIBER/HYBRIDOMA

JARANEE PHOUNGPHOSOP : PRODUCTION OF MONOCLONAL ANTIBODY AGAINST THYROID STIMULATING HORMONE USING HOLLOW FIBER BIOREACTOR. THESIS ADVISOR: ASSOC. PROF. AMORN PETSOM, Ph.D. THESIS CO-ADVISOR: MISS WIYADA CHAROENSIRIWATANA 117 pp. ISBN 974-17-4561-3

A study for the production of monoclonal antibody against thyroid stimulating hormone was carried out using hollow fiber bioreactor which was assembled using inexpensive hollow fiber dialysers. For the purpose of producing high yield of monoclonal antibody, the hollow fiber bioreactor was operated by alternating the direction of media flow before feeding to the cell culture cartridge in order to reduce the effects of pressure gradient. A total cell viability of 10^8 cells were inoculated to the extracapillary space of the cell culture cartridge. After inoculation, a 5-day batch with one direction of media flow was operated. Then, followed by the 24-hour circulating flow alternated clockwise and anticlockwise of the media throughout the culture period. In case that the viability of the cell was less than 10%, the frequency of reversing direction must be changed from every 24 hours to every 12 hours instead. In order to increase the yield of monoclonal antibody from harvest, the extracapillary port of cell culture cartridge must be positioned at angle of 90° from the vertical position. Additionally, when the culture was at the steady state, the amount of fetal bovine serum could be reduced gradually to 0% without any effects on monoclonal antibody production and cell metabolism. During the culture period, the medium circulation rate, the replacement of medium reservoir, and the harvest of product were based on metabolite products. Under the above conditions, the hollow fiber bioreactor could generate 750 mg of monoclonal antibody in 67 days.

สถาบันวิทยบริการ
จุฬาลงกรณ์มหาวิทยาลัย

Field of study Biotechnology Student's signature.....

Academic year 2003 Advisor's signature

Co-advisor's signature

ACKNOWLEDGEMENT

I would like to express my deepest gratitude to my advisor, Associate Professor Amorn Petsom, and co-advisor, Miss Wiyada Charoensiriwatana, for their excellent instruction, guidance and support throughout this thesis.

My gratitude is also extended to Dr. Supat Chareonpornwattana, Associate Professor Sirirat Rengpipat and Assistant Professor Nattaya Ngamrojnavanich for serving as thesis committee.

I gratefully acknowledge National Institute of Health, Department of Medical Sciences, for supplying hybridoma cell line and technical support of this thesis.

My special thanks to all members in the Radioisotope Laboratory section, National Institute of Health, Department of Medical Sciences and Program of Biotechnology, Faculty of Science, Chulalongkorn University for their assistant and friendship.

Finally, I am deeply grateful to my family and all my friends for their understanding and encouragement.



สถาบันวิทยบริการ
จุฬาลงกรณ์มหาวิทยาลัย

CONTENTS

	Page
THAI ABSTRACT.....	iv
ENGLISH ABSTRACT.....	v
ACKNOWLEDGEMENT.....	vi
CONTENTS.....	vii
LIST OF TABLES.....	x
LIST OF FIGURES.....	xii
LIST OF ABBREVIATIONS.....	xvi
CHAPTER I INTRODUCTION.....	1
1.1 Monoclonal antibody production.....	1
1.2 The purpose of research.....	2
CHAPTER II LITERATURES REVIEW.....	3
2.1 Hollow fiber membranes.....	3
2.2 Operational modes of hollow fiber system.....	4
2.3 Monoclonal antibody production in hollow fiber bioreactors.....	6
2.4 Barriers to scale up hollow fiber bioreactor.....	9
2.4.1 Heterogeneous nature of the hollow fiber bioreactor.....	9
2.4.2 Nutrient depletion.....	13
2.4.3 Accumulation of waste products.....	18
2.4.4 Oxygen transport limitation.....	23
CHAPTER III MATERIALS AND METHODS.....	29
3.1 Cell line and culture medium.....	29
3.2 Chemicals.....	29
3.3 Equipments.....	31
3.4 Assembly of hollow fiber bioreactor.....	32
3.4.1 The hollow fiber bioreactor with single flow direction.....	32
3.4.2 The hollow fiber bioreactor with reverse flow direction	32
3.5 Pre-incubation of the hollow fiber bioreactor.....	41

CONTENTS (continued)

	Page
3.6 Cell inoculation.....	41
3.7 Optimization procedures and control strategy.....	42
3.7.1 The hollow fiber bioreactor with single flow direction.....	42
3.7.2 The hollow fiber bioreactor with reverse flow direction.....	42
3.7.2.1 The hollow fiber bioreactor with operational mode 2.....	43
3.7.2.2 The hollow fiber bioreactor with operational mode 3	43
3.8 Statistical analysis.....	46
3.9 Analytical methods.....	46
3.9.1 Cell numbers and cell viability determination.....	46
3.9.2 Glucose determination.....	47
3.9.3 Lactate determination.....	47
3.9.4 Ammonia determination.....	47
3.9.5 Monoclonal antibody determination.....	48
3.9.5.1 Absorption of ultraviolet light.....	48
3.9.5.2 Enzyme linked immunosorbent assay (ELISA).....	48
3.10 Monoclonal antibody purification.....	49
3.10.1 Protein A Sepharose affinity chromatography.....	49
3.10.2 Expanded-bed rProtein A affinity chromatography.....	49
3.11 Denaturing polyacrylamide gel electrophoresis (SDS-PAGE).....	50
CHAPTER IV RESULTS.....	52
4.1 Optimization and control strategy.....	52
4.1.1 The hollow fiber bioreactor with single flow direction.....	52
4.1.2 The hollow fiber bioreactor with reverse flow direction.....	55
4.1.2.1 The hollow fiber bioreactor with operational mode 2.....	55
4.1.2.2 The hollow fiber bioreactor with operational mode 3.....	59
4.2 Comparative characterization of cells cultivation in different operational modes of the hollow fiber bioreactors	63
4.2.1 The metabolic activities.....	63
4.2.2 MAb-TSH production and viability.....	66
4.2.3 Purification of MAb-TSH from culture supernatant.....	68

CONTENTS (continued)

	Page
4.2.4 SDS-PAGE analysis of the purified MAb-TSH.....	71
CHAPTER V DISCUSSION.....	73
5.1 Assembly of hollow fiber bioreactor.....	73
5.2 Cells cultivation in different operational modes.....	74
5.3 Impact of gravity sedimentation on MAb-TSH concentration.....	76
5.4 Adaptation to low serum-supplemented medium.....	76
5.5 Evaluation of the hollow fiber bioreactor as an alternative for MAb-TSH production.....	77
CHAPTER VI CONCLUSION.....	80
REFERENCES.....	82
APPENDICES	88
BIOGRAPHY.....	117



 สถาบันวิทยบริการ
 จุฬาลงกรณ์มหาวิทยาลัย

LIST OF TABLES

Table	Page
1 Alternative designs and operating schemes for reducing the heterogeneous nature of hollow fiber bioreactor.....	13
2 The functional parts of the hollow fiber bioreactor with single flow and reverse flow direction.....	35
3 ANOVA table for the position of EC ports.....	58
4 Multiple comparisons of the position by LSD.....	59
5 ANOVA table for the reduction of serum concentration in basal medium...	62
6 Multiple comparisons of the reduction of serum concentration by LSD.....	63
7 Overview of the yield of purified MAb-TSH by expand-bed rProteinA affinity chromatography.....	70
8 Comparison of total MAb-TSH production in hollow fiber bioreactor and in murine ascites.....	77
9 Material costs of producing MAb-TSH in hollow fiber bioreactor under optimal conditions.....	79
10 Molecular weight and relative mobility of protein bands appeared in SDS-PAGE gel of Fig. 20.....	100
11 Molecular weight and relative mobility of protein bands appeared in SDS-PAGE gel of Fig. 22.....	102
12 Molecular weight and relative mobility of protein bands appeared in SDS-PAGE gel of Fig. 24.....	104
13 Molecular weight and relative mobility of protein bands appeared in SDS-PAGE gel of Fig. 26.....	106
14 Molecular weight and relative mobility of protein bands appeared in SDS-PAGE gel of Fig. 28.....	108
15 Molecular weight and relative mobility of protein bands appeared in SDS-PAGE gel of Fig. 30.....	110
16 Molecular weight and relative mobility of protein bands appeared in SDS-PAGE gel of Fig. 32.....	112
17 Molecular weight and relative mobility of protein bands appeared in SDS-PAGE gel of Fig. 34.....	114

LIST OF TABLES (continued)

Table	Page
18 Molecular weight and relative mobility of the protein bands appeared in SDS-PAGE gel of Fig. 36.....	116



สถาบันวิทยบริการ
จุฬาลงกรณ์มหาวิทยาลัย

LIST OF FIGURES

Figure	Page
1 Schematic diagrams of the types of membranes (Baker, 2000).....	3
2 The three modes of operation and the pressure distributions (Tharakan and Chau, 1986a).....	5
3 A simple hollow fiber system (Gramer and Poeschl, 1998).....	7
4 An analogous flow around capillaries known as staring flow (Piret and Cooney, 1990).....	10
5 Primary metabolism in mammalian cells exhibiting high rates of glucose and glutamine metabolism (Mancuso et al., 1994).....	14
6 Model for transport of NH_3 and NH_4^+ across cell membranes (Martinelle and Haggstrom, 1993).....	20
7 Schematic diagram of the hollow fiber bioreactor with single flow (A) and reverse flow (B and C) direction (modified from Altshuler et al., 1986; Honda-Corrigan, Nikolay, Jeffery et al., 1992).....	33
8 Four T- bore stopcocks rotated for clockwise (a) and anticlockwise (b) direction (modified from Altshuler et al., 1986; Honda-Corrigan, Nikolay, Jeffery et al., 1992).	39
9 The medium flow direction of system C turned clockwise (a) an anticlockwise (b) direction (modified from Altshuler et al., 1986; Honda-Corrigan, Nikolay, Jeffery et al., 1992).....	40
10 The position of EC ports during the steady state of MAb-TSH production (A) the vertical position (B) Angle of 90° from the vertical position (C) Angle of 135° from the vertical position	44
11 MAb-TSH production in the hollow fiber bioreactors with single flow direction. \triangle bioreactor 1 \square bioreactor 2 (A) MAb-TSH concentration in the samples of EC harvest from upstream and downstream port. opened symbols (\triangle , \square) harvested from downstream port closed symbols (\blacktriangle , \blacksquare) harvested from upstream port (B) MAb-TSH detection in the samples of IC medium.....	53

LIST OF FIGURES (continued)

Figure	Page
<p>12 IC pump rates plotted against the concentration of glucose (A), lactate (B) and ammonia (C) in the samples of IC medium of the hollow fiber bioreactors with single flow direction.</p> <p style="margin-left: 40px;"> —△— bioreactor 1 —□— bioreactor 2..... </p>	54
<p>13 MAb-TSH production in the hollow fiber bioreactors with reverse flow every 24 and 12 hrs</p> <p style="margin-left: 40px;"> —△— bioreactor 1 —□— bioreactor 2 </p> <p>(A) MAb-TSH concentration in the samples of EC harvest from upstream and downstream port.</p> <p style="margin-left: 40px;"> opened symbols (△, □) harvested from downstream port closed symbols (▲, ■) harvested from upstream port position of EC ports ↑ the vertical position ←○ angle of 90° from the vertical position ↙○ angle of 135° from the vertical position </p> <p>(B) MAb-TSH detection in the samples of IC medium.....</p>	56
<p>14 IC pump rates plotted against the concentration of glucose (A), lactate (B) and ammonia (C) in the IC medium of the hollow fiber bioreactors with reverse flow every 24 and 12 hrs.</p> <p style="margin-left: 40px;"> —△— bioreactor 1 —□— bioreactor 2..... </p>	57
<p>15 MAb-TSH production in the hollow fiber bioreactors with reverse flow every 12 hrs</p> <p style="margin-left: 40px;"> —△— bioreactor 1 —□— bioreactor 2 —○— bioreactor 3 </p> <p>(A) MAb-TSH concentration in the samples of EC harvest from upstream and downstream port.</p> <p style="margin-left: 40px;"> opened symbols (△, □, ○) harvested from downstream port closed symbols (▲, ■, ●) harvested from upstream port ① culture in 2.5% FBS ② culture in 1% FBS ③ culture in 0% FBS </p> <p>(B) MAb-TSH detection in the samples of IC medium.....</p>	60

LIST OF FIGURES (continued)

Figure	Page
16 IC pump rates plotted against the concentration of glucose (A), lactate (B) and ammonia (C) in the IC medium of the hollow fiber bioreactors with reverse flow every 12 hrs. —▲— bioreactor 1 —■— bioreactor 2 —○— bioreactor 3.....	61
17 Comparison of the GCR (A) , LPR (B), LPR/GCR ratios (C) and APR (D) of cells cultivation in difference operational modes of the hollow fiber bioreactors. —▲— mode 1 —■— mode 2 —○— mode 3.....	64-65
18 Comparison of the MAb-TSH concentration (A) and viability (B) of samples harvested in different operational modes of the hollow fiber bioreactors. —▲— mode 1 —■— mode 2 —○— mode 3.....	67
19 Elution profile of the purified MAb-TSH by using expanded-bed rProtein A affinity chromatography.....	69
20 SDS-PAGE gel of MAb-TSH purified from the supernatant of cells cultured in mode 1 using expanded-bed affinity chromatography.....	99
21 Molecular weight calibration curve obtained from SDS-PAGE gel of Fig. 20.....	100
22 SDS-PAGE gel of MAb-TSH purified from the supernatant of cells cultured in mode 2 of bioreactor 1 using expanded-bed affinity chromatography...	101
23 Molecular weight calibration curve obtained from SDS-PAGE gel of Fig. 22.....	102
24 SDS-PAGE gel of MAb-TSH purified from the supernatant of cells cultured in mode 2 of bioreactor 2 using expanded-bed affinity chromatography...	103
25 Molecular weight calibration curve obtained from SDS-PAGE gel of Fig. 24.....	104
26 SDS-PAGE gel of MAb-TSH purified from the supernatant of cells cultured in mode 3 of bioreactor 1 using expanded-bed affinity chromatography...	105
27 Molecular weight calibration curve obtained from SDS-PAGE gel of Fig. 26.....	106

LIST OF FIGURES (continued)

Figure	Page
28 SDS-PAGE gel of MAb-TSH purified from the supernatant of cells cultured in mode 3 of bioreactor 2 using expanded-bed affinity chromatography...	107
29 Molecular weight calibration curve obtained from SDS-PAGE gel of Fig. 28.....	108
30 SDS-PAGE gel of MAb-TSH purified from the supernatant of cells cultured in mode 3 of bioreactor 3 using expanded-bed affinity chromatography...	109
31 Molecular weight calibration curve obtained from SDS-PAGE gel of Fig. 30.....	110
32 SDS-PAGE gel of MAb-TSH purified from the supernatant of cells cultured in mode 3 of bioreactor 1 using Protein A sepharose affinity chromatography.....	111
33 Molecular weight calibration curve obtained from SDS-PAGE gel of Fig. 32.....	112
34 SDS-PAGE gel of MAb-TSH purified from the supernatant of cells cultured in mode 3 of bioreactor 2 using Protein A sepharose affinity chromatography.....	113
35 Molecular weight calibration curve obtained from SDS-PAGE gel of Fig. 34.	114
36 SDS-PAGE gel of MAb-TSH purified from the supernatant of cells cultured in mode 3 of bioreactor 3 using Protein A sepharose affinity chromatography.....	115
37 Molecular weight calibration curve obtained from SDS-PAGE gel of Fig. 36.....	116

จุฬาลงกรณ์มหาวิทยาลัย

LIST OF ABBREVIATIONS

%	percentage
A	absorbance
AA	generic aminoacid
Ac-CoA	acetyl-coenzyme A
ALA	alanine
alpha-KG	alpha-ketoglutarate
AMP	adenosine 5' monophosphate
APR	ammonia production rate
ASP	aspartate
ATP	adenosine 5' triphosphate
BSA	bovine serum albumin
° C	degree celsius
Car	carbonic anhydrase
cm	centimeter
CO ₂	carbon dioxide
CTP	cytosine 5' triphosphate
d _f	degree of freedom
DHAP	dihydroxy acetone phosphate
dl	deciliter
DMSO	dimethylsulfoxide
EC	extracapillary
ELISA	enzyme linked immunosorbent assay
F-1,6-DP	fructose-1,6-diphosphate
F-6-P	fructose-6-diphosphate
FAD/FADH ₂	flavin adenine dinucleotide oxidized/reduced forms
FBS	fetal bovine serum
G-6-P	glucose-6-phosphate
GA-3-P	glyceraldehyde-3-phosphate
GDP	guanosine 5'-diphosphate
GLCNT -6-P	gluconate-6-phosphate

LIST OF ABBREVIATIONS (continued)

GLN	glutamine
GLU	glutamate
GTP	guanosine 5'-triphosphate
GUR	glucose uptake rate
H ⁺	hydrogen ion
hr	hour
IC	intracapillary
K ⁺	potassium ion
KA	generic keto-acid
kDa	kilodalton
kg	kilogram
L	litre
LPR	lactate production rate
Lys	lysozyme
M	molar
MAb	monoclonal antibody
MAbPR	monoclonal antibody production rate
MAbs	monoclonal antibodies
MAb-TSH	monoclonal antibody against thyroid stimulating hormone
Mal-CoA	malonyl-coenzyme A
mg	milligram
um	micrometer
ug	microgram
min	minute
mM	millimolar
MWCO	molecular weight cut off
NAD/NADH	nicotinamide adenine dinucleotide oxidized/reduced forms
NADP/NADPH	nicotinamide adenine dinucleotide(phosphate) oxidized/reduced forms
NH ₃	ammonia
NH ₄ ⁺	ammonium ion
nm	nanometer

LIST OF ABBREVIATIONS (continued)

OAA	oxaloacetate
Ova	ovalbumin
PEP	phosphoenolpyruvate
PYR	pyruvate
R-5-P	ribose-5-phosphate
Rf	relative mobility
rpm	round per minute
SDS-PAGE	sodium dodecyl sulfate polyacrylamide gel electrophoresis
Sig	significance
Soy	soybean trypsin inhibitor
SUCC	succinate
SUCC-CoA	succinyl-coenzyme A
TCA	Tricarboxylic acid
V	voltage
vol	volume
X-5-P	xylose-5-phosphate



สถาบันวิทยบริการ
จุฬาลงกรณ์มหาวิทยาลัย

CHAPTER I

INTRODUCTION

1.1 Monoclonal antibody production

Since the discovery of hybridoma technology (Kohler and Milstein, 1975), Monoclonal antibodies (MAbs) have rapidly become one of the most important animal cell products. They have been widely used in various fields such as clinical diagnostics, therapeutics, and research (Nelson et al., 2000). The increasing demand of MAbs has led to an expansion of interest in developing tools to increase their productivity.

In vivo production in the peritoneal cavity of mice is also a reliable mean of producing research quantities of mouse monoclonal antibody (MAb). For a group of twenty mice, 4.07 to 8.37 mg/ml of MAb in 100 ml of peritoneal ascites fluid could be produced (Jackson et al., 1996). Although gram quantities of MAb can be conveniently and inexpensively produced from mouse ascites fluid, MAb production *in vivo* has several disadvantages.

Firstly, thousands of mice are required to produce kilograms of antibody. Secondly, some cautions must be taken to prevent rodent viral or bacterial infections. Thirdly, it is difficult and expensive to maintain sterile mouse colonies. Fourthly, synchronizing ascites production from thousand of animals is labor-intensive. Finally, MAb from ascites fluid can be contaminated with up to 20% endogeneous murine antibodies (Vetterlein, 1989). Therefore, *In vitro* methods of hybridoma cultivation have been alternatively chosen to produce MAb in order to avoid all difficulties.

Mammalian cells can be cultured either in suspension or anchorage-dependent cultivation system. For suspension culture, cells are grown in bioreactor with either mechanical stirring or air sparging to keep cells in suspension, for example, spinner culture, stirred bioreactor or airlift fermenter. In contrast, anchorage-dependent cultivation, the cells require the extra surface for cell growth, for example, roller culture, glass bead immobilized beads or microcarrier culture (Griffiths, 2001). Although the above cultivation systems can be applied for the production of MAb, antibody product obtained is generally less concentrated than that produced in mouse ascites. In suspension culture, cell cannot easily be retained

in the reactor when the fluid is replaced with fresh medium. As a result, the maximum cell concentration achievable in suspension culture is lower than that obtained in mouse ascites. The antibody concentration in suspension culture can be a hundredfold lower than that in ascites fluid (10-50 µg/ml as apposed to 1-5 mg/ml in ascites fluid). For microcarrier culture, the cell concentration may be able to be increased by increasing the microcarrier concentration. However, cells often slough off from the microcarriers after reaching confluence. Besides these problems, hybridoma cells are sensitive to the shear force caused by agitation in a stirred vessel. To overcome these problems, various techniques or devices have been developed to increase the cell concentration (Hu and Dodge, 1985).

Hollow fiber bioreactor is one of the developments to prevent cell wash out. A high cell concentration is achieved because of the ability of the capillary network to allow for diffusion of nutrients to and metabolic waste away from the cells without washing out the cells. In these system, the cell density of 10^8 cells/ml is achieved which means the MAb concentrations approaching that of ascites fluid can be obtained (Griffiths, 1991). In reports comparing antibody production using different cell culture system, hollow fiber bioreactors consistently produced the most concentrated products, ranging from 0.71 to 11.10 mg/ml (Altshuler et al., 1986; Gorter et al., 1993; Heifetz et al., 1989; Jackson et al., 1996; Scott et al., 2000).

In addition to the production of a highly concentrated product, these systems also have many advantages in terms of smaller process equipments which reduce nutritional requirements, especially the expensive fetal bovine serum. It is economically important to reduce fetal bovine serum in the culture media without significant inhibitory effect on production (Altshuler et al., 1986; Klerx et al., 1988). Moreover, downstream purification is made cheaper and easier because the hollow fiber product is not only more concentrated but also contains lower concentration of contaminant than the MAb produced in ascites. Therefore, hollow fiber bioreactor systems can be served as an alternative for the production of MAb in commercial scale.

1.2 The purpose of research

The purpose of this research is to assemble the simple hollow fiber bioreactor for the production of MAb-TSH and to determine the optimal condition for producing high yield of MAb-TSH.

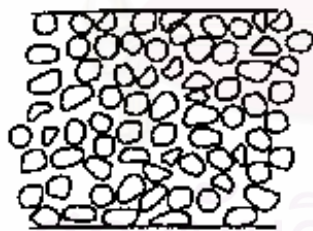
CHAPTER II

LITERATURES REVIEW

2.1 Hollow fiber membranes

Hollow fiber membranes in the form of thin tubes or fibers were developed during the 1960s. An important advantage of hollow fiber membranes is that compact modules with very high membrane surface area can be formed. However, this advantage is offset by the generally lower fluxes of hollow fiber membranes compared to those of flat-sheet membrane made from the same materials. The fiber membranes can be isotropic or anisotropic (Fig. 1). For isotropic, fiber can be made with a uniformly dense structure. However, preferably are formed as a microporous structure having a dense selective layer on either the outside or the inside surface while the anisotropic membrane consists of dense selective layer which can be either integral with the fiber or separate layer coated onto the porous support fiber. The separation properties and permeation rates of membrane are determined by the surface layer. Many fibers must be packed into bundles and potted into tubes to form a shell and tube configuration (Baker, 2000; Kelsey, Pillarella and Zydney, 1990).

Isotropic membranes

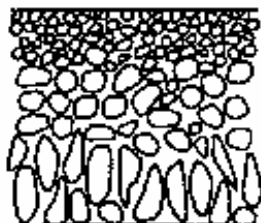


microporous membrane



nonporous dense membrane

Anisotropic membranes



loeb-sourirajan



thin-film composite

Fig. 1 Schematic diagrams of the types of membranes (Baker, 2000).

The most common membrane material for hollow fibers is regenerated cellulose. Cellulose has a very regular structure and is able to form strong intermolecular hydrogen-bonds between the several hydroxy groups. As a result, cellulose is practically insoluble in almost all solvents. Although cellulose membranes are widely used in applications where low fouling characteristics are required, the hydraulic permeability of cellulose is relatively low. Recently, synthetic polymers have begun to replace cellulose. These membrane materials are substituted cellulose derivatives, specifically cellulose acetate or polymers such as polyacrylonitrile, polysulfone, polycarbonate, polyamide and poly(methyl methacrylate). These synthetic fiber membranes are generally microporous with a finely microporous skin layer on the inside. The hydraulic permeability of these fibers is up to 10 times that of cellulose membranes and they can be tailored to achieve a range of molecular weight cut offs by using different preparation procedures (Baker, 2000; Nune and Peinemann, 2001).

The diameter of hollow fibers varies over a wide range from 50 to 3,000 μm . Fibers of 50-200 μm diameter are usually called hollow fine fibers. They are used in reverse osmosis or high pressure gas separation applications. The feed fluid is applied to the outside (shell-side) of fibers, and permeates the fiber bore. When the fiber diameter is greater than 200 to 500 μm , the feed fluid is commonly applied to the inside bore of fiber, and permeates through the outer shell. This technique is used for low pressure gas separations and for applications such as hemodialysis or ultrafiltration. Fibers with a diameter greater than 500 μm are called capillary fibers (Baker, 2000).

2.2 Operational modes of hollow fiber system

Tharakan and Chau (1986a) reviewed three operation modes of the hollow fiber system (Fig. 2). The first and second mode employed an axial feed to the fiber lumen. The first one was open shell mode. In the continuous open shell mode, the feed stream was introduced to the tube side, permeated through the hollow fibers and exited continuously through a shell port. The retention flowed out of the downstream end of tube. As second method, in the closed shell mode, the feed was still through the lumen, but there was no effluent from the shell. The third possibility was to consider shell-side crossflow. The feed stream was delivered to the shell-side and distributed uniformly along the length of fiber. The feed flowed across the fiber bed

while simultaneously permeated the fiber wall and exited from the tube side of cartridge.

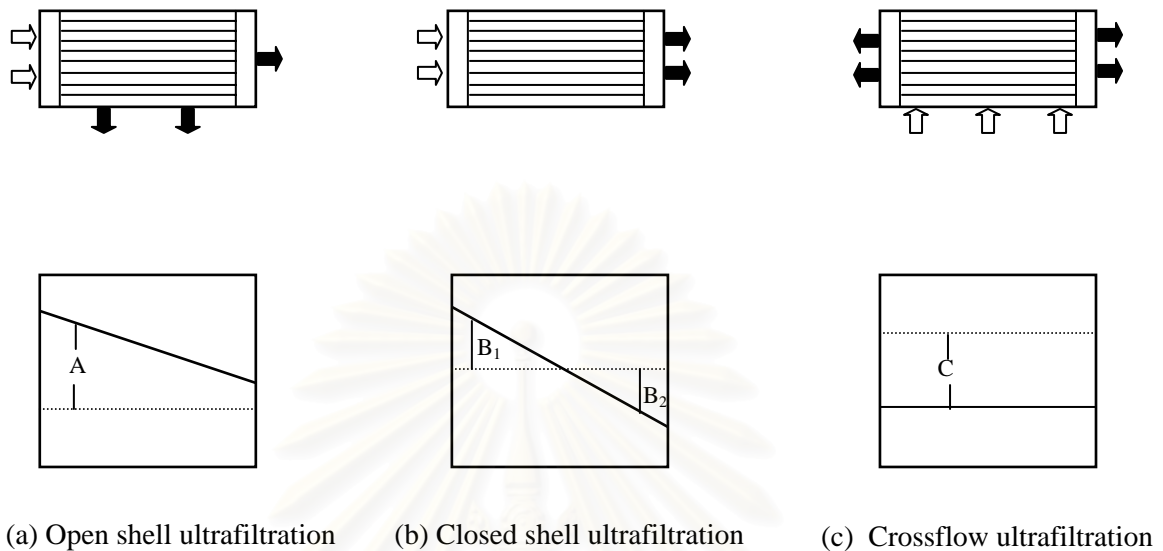


Fig. 2 The three modes of operation and the pressure distributions (Tharakan and Chau, 1986a).

opened arrow (\Rightarrow) indicates feed inlet.

closed arrow (\Rightarrow) indicates effluent stream.

solid line (—) represents the tube side pressure

dashed line (---) represents the tube side pressure.

(a) open shell ultrafiltration and transmembrane pressure difference, A.

(b) closed shell ultrafiltration and transmembrane pressure difference, B_1 and B_2 .

(c) cross flow ultrafiltration and transmembrane pressure difference, C.

They also presented data of pressure distribution in the three operational modes (Fig. 2). In the open shell mode, the tube side pressure was always greater than the shell-side but decrease linearly along the fiber unit. The shell pressure was usually uniform and thus the transmembrane flux was positive toward the shell-side and flow was always into the shell. In the limit that the tube side exit pressure was the same as the shell-side exit, the transmembrane pressure drop decreased to zero at this axial position.

In the crossflow operation, the results indicated that the shell-side pressure was always greater than the tube side pressure and thus the transmembrane pressure

flux were always positive into the tube side of fiber. In cases which an air/CO₂ mixture was passed through the fiber lumen. The data revealed that the lumen air flow rate had a negligible effect on the transmembrane flux. The shell-side pressure increased linearly with the crossflow rate, regardless of tube side pressure or the lumen airflow rate.

For the closed shell mode, the shell-side pressure remained constant along the length of unit. At the tube inlet, the tube side pressure was maintained above the shell pressure but decreased linearly along the fiber. When a crossover point was reached within 30% of the fiber unit length, the tube side pressure became less than of the shell. As the results, the transmembrane pressure drop was initially positive into the shell and became negative and flux was directed back into the tube side from the shell.

2.3 Monoclonal antibody production in hollow fiber bioreactors

For cell culture work, closed shell mode is the preferable mode of operation. A diagram of a simple hollow fiber system which operate in closed shell mode is shown in Fig. 3. The system consisted of hollow fiber cartridge, gas exchanger and medium reservoir. The system were housed with in a CO₂ incubator. Cells were inoculated into the shell-side in the extracapillary (EC) space of hollow fiber cartridge. Medium was circulated with a peristaltic pump from the reservoir, through the gas exchanger, through inside the fiber in the intracapillary (IC) space of hollow fiber cartridge, and was returned back to the reservoir. The hollow fiber membranes that separated the cells and the circulating medium, allowing diffusion of nutrient such as glucose, glutamine and oxygen fed to the cells through the fibers, and waste products such as lactate and ammonia were removed through the fibers and diluted in the medium reservoir. Large molecular weight growth factors in serum were supplied to the medium in the EC space where the cells were. The medium reservoir was always changed every 1-2 days to provide fresh basal nutrients. The EC medium was also changed every few days to replenish the high molecular weight growth factors and to harvest the product which was retained on the EC side along with the cells (Gramer and Poeschl, 1998).

Hollow fiber bioreactors have become widely used for MAb production due to the advantage among other systems, that MAb concentration approaching that of traditional method of ascites production. Furthermore, these systems have many

advantages in term of smaller process equipments, higher cell densities, reduced nutritional requirement and downstream purification is made cheaper. The following reviews demonstrated the advantages and some characteristics of hollow fiber bioreactors.

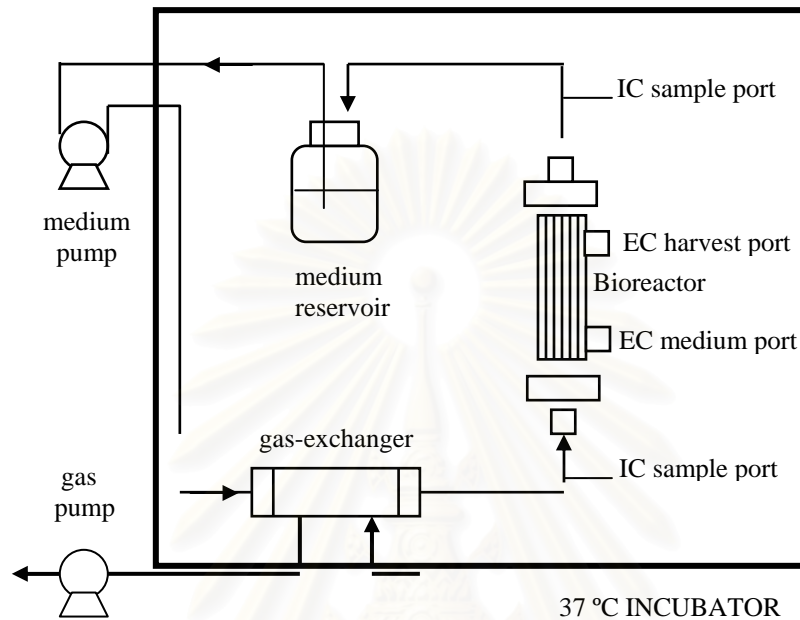


Fig. 3 A simple hollow fiber system (Gramer and Poeschl, 1998).

Altshuler et al. (1986) evaluated polysulfone hollow fiber membrane modules which had the different molecular weight cut off at 10, 50 and 100 kDa. The volume of medium in the EC space and in the reservoir were 2.5 and 125 ml respectively. The system was operated in a CO₂ incubator and controlled at 37°C with 5% CO₂. In the case of increasing the molecular weight cut off of hollow fiber membrane, the results showed a steady increase in the IgG concentration. The maximum IgG concentration in the shell space were 80, 150 and 740 µg/ml for the 10, 50 and 100 kDa hollow fiber module runs respectively. However, the IgG concentration was measured at 260 µg/ml in the reservoir for the 100 kDa hollow fiber membrane module. This occurrence resulted in back diffusion of IgG from the shell space to the lumen. In addition, the cells in 50kDa hollow fiber membrane module were able to decrease the concentration of FBS in the medium from 20% to 6.9%.

Klerx et al. (1988) constructed a compact, portable hollow fiber cell culture. An inexpensive hemodialyzer with a 10 kDa molecular weight cut off was

used as hollow fiber cell culture cartridge. The EC space volume was 120 ml and the volume of medium in the reservoir was 3.5 litres. The medium circulation rate was initially 150 ml/min and was increased to 500 ml/min. This system was housed in the CO₂ incubator and cell culture was maintained at 37°C with 5% CO₂. In this system, the serum in the EC space was carefully decreased until 2%. Although hybridoma cells could be adapted to this condition, antibody production was decreased as well. However, the production of antibody was markedly higher under serum free condition than when using low serum-supplemented culture medium (2% vol/vol). This may have been due to a negative effect of serum on antibody secretion by the hybridoma.

Heifetz et al. (1989) demonstrated two large-scale sized of the commercial hollow fiber systems using serum free medium. The pre-steriled VITAFIBER II and VITAFIBER V bioreactors were operated in a 37°C incubator. Gassing with CO₂ was not required because the medium was formulated for air equilibration by the gas exchange unit. The EC space volume of VITAFIBER II and VITAFIBER V were 28 and 91 ml respectively whereas the medium circulation rate of VITAFIBER II and VITAFIBER V were 100-200 ml/min and 200-500 ml/min respectively. The results showed that gram quantities of MAb were produced during the 40 days of experiment. Moreover, MAb produced in VITAFIBER hollow fiber bioreactors using serum free medium was relatively pure and quite concentrated.

Gorter et al. (1993) measured the feasibility of producing high amount of bi-specific MAb using an automated hollow fiber bioreactor (ACUSYST - Jr). In this system, quadroma cells were adapted to culture medium containing only 1% fetal calf serum in the EC space and optimal culture conditions were maintained by computer controlled regulation of pH, media feed rates, temperature and dissolve oxygen. In 38 days, the yield of bi-isotypic MAb after the purification procedure was 79 mg. This amount of bi-isotypic MAb was similar to the amount obtained from ascites fluid produced by 200 mice or 38 litres of tissue culture flask supernatant.

Lowrey, Murphy and Goffe (1994) examined the differences in cell culture performance between eight hollow fiber cartridges with both adherent and non-adherent cells. Eight different hollow fiber cartridges which varied in molecular weight cut off, surface area, fiber material and ultrafiltration rate were compared in the Cell-Pharm 2000 cell culture instrument. The results demonstrated marked differences between bioreactors in both cell metabolism and production. Cellulose

and cuprammonium rayon cartridges were uniformly undesirable for adherent cells. This was likely due to the relatively hydrophilic nature of these materials and the affinity of adherent cells for more polar or charged surfaces. In contrast, cellulose acetate and polymethylmethacrylate cartridges were less hydrophilic and more polar or ionically charged and were therefore better substrates for adherent cell growth. It would appear that the high ultrafiltration rate provided by increasing the molecular weight cut off of hollow fiber membranes overcame the undesirable surface effect by providing more desirable perfusion conditions.

Jackson et al. (1996) compared MAb production in hollow fiber bioreactor systems and murine ascites. The three hollow fiber systems used in this study were the Cellmax Quad (Cellco), the MiniMouse (Unisyn technologies) and the Technomouse (Integra Biosciences). Techniques for bioreactor system set up, operation, and maintenance were performed as recommended by each respective manufacturer. Three hybridoma cell lines were grown in each of three different hollow fiber bioreactor systems and in a group of 20 mice. Mean MAb concentration ranged from 4.07 to 8.37 mg/ml in murine ascites, and from 0.71 to 11.10 mg/ml in hollow fiber bioreactor systems. Although time and material costs were generally greater for the bioreactors, these results suggested that hollow fiber bioreactor systems merit further investigation as potentially viable *in vitro* alternatives to the use of mice for small scale (≤ 1 g) MAb production.

2.4 Barriers to scale up hollow fiber bioreactor

2.4.1 Heterogeneous nature of the hollow fiber bioreactor

When a hollow fiber bioreactor is operated in the closed shell mode, the pressure gradient is occurred (Fig. 2). In the entrance half of bioreactor, the pressure is higher in the fiber lumen than in the EC space and flow of nutrients enters the EC space. In the distal half, where the lumen pressure is lower than the EC space pressure, fluid from the EC space returns to the lumen and exits the bioreactor. This phenomenon causes the cells at the downstream end of unit only receive medium that has already been utilized by cells at the upstream end of device. This nutrient deficiency will foster nonuniform growth of cell mass in the shell-side. The result is dense cell growth at the inlet end of device and negligible cell growth in the downstream half. Moreover, the pressure gradient drives a secondary flow in the EC

space which passes into the shell-side upstream and back into the recycle downstream. An analogous flow around capillaries known as starring flow (Fig. 4).

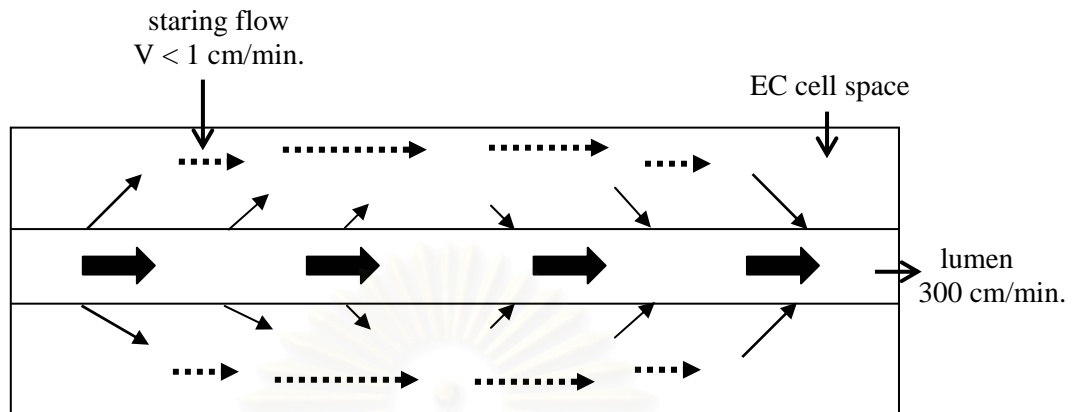


Fig. 4 An analogous flow around capillaries known as starring flow (Piret and Cooney, 1990).

The starring flow causes the cells, nutrients and metabolic products to be entrained and accumulated at the downstream end of the device. (Brotherton and Chau, 1996; Piret and Cooney, 1990; Thanakan and Chau, 1986a).

Thus, hollow fiber system operated in the closed shell axial feed mode will never have a uniform distribution of biomass and this problem will cause great difficulties in process control schemes and reduce reactor productivity. There are many reports investigated this limitation and also presented alternative methods which could be alleviated this problem.

Tharakan and Chau (1986b) developed a radial flow hollow fiber bioreactor that maximizes the utilization of fiber surface for cell growth while eliminating nutrient and metabolic gradients inherent in conventional hollow fiber cartridges. The reactor consisted of a central flow distributor tube surrounded by an annular bed of hollow fibers. The central flow distributor tube ensured an axially uniform radial convective flow of nutrients across the fiber bed. Cells attached and proliferated on the outer surface of fibers. The fiber were pretreated with polylysine to facilitate cell attachment. A mixture of air and CO_2 was fed through the tube side of hollow fibers. Spent medium diffused across the cell layer into the tube side of fibers and was convected away along with the spent gas stream. The operation of the reactor system as a high recycle unit was successful in that there was a fairly high

utilization of substrate while no significant nutrient and waste product gradient developed.

Chresand, Gillies and Dale (1988) constructed a high surface area hollow fiber reactor which employed either collagen or agar gel as an interfiber support matrix. The gel matrix greatly increased the surface area available for support of cells in the interfiber region. In this study, collagen gels were used for anchorage - dependent 3T3 mouse fibroblasts while agar gels were used for nonanchorage - dependent Ehrlich ascites tumor cells. The use of collagen or agar in the EC space as a support matrix avoided the problem of pressure induced flow in the shell-side. The gel was rigid enough so that no convective flow was possible at the pressure used. However, the disadvantage of gel matrix was that shell-side harvesting was difficult.

Piret and Cooney (1990) investigated the heterogeneous protein and cell distributions on the shell-side of hollow fiber bioreactors. At the end of each experiment, the shell-side of cartridge was studied by rapidly freezing the cartridges in liquid nitrogen and were cut into 7 or 8 axial sections to obtain samples of cell culture environment and of immobilized cells. The axial sectioning analysis revealed downstream polarization of the high molecular weight proteins. This distribution resulted from shell-side convective fluxes which caused a concentration polarization of proteins retained by the ultrafiltration membranes. Measurements of axial hybridoma cell distribution also revealed a downstream concentration of viable cells during the first month of perfusion operation. This was believed to result from the shell-side convective flow and its influenced on the inoculum and high molecular weight growth factor distribution. The heterogeneous nature could be reduced significantly by periodic alternation of the direction of recycle flow and the reactor antibody productivity were doubled.

Piret, Devens and Cooney (1991) investigated nutrient and metabolite gradients in the shell-side of ultrafiltration hollow fiber bioreactors. In the axial dimension, oxygen depletion was measured in the recycle stream and was identified as the critical, axial scale limiting factor in this reactor whereas soluble nutrients such as glucose and glutamine were easily supplied at levels when they were not limiting. Moreover, the accumulation of lactate and ammonium in the recycle stream were insufficient to impact growth and antibody productivity. To investigate radial lactate, ammonium, glucose and glutamine gradient, the hollow fiber cartridges were rapidly frozen in liquid nitrogen and were cut into 7 or 8 sections to recover samples

of shell-side environment. The result showed downstream skewing of nutrient and metabolite concentration. However, the cell distribution and activity were more homogeneous and not skewed downstream when the reactor operated with cycling of flow direction.

Patkar, Bowen and Piret (1993) measured lumen and EC space pressures in Flo-Path 7000 cartridges. At a lumen recycle flow rate of 1200 ml/min, the average EC space pressure drop was about 56% of the lumen inlet pressure. This slight deviation from symmetry could be due to partial blocking of fiber inlet by small particle in the fluid. To observe the effect of protein loading on the EC space distribution, the experiment was carried out using azoalbumin. In the absence of protein, the EC space pressure profile was asymmetric about the reactor midplane, with a higher pressure drop in the downstream region. Conversely, the decrease in the EC space pressure drop with increased protein loading could be occurred as a consequence of two separate effects: membrane fouling and osmotic effect.

Brotherton and Chau (1995) performed an intercalated spiral alternate - dead-ended hollow fiber bioreactor. The hollow fiber cartridge consisted of two fiber sets which were blocked at opposite ends and laid out as sheets upon one another. The fiber sets were rolled together to form two intercalated spirals. The intercalated-spiral bioreactor demonstrated not only a higher viable cell density, but also a more uniform distribution of cells along the bioreactor length. In addition, nutrient transport limitation can be eliminated when the convective flux through the EC space was sufficient high.

Gramer et al. (1999) operated hollow fiber bioreactor up to 60 days using three different harvesting protocols. The first method was a control consisting of a closed shell EC space with batch harvesting where starting flow the dominant convective force in the EC space. The second method, EC circulation was to slowly circulate the EC medium from one end of bioreactor to the other. The third method, EC cycling was to ultrafilter the medium from IC space to the EC space and back. In contrast to the batch harvest and EC circulation, there was no apparent channel in the EC cycling system. Cells were evenly distributed with a consistent light cream color throughout the bioreactor. The perpendicular flow forced across the fibers by EC cycling was apparently keeping flow channels open throughout the entire cell mass. These results demonstrated the importance of inducing the proper flow distribution in the EC space to allow consistent and stable production in hollow fiber bioreactors.

From literatures review, it is found that the heterogeneous nature of hollow fiber bioreactor which operate in the closed shell axial feed mode lead to reduce cell numbers and reactor productivity. To alleviate this problems, alternative designs and operating schemes had been proposed and summarized in Table 1.

Table 1 Alternative designs and operating schemes for reducing the heterogeneous nature of hollow fiber bioreactor.

System	Comments	References
radial flow	the central flow distributor system to achieve dominant radial flow.	Tharakan and Chau (1986b)
interfiber support matrix	the use of collagen or agar as an interfiber support matrix to reduce a shell-side convective flow.	Chresand, Gillies and Dale (1988)
reverse-flow cycling	operating strategy on an axial-flow bioreactor to reduce nutrient gradient.	Piret and Cooney (1990) Piret, Devens and Cooney(1991)
alternate-dead-ended	intercalate – spiral fiber set to eliminate nutrient transport limitations	Brotherton and Chau (1995)
EC space cycling	operating strategy on an axial-flow bioreactor to reduce a shell-side convective flow	Gramer et al. (1999)

2.4.2 Nutrient depletion

Glucose and glutamine are the major carbon and energy sources used by mammalian cells in culture. As shown in Fig. 5, both nutrients have essential

anabolic roles but are complementary for the production of other metabolites and energy.

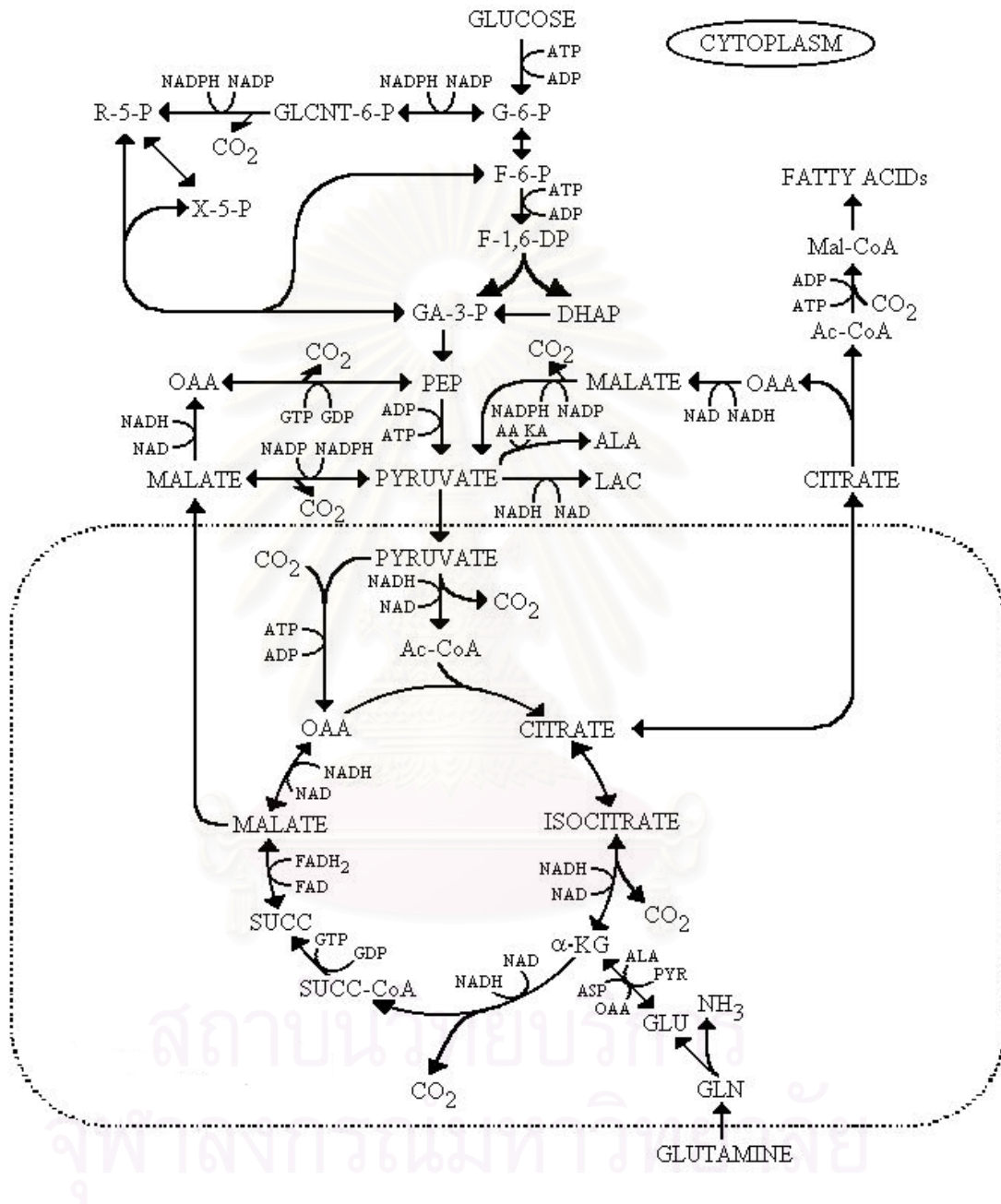


Fig. 5 Primary metabolism in mammalian cells exhibiting high rates of glucose and glutamine metabolism (Mancuso et al., 1994).

Glucose is metabolized to pyruvate for energy in mammalian cells via glycolytic pathway whereas the predominant source of pyruvate is the glycolytic pathway, some may also be formed the pentose phosphate pathway, the malate shunt

(conversion of malate to pyruvate), and the pyruvate/malate shuttle associated with lipid synthesis (conversion of citrate to cytosolic acetyl CoA and oxaloacetate). Pyruvate can enter the TCA cycle by two main enzymes, pyruvate dehydrogenase and pyruvate carboxylase. For energy production, pyruvate enters predominantly through pyruvate dehydrogenase whereas cells exhibiting high rates of lipid synthesis have significant fluxes through pyruvate carboxylase (Stryer, 1995).

Glutamine is also catabolized to produce energy. There are three pathways in which glutamine can be catabolized. The first one is the complete oxidation to CO_2 through the TCA cycle. The second is the partial oxidized to lactate. The last is another partial oxidation to aspartate by aspartate aminotransferase or to alanine by alanine aminotransferase. Additionally, the amide of glutamine is a source of nitrogen in the biosynthesis of a variety compound, such as tryptophan, histidine, asparagine, carbamoyl phosphate, glucosamine 6 - phosphate, CTP and AMP (Stryer, 1995; Tildon and Zeilke, 1988).

Miller, Wilke and Blanch (1989a) examined the transient and steady state responses of hybridoma growth and metabolism to glucose pulse and step changes. The specific glucose consumption rate increased by 100-200% immediately after glucose was added to the reactor, and the increase glycolytic ATP production appeared to be responsible for the concurrent rapid decrease in the specific oxygen uptake rate. The effects on glutamine consumption were delayed, probably due to buffering by the TCA cycle and interrelated pathways. A period of increase biosynthetic activity, as evidence by an increase in the estimated specific ATP production rate and lower by product yield from glutamine, preceded the increase in cell concentration after the glucose step change. The estimated 22% ATP production due to glycolysis was twice as great as that before the step change.

Miller, Wilke and Blanch (1989b) examined the transient and steady state responses of hybridoma growth and metabolism to glutamine pulse and step changes. The specific glutamine consumption rate increased rapidly after glutamine was added to the reactor. The responses of glucose and oxygen consumption rates and the cell concentration were found to depend on the initial feed glutamine concentration. Glutamine has been shown to increase glucose oxidation via the pentose phosphate pathway, so a portion of increase in oxygen consumption rates was probably due to the increased rate of ribose 5-phosphate synthesis in preparation for more rapid cell division. The glucose consumption rate was 1.4 -10.9 times that

of glutamine and serine and branched-chain amino acids were consumed in larger amounts at the higher glucose:glutamine uptake ratios.

Flickinger et al. (1992) studied the addition of L-glutamine to batch culture of hybridoma cells in microcarrier spinner flasks. The addition of L-glutamine to a final concentration of 5-40 mM was found to stimulate the growth of hybridoma cells as well as the secretion of MAb per cell, particularly in slowly growing cells. These responses indicated that during slow growth, the addition of L-glutamine increased the availability of cellular ATP generated by mitochondrial respiration which stimulated some posttranscriptional step in the pathway of MAb secretion.

Mancuso et al. (1994) studied primary metabolism of murine hybridoma by probing with ^{13}C nuclear magnetic resonance spectroscopy. Cells cultured in hollow fiber bioreactor were serially infused with [1- ^{13}C] glucose, [2- ^{13}C] glucose, [3- ^{13}C] glutamine. Estimates made from labeling patterns in lactate indicated that 76% of pyruvate was derived directly from glycolysis; some was also derived from the malate shunt, the pyruvate/malate shunt associated with lipid synthesis and the pentose phosphate pathway. The rate of formation of pyruvate from the pentose phosphate pathway was estimated to be 4% of that from glycolysis; this value was a lower limit and the actual value may be higher. Most pyruvate carbon entered the TCA cycle through pyruvate dehydrogenase. No flux through pyruvate carboxylase was detected. A significant amount of glutamine was converted to pyruvate through the malate shunt. The rate of incorporation of glucose-derived acetyl-CoA into lipids was 4% of glucose uptake rate. The TCA cycle rate between isocitrate and α -ketoglutarate was 110% of the glutamine uptake rate.

Sharfstein et al. (1994) described an nuclear magnetic resonance (NMR) study of hybridoma metabolism at two feed glutamine concentration, 4.0 and 1.7 mM. Hybridoma cells were grown in a hollow fiber bioreactor to provide high cell densities at a constant pH and dissolved oxygen (DO) level, and were then fed ^{13}C -labeled glucose or glutamine. Decreasing the feed glutamine concentration significantly increased antibody productivity in concert with decreased glutamine uptake and no apparent change in glycolytic metabolism suggested that antibody productivity was not energy limited. Metabolic flux calculations indicated that (1) approximately 92% of glucose consumed proceeded directly through glycolysis with 8% channeled through the pentose shunt; (2) lipid synthesis appeared to be

greater than malate shunt activity; and (3) considerable exchange occurred between TCA cycle intermediates and amino acid metabolic pools, leading to substantial loss of ^{13}C label from the TCA cycle.

Jeong and Wang (1995) investigated the effects of glutamine on cell growth kinetics, MAb productivity and cell metabolism of hybridoma cells in 25 and 75 cm^3 tissue culture flasks. Glutamine showed a mono-type effect on specific cell growth rate with a very small Monod constant of 0.089 (mM). MAb production was also strongly dependent on glutamine concentration. Glutamine enhanced MAb production not only by stimulation of cell growth, but also by increasing the specific MAb productivity. Increasing glutamine concentration stimulated specific glutamine consumption rate and specific ammonium ion production. The specific glucose consumption rate decreased with increasing glutamine concentration up from 0 to 0.1 mM and then increased. The specific lactate production rate decreased as glutamine concentration decreased.

Sanfeliu et al. (1996) carried out a series of batch experiments to determine the effect of different initial glucose and glutamine concentrations on cell growth, MAb production and metabolism. Cells were cultured in tissue culture flasks to give an initial concentration of 10^5 viable cells/ml. It could be observed that the maximum number of viable cells obtained at the end of exponential growth phase increased with increasing the initial glucose concentration in the medium. However, the influence of glutamine seemed to be irrelevant regarding this aspect. The maximum growth rate, glucose and glutamine uptake rates did not change with different initial glucose and glutamine concentration.

Mancuso et al. (1998) examined the effect of changes in extracellular glutamine level on metabolism of a murine hybridoma by probing ^{13}C nuclear magnetic resonance spectroscopy. Cells were cultured in hollow fiber bioreactor at high cell density. Steady infusions of [1 - ^{13}C] glucose were used to label glycolytic and TCA cycle intermediates during changes in environmental glutamine level. For a brief reduction in feed glutamine concentration from 4 to 0 mM (which produced a rapid change from 0.67 to 0 mM of residual glutamine in the circulating medium), energy metabolism was perturbed as indicated by increasing in the rate of glycolysis. The changes were detected after the residual glutamine level had dropped to only 0.37 mM. Antibody synthesis was also strongly stimulated and nitrogen metabolism was significantly altered. For a more prolonged reduction from 2.4 to 1.2 mM (which

produced a slower reduction from 0.30 to 0.08 mM of residual glutamine in the circulating medium), the rate of glycolysis were slightly reduced. Energy metabolism did not appear to be limited by glutamine at 0.08 mM, which suggested that significant futile cycling would be occurred in energy producing pathways when excess glucose and glutamine were available. However, the concentration of extracellular glutamine appeared to affect some anabolic pathways which required amino groups from glutamine.

2.4.3 Accumulation of waste products

In mammalian cell culture, waste products excreted by the mammalian cell itself have significant effect on cell growth and metabolite production. Lactate and ammonia are the two major waste products formed during mammalian cell growth. Lactate is mainly produced from glucose metabolism. In the absence of oxygen, pyruvate is reduced by NADH to lactate. Additionally, lactate can also be produced in small amounts from glutamine (Stryer, 1995). The source of ammonia formation originates from the nonenzymatic degradation of amide group of glutamine which is unstable under normal conditions during animal cell cultivation. The second source is the enzymatic degradation of amide group of glutamine, which occurs in the mitochondria and is catalyzed by glutaminase. The third source is the enzymatic hydrolysis of amino group of glutamine. The last source of ammonia formation comes from other essential amino acids via glutamate hydrolysis (Xie and Wang, 1994).

The problems with lactate and ammonia accumulation in mammalian cell cultures have been addressed by many workers and the following mechanism of toxicity was proposed.

Luan, Mutharasan and Magee (1987) examined the effect of growth rate and pH on lactate formation in batch cultures of hybridoma cell line. The experiments were conducted in tissue culture flasks. The results showed that high glucose concentration led to extensive lactate formation only during growth phase and not during stationary phase. Lactate formation also served to regulate extracellular pH at pH 6.8, provided conditions were favorable to maintain viability and if sufficient nutrients were presented in the medium.

Glacken, Adema and Sinskey (1988) determined the initial metabolism of hybridoma cells, such as growth rate and the specific antibody

productivity. Hybridoma cells were grown in tissue culture flasks. The rate were measured over brief time intervals and at low cell concentration. The results indicated that decreased FBS and medium concentrations, and increase ammonia levels reduced the growth rate. The hypothesis of ammonia 's inhibitory effect may be the result of destruction of electrochemical gradients that may occurred due to ammonia 's basic nature. Although lactate levels as high as 40 mM did not significantly affect the growth rate, lactate was found to be the only environmental parameter that significantly inhibited MAb production.

Mcqueen and Bailey (1990) investigated the effects of NH_4Cl addition on batch hybridoma cell growth at different external pH values (pHe). Cells were cultured in tissue culture flasks and a bioreactor at constant pH and dissolved oxygen concentration. The effects of pHe and NH_4Cl concentration on cell metabolism gave similar results for cells grew in flasks and in the bioreactor. The pHe over the range 6.8-7.6 had minor effect on growth. Addition of 3 mM NH_4Cl had little effect on cell growth while 10 mM NH_4Cl caused a substantial growth inhibition. Increases in NH_4Cl concentration were shown to decrease pHe and were shown to decrease the integral cell yield on glucose and glutamine. Change in pHe and NH_4Cl concentration caused growth inhibition but no effect on the specific antibody production rate, and the quality of antibody produced.

Ozturk, Riley and Palsson (1992) investigated the murine hybridoma cell during batch culture in tissue culture flasks for the influence of ammonia and lactate on cell growth, metabolism, and antibody production rates. The specific growth rate was reduced by one-half in the presence of an initial ammonia or lactate concentration at 4 mM or 55 mM respectively. Specific metabolic rates were accelerated at higher ammonia or lactate concentration. Specific antibody productivity was not influence by ammonia concentration. Cultures at higher ammonia level result in lower antibody levels due to the low cell concentrations obtained. However, at higher lactate concentrations specific antibody productivity increased, possibly due to the increase in medium osmolarity. The specific oxygen uptake rate was insensitive to ammonia and lactate concentrations. Decreasing external pH and increasing ammonia concentrations caused cytoplasmic acidification. Effects of lactate on intracellular pH was insignificant, whereas increasing osmolarity caused cytoplasmic alkalization.

Omasa et al. (1992) reported on the effects of lactate on hybridoma cell growth and antibody production. A glass spinner flask was used for the fed-batch culture in a serum-free medium. With an increase of average osmotic pressure, the specific growth rate decreased and the specific death rate increased. When the osmotic pressure was adjusted to the same condition as that of lactate using sodium chloride, the specific growth data showed the same degree of growth inhibition. Therefore, the effect of lactate on the specific growth and death rates was mainly due to the increase of osmotic pressure. The production of lactate from glucose was found to be inhibited by the lactate itself which might be attributed to inhibition of L-lactate dehydrogenase reaction by L-lactate.

Martinelle and Haggstrom (1993) presented a model for transport of NH_3 and NH_4^+ across cell membranes as shown in Fig. 6. Formation of $\text{NH}_3/\text{NH}_4^+$ in the cells occurred mainly in the mitochondria by the mitochondrial enzymes glutaminase and glutamate dehydrogenase. These reactions liberated NH_4^+ which only slightly decreased the mitochondrial pH as the equilibrium with NH_3 was formed. The outflow of NH_3 forced formation of new $\text{NH}_3 + \text{H}^+$ from NH_4^+ to reestablish the equilibrium in the mitochondria while NH_3 readily diffused through the extremely ion impermeable inner mitochondrial membrane and transiently increased the cytoplasmic pH. Ammonia that diffused from the cytoplasm to the outside of cell could be transported back across the cytoplasmic membrane via

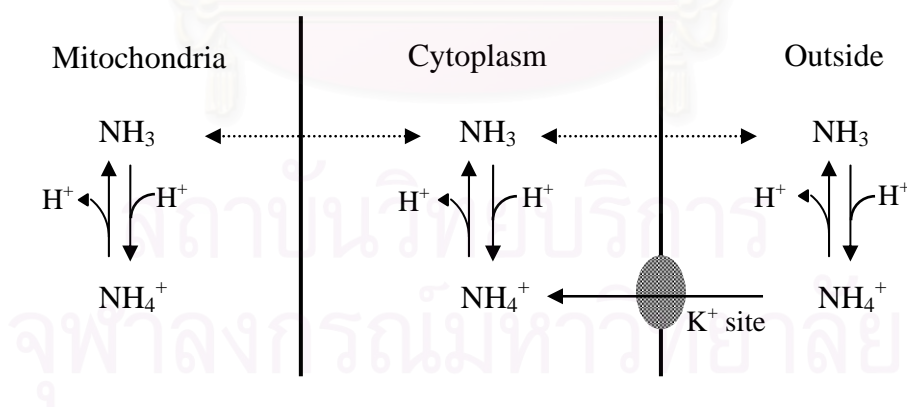


Fig. 6 Model for transport of NH_3 and NH_4^+ across cell membranes (Martinelle and Haggstrom, 1993).

certain transport proteins as NH_4^+ , in competition with K^+ . The transport occurred against a concentration gradient but intracellularly NH_4^+ equilibrated immediately with NH_3 which again diffused out the cell. Thus, mitochondrial formation of

$\text{NH}_3/\text{NH}_4^+$ decreased both the mitochondria and the cytoplasmic pH. The cytoplasm becoming progressively more acid by time. Other cellular compartments would turn alkaline as NH_3 diffused into them. Experiments which verified the model were performed by measurement of pHe in a concentrated myeloma cell suspension in buffer. The result showed that addition of NH_4^+ caused a time-dependent pHe (extracellular pH) increased and NH_4^+ which transported in the murine myeloma cell line was inhibited by an excess of K^+ . It was postulated that one important toxic effect of $\text{NH}_3/\text{NH}_4^+$ was an increased demand for maintenance energy, caused by the need to maintain ion gradients over the cytoplasmic membrane. The results also suggested that K^+ could be used to detoxify $\text{NH}_3/\text{NH}_4^+$ in animal cell cultivations.

Kromenaker and Srienc (1994) studied the effects of lactic acid concentration on the cell cycle kinetics of hybridoma cell growth and antibody production in batch culture using spinner flasks based on population-average data analysis and using flow cytometry based on single-cell data analysis. When 33 mM lactic acid was initially presented, the true specific growth rate was reduced by 37% and the cell specific antibody production rate increased by a factor of 2.6 relative to a control culture with no addition of lactic acid. DNA content distributions measured during balanced exponential growth were not affected by lactic acid concentration indicating lactic acid had a uniform effect on cell growth throughout the cell cycle.

Cherlet and Marc (1998) studied the behavior of hybridoma cells by monitoring the intracellular pH (pHi) during batch and continuous bioreactor cultures under normal real culture conditions. The results of batch culture without control of medium pH indicated that a decrease of extracellular pH induced an acidification of cytoplasm at short term, before the cell could adapted to this decrease. During the continuous culture, a decrease of medium pH of its value of 7.0 to 6.7 did not necessarily result in cytoplasmic acidification but at pH 6.7 the growth inhibition was observed. The growth inhibitory effect could be explained by the combination of increased demand for maintenance energy associated with the higher ΔpH gradient maintained across the cell membrane. This increase was accompanied by a drastic decrease of specific glucose consumption rate. The results also indicated that increased ammonium ion concentrations did not lower pHi. This observation together with the results of batch culture carried out at a more alkaline pH, indicated that the form NH_3 , and not the form NH_4^+ had negative effect on cell growth.

Several strategies for reducing the production of lactic acid and ammonia by mammalian cells are proposed and there are summarized as follows:

Glacken, Fleischaker and Sinsky (1986) demonstrated strategies for reducing the production of lactic acid and ammonia via controlled addition of glucose and glutamine. Human foreskin fibroblasts grown on microcarriers were cultured in 14 L aerated vessel which was equipped to monitor and control pH, dissolved oxygen, and glucose levels via a computer. By either replacing glucose with galactose or by controlling glucose at low levels, the specific lactic acid productivity drastically reduced. Additionally, glutamine and ammonium kinetics for Madin-Darby canine kidney (MDCK) cells were described mathematically. From mathematical relations, cultures maintained at these low glutamine levels exhibited reduced ammonium production compared to standard batch cultures.

Kurokawa et al. (1994) developed an online system using high-performance liquid chromatography (HPLC) for the measurement of glucose, glutamine, and lactate in fed-batch culture of hybridoma cells in spinner flask. When glucose concentration was controlled at low level 0.2 g/L, the intracellular lactate dehydrogenase activity decreased by one-half and the lactate concentration by one-third. On the other hand, ammonia production increased when glucose concentration was kept low. To reduce the production of lactate and ammonia, and improved antibody production rate, the concentrations of glucose and glutamine were controlled at 0.2 and 0.1 g/L respectively. With these low concentrations of glucose and glutamine, the cell concentration and antibody production both increased about twofold compared with the amounts when glucose was controlled at higher levels.

Capiaumont et al. (1995) used two strategies to reduce accumulation of ammonia in hybridoma cell cultures. The first strategy was to adapt the cells to a non-ammoniogenic medium. Ammonia production was limited by replacing glutamine with glutamate. Batch culture were maintained in spinner flasks. Replacing the medium containing 1 mM glutamine and 3 mM glutamate reduced the quantity of ammonia produced to 0.5 mM during the whole culture while cell growth and MAb production were reduced by 30%. The second strategy was removed the ammonia produced by two methods. Firstly, batch cultures were carried out in the bioreactor which connected to a column packed with Na-regenerate clinoptilolite for detoxification. Removing ammonia with clinoptilolite slightly increased cell proliferation, but had no effect on antibody production. The use of clinoptilolite

required constant ion rebalancing of medium to replace the adsorbed K^+ after each cycle. Secondly, batch cultures were run in the bioreactor which connected to a hydrophobic microporous hollow fiber module. The ammonia was eliminated by diffusion of gas through the membrane into the EC space. Membrane detoxification reduced the ammonia concentration in the culture at 1 mM without ionic imbalance. The lower ammonia concentration led to increase in cell density, but to only a small increase in MAb production.

Chen et al. (2001) reduced lactate formation in the cell culture by genetically manipulating the pathway of lactate synthesis. Disruption the LDH-A gene by homologous recombination in hybridoma cell (ATCC-CRL-1606). A variant cell LDH-neo21 was identified through this screening method and was characterized. The specific productivity of lactate by LDH-neo21 cell was 50% lower than that of parental cells. Intracellular LDH enzyme activity was significantly reduced. The cell growth was improved both in terms of cell density and cell viability. The antibody production of LDH-neo21 cells was threefold greater than that of parental cells during 5 days batch culture. Polymerase chain reaction results showed that at least one copy of LDH-A gene was disrupted in the LDH-neo21 cells. The variant of hybridoma cell exhibited a significant advantage of reduced lactate formation in the cell culture with a high concentration of glucose, which led to a higher production of MAb.

2.4.4 Oxygen transport limitation

Oxygen transport is a major limitation in large-scale hybridoma cell culture. This is due in part to the low solubility of oxygen in water (0.22 mmole/L at 37°C in equilibrium with air) and the high rate of oxygen consumption by the cell (Piret, Devens and Cooney, 1991). In suspension bioreactors, the high degree of agitation can increase the rate of oxygen transfer. However, hybridoma cells do not have a protective cell wall and thus cannot tolerate excessive agitation. On the other hand, in immobilized bioreactor systems where the cells are protected from shear, diffusional resistances limit the transfer rate of oxygen, and oxygen limitation becomes unavoidable at high cell densities (Ozturk and Palsson, 1990). The effect of oxygen on hybridoma cell growth, metabolism and MAb production have been studied extensively.

Miller, Wilke and Blanch (1987) investigated the effects of dissolved oxygen concentration (DO from 0.1 to 100% saturation in air) on mouse hybridomas using continuous suspension culture. The steady state concentration of viable cells increased with decreasing DO until a critical dissolved oxygen concentration of 0.5% of air saturation was reached. The cell viability was higher at lower DO may be due to less oxidative damage to cellular components. Below 0.5% DO, the cell concentration declined because the energy loss caused by incomplete glutamine oxidation, and the specific lactate production from glucose increased to offset the reduced energy production from glutamine. The specific oxygen uptake rate was essentially constant for DO above 10% of air saturation and then decreased with decreasing DO. The P/O ratio (ATP molecules produced per O atom consumed) appeared to change from 2 to 3 between 10% and 0.5% DO. The optimum DO of 50% for antibody production was different than the optimum DO of 0.5% for cell growth.

Ramirez and Mutharasan (1990) revealed a direct correlation between average cell volume and progression through the cell cycle by determination of cell size and DNA content of hybridomas. Semicontinuous experiments in tissue culture flasks showed that G₁ cells as estimated from cell size measurements, secreted MAb at rates higher than those of cells in other stages of interphase and mitosis. Similarly, fed-batch and batch experiments suggested that specific oxygen uptake rate was also a function of cell cycle, being minimum for cell in G₀ and G₁ phase. In batch cultivation in reactor, the oxygen uptake rate steadily increased as the cells went from the lag to the midexponential phase, and the specific oxygen uptake rate increased during the early exponential phase where it remained relative constant. Several hours before maximum cell concentration was reached, oxygen uptake rate and the specific oxygen uptake rate rapidly decreased to levels below those observed at inoculation. The time at which the shift in the oxygen uptake rate and the specific oxygen uptake rate occurred and the onset of decrease in the average cell size corresponded to the time of glutamine depletion.

Ozturk and Palsson (1990) examined the effect of dissolved oxygen concentration (DO) on hybridoma cell physiology in a continuous stirred tank bioreactor. Cell growth was relatively constant between 5% and 78% DO, and a decrease was observed at 100% air saturation and below 5% air saturation. Lower cell concentrations were observed at low DO due to the oxygen limitation whereas

the cells were very viable at zero DO which was probably due to lower oxidative damage to the cells. At steady state of culture, glucose and oxygen consumption rate changed little by decreasing oxygen concentration until 1.2% DO was reached. Between 100% and 1.2% DO, only the consumption rate of glutamine changed significantly. The glutamine consumption rate was higher at higher oxygen concentrations in this range. The metabolic rates of glucose, glutamine, lactate and ammonia increased 2-3 fold as the DO dropped from 1% to 0%. The consumption rate of amino acid changed little above 1% DO, but under anaerobic conditions the consumption rates of all amino acids increased severalfold. These changes in metabolic rates at low DO showed the adjustment of cellular metabolism to the oxygen-deprived environment. Cells obtained most of their metabolic energy from glutamine oxidation but glucose was preferred over glutamine when oxygen was limiting. The specific ATP production rate obtained was constant at all oxygen concentration, except at zero oxygen where the cells exhibited a higher ATP production rate. Antibody concentration was highest at 35% DO while the specific antibody production rate was insensitive to DO.

Zhang, Honda-Corrigan and Spier (1993) investigated the oxygenation of high-density hybridoma cell cultures. The culture system was composed of stirred-tank bioreactor, which was connected to a hollow fiber cartridge for medium perfusion. Cell growth and antibody production were examined with large bubble (~5 mm in diameter), micron-sized bubble (~80 μm in diameter) and silicone tubing oxygenation techniques. For the micron-sized bubble oxygenation, consistent increases in both the cell and MAb concentrations were obtained at the cultivation progress. However, large air bubble sparging could not supply enough oxygen when a cell density of 5×10^6 cells/ml was attained. Subsequently, pure oxygen sparging was used for the large bubble oxygenation, and the dissolved oxygen tension was maintained successfully at 30% air saturation. Relatively low cell growth and MAb production were attained with the bubble-free silicone tubing-oxygenation. It was concluded that direct bubble oxygenation could be applied successfully in high-density animal cell cultures and the micron-sized bubble oxygenation method was highly recommended for high density animal cell cultures, provided that Pluronic F-68 was supplemented into the culture medium. The accumulation of ammonia in the culture medium rather than oxygen limitation was found to inhibit cell growth.

Shi, Ryu and Park (1993) compared the two different perfusion culture systems under oxygen limited and non-oxygen limited conditions. The culture system was consisted of stirred-tank bioreactor, which was connected to a hollow fiber cartridge for cell recycling. When oxygen was a limiting factor during perfusion culture, both specific glucose uptake and lactate production rate increased, compared to non-oxygen limited condition by a factor of 1.6 and 1.3 respectively. The specific glutamine uptake rate under oxygen limited conditions was almost 4 times higher than under non-oxygen limited conditions. This was suggested that more ATP was consumed under oxygen limited cultivation conditions in a high cell density perfusion culture. There was a 3.2 times higher specific rate of lactate dehydrogenase activity released by dead cell in oxygen limited cultures than in non-oxygen limited cultures. The rate of lactate dehydrogenase activity increased mainly because of an increase in the rate of lactate formation. The specific MAb production rate was not significantly affected by the oxygen transfer conditions during the rapid cell growth period.

Riley, Muzzio and Reyes (1997) described the model of immobilized cell behavior. The model assumed that cellular productivity was limited only by the supply of oxygen and the growth media was continually replenished. Model predictions agreed with experiment measurements reported in the literature and indicated that for long operation time the supply of oxygen, biocatalyst size, and cell kinetics have a significant effect on biocatalyst performance whereas the cell loading has only a relatively small effect. Under culture conditions found that oxygen penetrated to a maximum depth of about 0.4 mm. Accordingly, cells immobilized farther than this threshold distance received an insufficient supply of oxygen.

In hollow fiber bioreactor, oxygen depletion is expected to be the major limiting factor for both radial and axial-scale. This is due to the low solubility of oxygen in water, and oxygen transport through tissues is hindered by the packed cell protein and membrane component. Therefore, high liquid flow rates through the reactor are required to supply the oxygen needed. However, mechanical strain on the fibers and a very high liquid shear rate inside the fiber, potentially causing denaturation of serum or product proteins.

Adema and Sinskey (1987) analysed the mathematical model for oxygen transport through the cell mass. The analysis indicated that diffusion oxygen transport from the fiber wall to the cells can be enhanced by increasing the surface

area for oxygen and/or decreasing the penetration depth. One strategy for improving of surface area to penetration depth ratio was to increase the number of fibers in the reactor. An alternative way to manipulate this ratio was to grow the cells inside the fibers rather than on the outside. The theoretical analysis indicated that this was favorable when the volume of EC space exceeded that of fiber lumen by a factor four or more. Therefore, the hollow fiber bioreactor with crossflow operation could be set up for nutrient diffusion through cell mass growing inside the fibers. The fibers where the cells were grown on the inside were considerably larger than used in the conventional reactors for reducing the likelihood of a broken fiber. On the other hand, if one were used the very small (150-200 μm) fibers in a crossflow reactor, the amount of cell per fiber would be very small but gradients in oxygen concentration were minimized. A disadvantage of crossflow mode was that high molecular weight products such as MAb had to be recovered from the circulating medium whereas in the traditional design they were concentrated in the EC space.

Piret, Devens and Cooney (1991) investigated oxygen depletion in the shell-side of ultrafiltration hollow fiber bioreactors. At the recycle flow rate of 100 ml/min, a 0.05 mM decreased in the oxygen concentration in the recycle stream was measured between the inlet and outlet of bioreactor. At a lower (12.5 ml/min) recycle flow rate, the oxygen concentration measured at the recycle outlet was nearly completely depleted. Moreover, at the low recycle flow rate revealed a decline in viable cell numbers from the inlet to the outlet end of bioreactor. Therefore, in high density immobilized cell bioreactors the medium oxygen should be maintained high to minimize axial and radial limitations.

Shi, Sardonini and Goffe (1998) investigated the use of chemical oxygen carriers to enhance growth and MAb production of hybridomas in hollow fiber bioreactor systems. These oxygen carriers include natural bovine haemoglobin, ErythrogenTM-1, Formula-1TM, polyethylene glycol cross-linked haemoglobin, and perfluorocarbon emulsion. Oxygen carriers were added to the medium reservoir of hollow fiber bioreactors to test for any increases in culture. Although these additives displayed no beneficial effects in tissue flask cultures, they were found to improve the output of antibody over control culture containing no additives when tested in hollow fiber systems. Production enhancements ranged from 104% using erythrogen, 20% using the polyethylene glycol cross-linked haemoglobin, 40% using Formula-1TM and 78% using perfluorocarbon emulsion. No increase in production was

observed for natural bovine haemoglobin. Haemoglobin additives that resulted in an increase in antibody output were found to decrease the ratio of lactate production rate to glucose consumption rate (LPR/GUR) which used as a measure of efficiency of oxygen usage.

From literatures review, it is noticed that in order to produce high yield of MAb by the hollow fiber bioreactor, the following factors have to be considered. Firstly, reducing nutrient and metabolite gradients in the shell-side of hollow fiber cartridge by using alternative designs and operation schemes. Secondly, nutrient should be maintained above limiting levels whereas the waste products should be controlled under limiting level. Finally, maintain the oxygenated region in the immobilized phase at high levels.



สถาบันวิทยบริการ
จุฬาลงกรณ์มหาวิทยาลัย

CHAPTER III

MATERIALS AND METHODS

3.1 Cell line and culture medium

Hybridoma TSH II was formed from the fusion of spleen cells from an immunized Balb/c mouse with the Sp2/0-Ag14 myeloma fusion partner. This hybridoma secretes IgG₁ antibody directed against β chain of thyroid stimulating hormone. Basal medium consisted of RPM I - 1640 with 4 mM glutamine, 1 mM sodium pyruvate, 4.5 g/L glucose and 2 g/L sodium bicarbonate. serum-supplemented medium was prepared by adding FBS to basal medium. Cells were routinely propagated in 5% serum-supplemented medium at 37°C in an incubator with 5% CO₂.

3.2 Chemicals

3,3',5,5'-tetramethylbenzidine (TMB)	Roche
Acetic acid	Merck
Acrylamide	Sigma
Ammonia kit(171-C)	Sigma
Ammonium persulfate	Sigma
Bovine serum albumin	Boeringer mannheim
Bromophenol blue	Sigma
Citric acid	Merck
Coomassie brilliant blue R-250	Sigma
D-glucose	Fluka
Disodium hydrogen phosphate	Merck
Fetal bovine serum	Hyclone
Glucose kit (510-A)	Sigma
Glycerol	Merck
Glycine	Sigma
Goat anti-mouse immunoglobulins	DAKO
Hydrochloric acid	Merck
Hydrogen peroxide	Merck

Lactate reagent (735-10)	Sigma
Lactate standard; 40mg/dl (826-10)	Sigma
L-glutamine	Sigma
Mercaptoethanol	Sigma
Metabolite control (S 3006)	Sigma
Methanol	Merck
Mouse IgG-technical grade	Sigma
N,N,N,N/- tetramethyl ethylene diamine (TEMED)	Sigma
N,N/-methylene-bis-acrylamide	Sigma
Peroxidase-conjugated rabbit anti-mouse immunoglobulins	DAKO
Potassium chloride	Merck
Potassium dihydrogen phosphate	Merck
Protein A Sepharose 4 fast flow	Pharmacia biotech
RPM I medium (powder for 10 L)	Hyclone
Sodium carbonate	Merck
Sodium chloride	Merck
Sodium citrate	Sigma
Sodium dihydrogen phosphate	Merck
Sodium dodecyl sulfate (SDS)	Sigma
Sodium hydrogen carbonate	Merck
Sodium hydroxide	Merck
Sodium pyruvate	Sigma
Standard marker protein for SDS-PAGE	Bio rad
Streamline rProteinA	Pharmacia biotech
Sucrose	Merck
Sulfuric acid	Merck
Tris (hydroxymethyl) aminomethane	Sigma
Trypan blue	Merck
Tween 20	Merck
Tween 80	Merck

3.3 Equipments

Autoclave / HV-110	Hirayama
Centrifuge tube (50 ml)	Nunc
Centrifuge / CF7D2	Hitachi
Conical centrifuge tube (200 ml)	Nunc
Connector for the IC space of the cartridge	Terumo
Coupling connector (KECK connector)	Duran
Dialysis connector	Gambro dasco
Electrophoresis power supply / EPS 300	Pharmacia biotech
Electrophoresis unit / Mighty small SE 245	Pharmacia biotech
Female-female connector	Vygon
Freeze dry system	Labconco
Glass bottle (5 L)	Duran
Haemocytometer	Boeco
Hollow fiber dialyzer / T175	Terumo
Hydrophilic filter 0.2 μm / Vacucap 90	Gelman-science
Hydrophobic filter 0.2 μm / Midisart 2000	Sartorius
Inverted microscope	Nicon
Liquid chromatography system (AKTA explorer)	Pharmacia biotech
Maprene tube (tube bore 4.8 mm. , thick 2.4 mm.)	Watson-marlow
Microbiological safety cabinet / Atlas 2000	Flufrance
Microtiterplate 96 wells	Nunc
Microtiterplate reader / multiskan MS	Labsystem
Needle (18G x 1 $\frac{1}{2}$ inches)	Terumo
Peristaltic pump / 505S	Watson-marlow
Pumphead /505L	Watson-marlow
Screw cap GL 45	Duran
Silicone tube (tube bore 4.8 mm. , thick 1.6 mm.)	Watson-marlow
Spectrophotometer / Ultrospec 3000	Pharmacia biotech
Streamline-25 column	Pharmacia biotech
Syringe (50 ml)	Terumo

T-bore (three-way) stopcock	Brand
Three-way stopcock	B. Braun
Three-way valve	Watson-marlow
Tissue culture flask (25 ,75 and 175 cm ²)	Nunc
Tubing clip (Hoffmanntype)	Labsco
Tubing connector (KECK connector)	Duran
Vacuum pump	Millipore
Water bath	Heto
Water jacket incubator / 3121 series	Forma scientific

3.4 Assembly of hollow fiber bioreactor

3.4.1 *The hollow fiber bioreactor with single flow direction*

The hollow fiber bioreactor was operated by medium flow was fed to the cell culture cartridge with single flow direction. The hollow fiber with single flow direction was referred as system A. The assembly and functional parts of this system are presented in Fig. 7A and Table 2 respectively.

3.4.2 *The hollow fiber bioreactor with reverse flow direction*

The hollow fiber bioreactor was operated by periodically alternating the direction of medium flow before feeding into the cell culture cartridge. The hollow fiber with reverse flow direction was assembled in two different systems, which were referred as system B and C. The assembly of system B and C, and their functional parts are presented in Fig. 7B, 7C and Table 2 respectively.

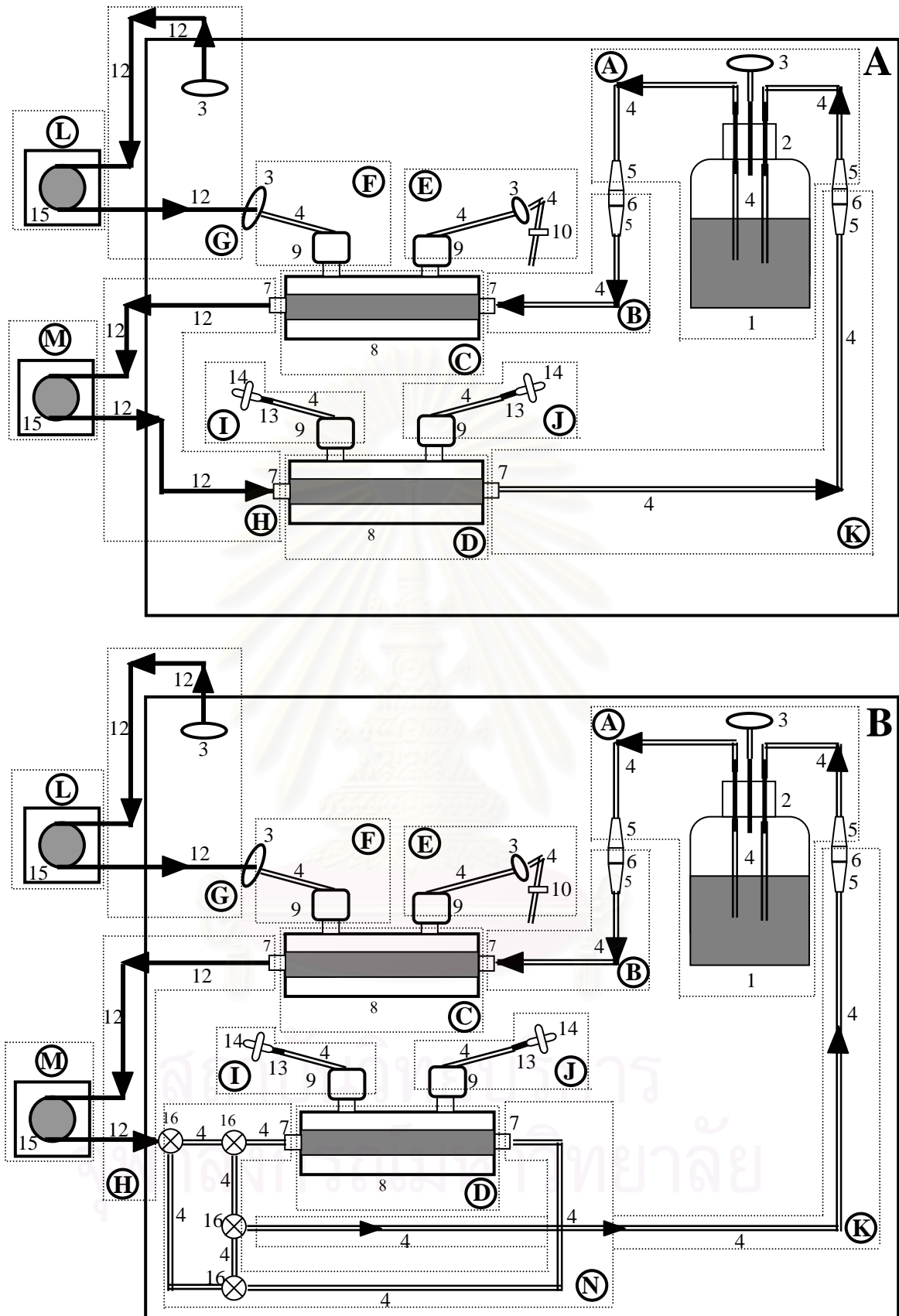


Fig. 7 Schematic diagram of the hollow fiber bioreactor with single flow (A) and reverse flow (B and C) direction (modified from Altshuler et al., 1986; Honda-Corrigan, Nikolay, Jeffery et al., 1992).

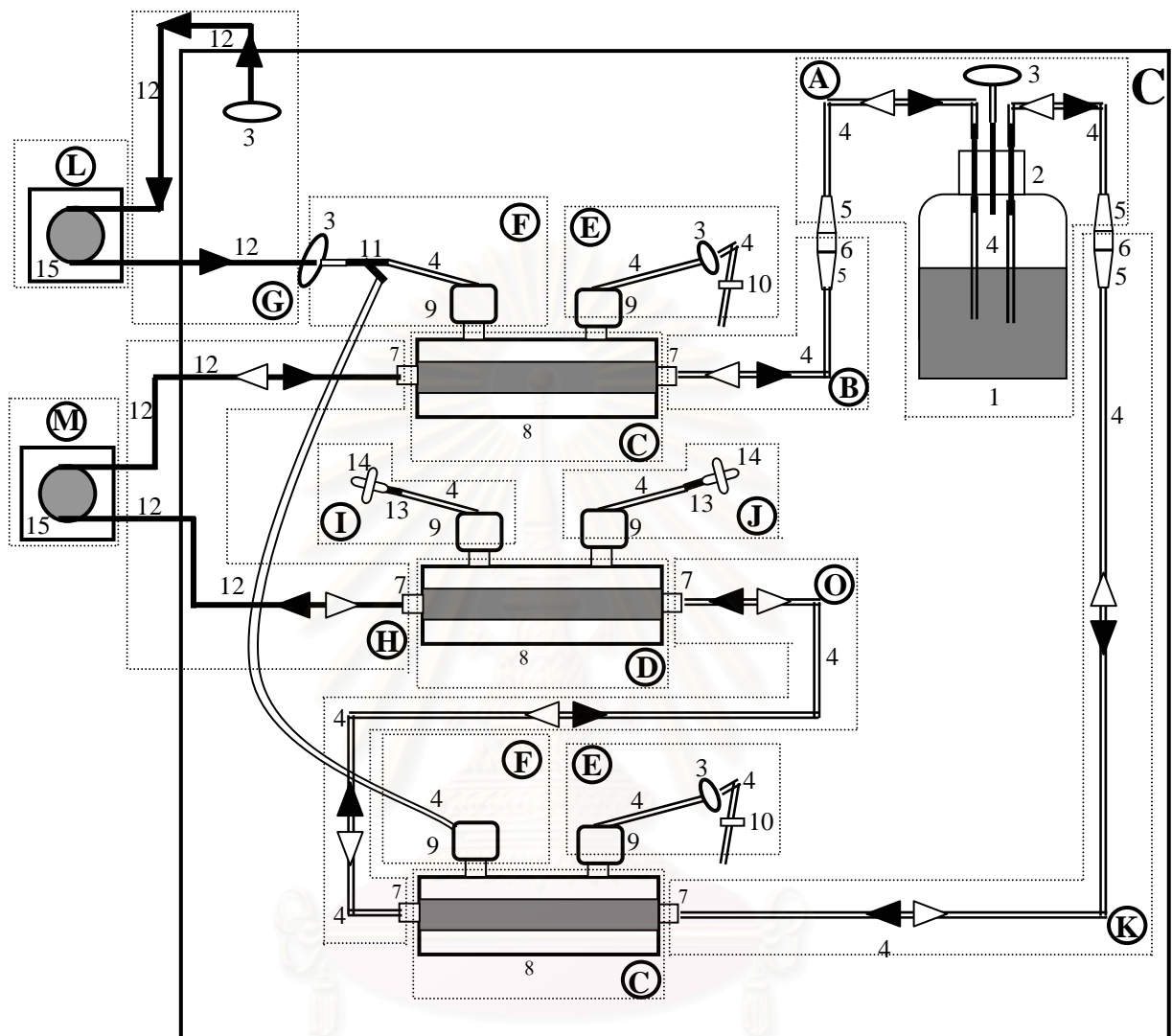


Fig. 7 Schematic diagram of the hollow fiber bioreactor with single flow (A) and reverse flow (B and C) direction (modified from Altshuler et al., 1986; Honda-Corrigan, Nikolay, Jeffery et al., 1992).

Table 2 The functional parts of the hollow fiber bioreactor with single flow and reverse flow direction.

Part	Part Definition	Components	Description
Ⓐ	Medium reservoir	<p>1 = five-litres glass bottle</p> <p>2 = cap with three ports</p> <p>3 = hydrophobic filter</p> <p>4 = silicone tube</p> <p>5 = tubing connector</p>	<p>Five - litres glass bottle equipped with three ports on the top. One of the top port was attached with a hydrophobic 0.2 μm filter for pressure equilibration. The others were used for medium inlet and outlet port respectively. The medium reservoir contained 3 L of basal medium.</p>
Ⓑ	-	<p>4 = silicone tube</p> <p>5 = tubing connector</p> <p>6 = coupling connector</p> <p>7 = connector for the IC space of cartridge</p>	<p>This part was used to convey medium between the medium reservoir and the IC space of gas exchange cartridge.</p>
Ⓒ	Gas exchange cartridge	<p>8 = hollow fiber dialyser</p>	<p>The gas exchange cartridge was used for permeating the gas mixture (5% CO_2 in air) to the circulating medium. The fiber membrane of cartridges is cellulose which has 35 kDa MWCO. The total surface area of fiber is 1.75m^2. The EC volume of cartridge is 120 ml.</p>

Table 2 (continued)

Part	Part definition	Components	Description
Ⓓ	Cell culture Cartridge	8 = hollow fiber dialyser	Cells were cultured in the EC space of cell culture cartridge. The specifications of cell culture cartridge are the same as gas exchange cartridge.
Ⓔ	Upstream EC port of gas exchange cartridge	3 = hydrophobic filter 4 = silicone tube 9 = dialysis connector 10 = tubing clip	This part was used as an outlet port for gas mixture (5% CO ₂ in air).
Ⓕ	Downstream EC port of gas exchange cartridge	3 = hydrophobic filter 4 = silicone tube 9 = dialysis connector 11 = three-way valve (used in system C only)	This part was used as an inlet port for gas mixture (5% CO ₂ in air).
Ⓖ	-	3 = hydrophobic filter 12 = maprene tube	This part was used to convey gas mixture (5% CO ₂ in air) from CO ₂ incubator to the downstream EC port of gas exchange cartridge.
Ⓗ	-	7 = connector for the IC space of cartridge 12 = maprene tube	This part was used to convey medium between the gas exchange cartridge and the IC space of cell culture cartridge.

Table 2 (continued)

Part	Part Definition	Components	Description
Ⓘ	Upstream EC port of cell culture cartridge	4 = silicone tube 9 = dialysis connector 13 = female-female connector 14 = three-way stopcock	This part was used to connect with a syringe in order to inject fresh medium or harvest of product.
Ⓙ	Downstream EC port of cell culture cartridge	4 = silicone tube 9 = dialysis connector 13 = female-female connector 14 = three-way stopcock	This part was used to connect with a syringe in order to inject fresh medium or harvest of product.
Ⓚ	-	4 = silicone tube 5 = tubing connector 6 = coupling connector 7 = connector for the IC space of cartridge	For system A and B, this part was used to convey medium from the cell culture cartridge to the medium reservoir. For system C, this part was used to convey medium between the gas exchange cartridge and the medium reservoir.
Ⓛ	Gas pump	15 = peristaltic pump	This part was used to supply gas mixture (5% CO ₂ in air) to the gas exchange cartridge.

Table 2 (continued)

Part	Part definition	Components	Description
Ⓜ	Medium pump	15 = peristaltic pump	This part was used to circulate medium through the IC space of cartridges.
Ⓝ	-	4 = silicone tube 16 = T-bore (three- way) stopcock 7 = connector for the IC space of cartridge	This part was used to reverse the direction of medium flow before feeding to cell culture cartridge.
Ⓞ		4 = silicone tube 7 = connector for the IC space of cartridge	This part was used to convey medium between the cell culture cartridge and the gas exchange cartridge

As shown in Fig. 7B, the four T-bore (three way) stopcocks (Part Ⓝ) were additionally connected to system B in order to reverse the direction of medium flow before feeding to cell culture cartridge. To reverse the direction between clockwise and anticlockwise, all four stopcocks must be rotated to the positions as shown in Fig. 8a and 8b respectively. On the other hand, Part Ⓢ, Ⓣ, Ⓤ and Ⓞ were additionally connected to system C (Fig. 7C) in order to reverse the direction of medium flow between clockwise and anticlockwise as shown in Fig. 9a and 9b respectively.

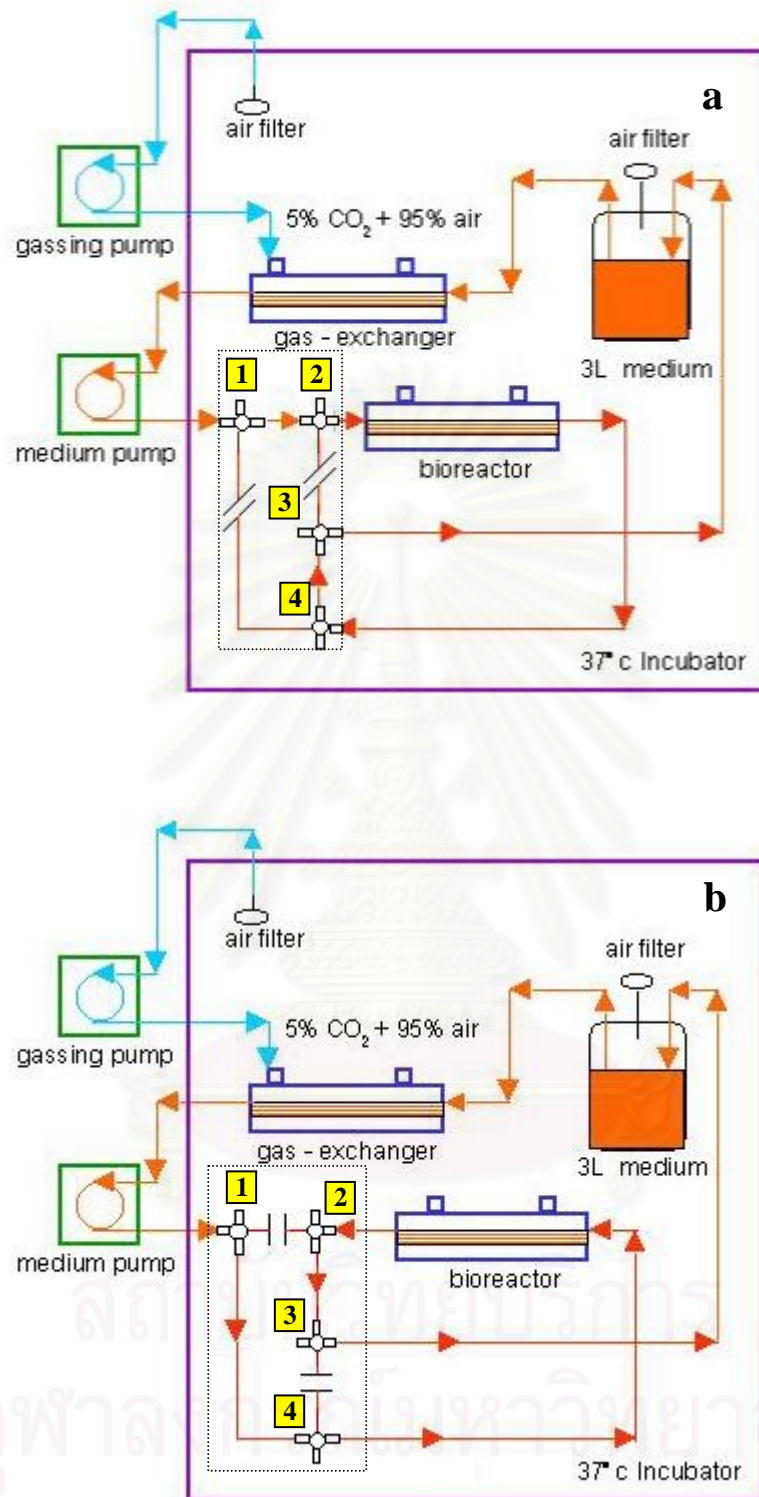


Fig. 8 Four T-bore stopcocks rotated for clockwise (a) and anticlockwise (b) direction (modified from Altshuler et al., 1986; Honda-Corrigan, Nikolay, Jeffery et al., 1992).

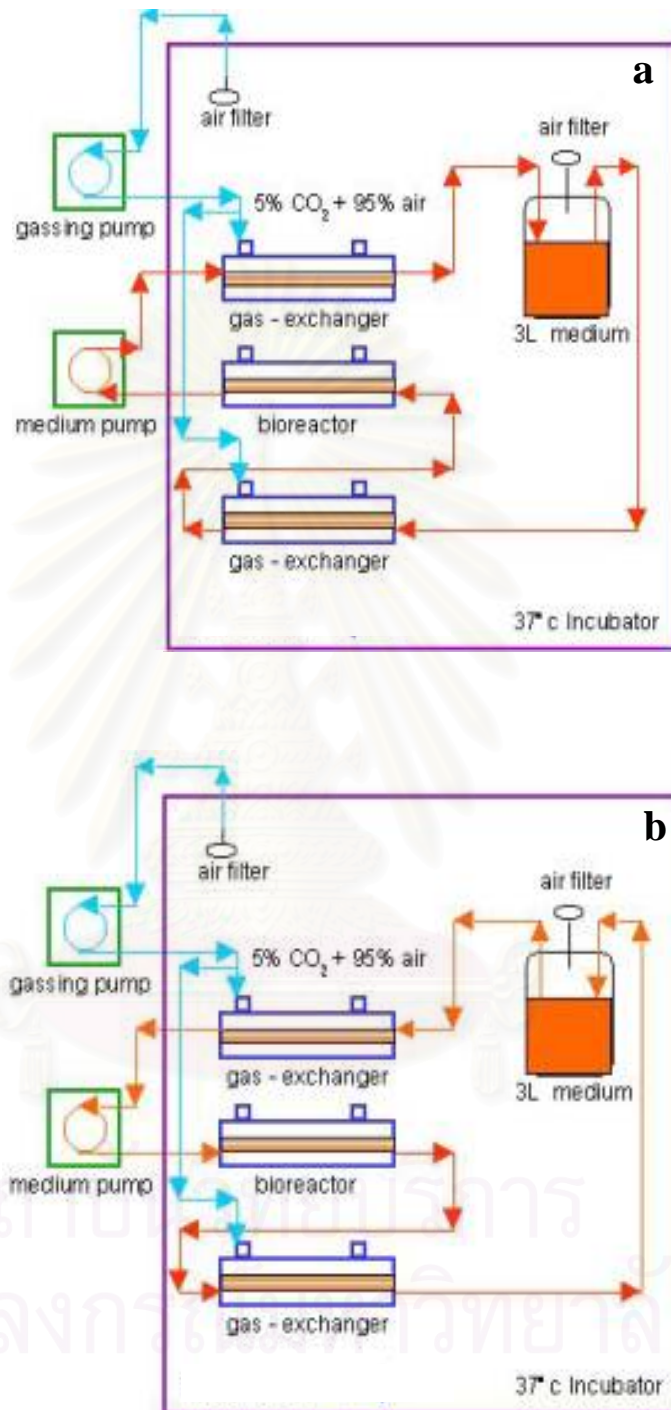


Fig. 9 The medium flow direction of system C turned clockwise (a) and anticlockwise (b) direction (modified from Altshuler et al., 1986; Honda-Corrigan, Nikolay, Jeffery et al., 1992).

The hollow fiber cartridges and lockable three way valves were supplied in sterilized condition. The other components were steam-sterilized before assembling inside a laminar flow cabinet. Afterward, the EC space of cell culture cartridge was filled with 100 ml of 5% serum-supplemented medium by injecting through the upstream EC ports. Then, the entire system was placed inside the CO₂ incubator that maintained at 37 °C with 5% CO₂ in air. Finally, the maprene tube of medium pump and gas pump were locked into the position of the pump.

3.5 Pre-incubation of the hollow fiber bioreactor

Prior inoculation, the IC space of both cartridges was filled by pumping basal medium from the medium reservoir at the maximum pump rate of 999 ml/min. Once filled, the system was equilibrated with the medium circulation rate at 100 ml/min while the gas mixture was also pumped into the system at flow rate of 50 ml/min. After a period of 3-days, the system was placed inside a laminar flow cabinet. The new medium reservoir was replaced and the EC space of cell culture cartridge was also filled with 5% serum-supplemented medium by injecting 100 ml of the medium through the upstream EC port, resulting in a collection of the replaced medium by a syringe at the downstream EC port. The system was then placed back inside the CO₂ incubator and equilibrated again for another 3 days under the same conditions.

3.6 Cell inoculation

Stock of hybridoma cells were previously stored in a solution composed of 95% FBS and 5% DMSO, and maintained frozen in liquid nitrogen. Cells were then thawed and grown in 5% serum-supplemented medium and then were expanded in 175 cm² tissue culture flasks for a total cell viability of 10⁸ cells prior to inoculating into the system. The cell suspension was aliquoted in 4x175 ml sterilized conical centrifuge tubes and centrifuged for 4 minutes at the speed of 1,250 rpm. The supernatant was decanted and the cell pellets were pooled into 50 ml supernatant. The system was then placed inside a laminar flow cabinet. The new medium reservoir was replaced, then 50 ml of cell suspension was pushed to the upstream EC port of cell culture cartridge with a syringe. With this action, the second syringe was connected to the downstream EC port to collect the replaced medium. Finally, the system was placed back inside the CO₂ incubator under the previous conditions.

3.7 Optimization procedures and control strategy

3.7.1 The hollow fiber bioreactor with single flow direction

Hybridoma cells were cultured by the hollow fiber bioreactor with single flow direction. The system was assembled and operated as described in section 3.4.1, 3.5 and 3.6. After inoculation, the system was then operated under the following conditions.

- A 5-day batch culture was operated, then followed by replacing medium reservoir and EC medium of the cell culture cartridge on every 3 days throughout the culture period.
- The medium circulation rate was initially set 100 ml/min and then increased 150 ml/min and 200 ml/min respectively on every nine days. Then, the rate was maintained at 250 ml/min through the rest of culture period.
- The gas mixture of 5% CO₂ in air was pumped into the system at constant flow rate of 50 ml/min.
- Cells were cultured in 5% serum-supplemented medium throughout the culture period.
- The EC ports of cell culture cartridge were positioned at angle of 90° from the vertical position and turned interchangeably between 90° clockwise direction and 90° anticlockwise direction every time after harvest throughout the culture period.

The operation under the above conditions was classified and designated as operational mode 1. The hollow fiber bioreactor with operational mode 1 were done duplicate, which were referred as bioreactor 1 and 2.

3.7.2 The hollow fiber bioreactor with reverse flow direction

Hybridoma cells were cultured by the hollow fiber bioreactor with reverse flow direction. The experiments were set up in two different reverse timing modes: 1) reverse every 24 and then 12 hours as designated as mode 2 2) reverse every 12 hours from the beginning of operation as designated as mode 3.

All reverse flow operations were assembled and operated as described in section 3.4.2, 3.5 and 3.6. The gas mixture of 5%CO₂ in air was pumped into the system at constant flow rate of 50 ml/min. After inoculation, a 5-day batch with one

direction of medium flow was operated. Then, the bioreactor systems were operated under the following conditions.

3.7.2.1 The hollow fiber bioreactor with operational mode 2

The hollow fiber bioreactor with operational mode 2 were done duplicate, which were referred as bioreactor 1 and 2.

- The medium flow direction was periodically reversed every 24 hrs during the increasing state of MAb-TSH production, and then reversed every 12 hrs during the steady state of MAb-TSH production.
- Cells were cultured in 5% serum-supplemented medium throughout the culture period.
- Before entering the steady state of MAb-TSH production, the EC ports of cell culture cartridge were positioned at angle of 90° from the vertical position and turned interchangeably between 90° clockwise direction and 90° anticlockwise direction every time after harvest.
- During the steady state of MAb-TSH production, the position of EC ports after harvest were changed every 10 days to the vertical position, to angle of 90° from the vertical position, and to angle of 135° from the vertical position in order to investigate the impact of gravity sedimentation on the concentration of MAb-TSH produced. The position of EC ports during the steady state of MAb-TSH production is shown in Fig. 10.
- The results of metabolite products in experiment 3.7.1 were used as a tool for monitoring the medium circulation rate, the replacement of medium reservoir, and the replacement of EC medium.

3.7.2.2 The hollow fiber bioreactor with operational mode 3

The hollow fiber bioreactor with operational mode 3 were done duplicate by gradually reducing the amount of FBS, which were referred as bioreactor 2, and 3. In addition, another bioreactor was set up with 5% FBS as a control system, which were referred as bioreactor 1.

- The medium flow direction was periodically reversed every 12 hrs throughout the culture period.

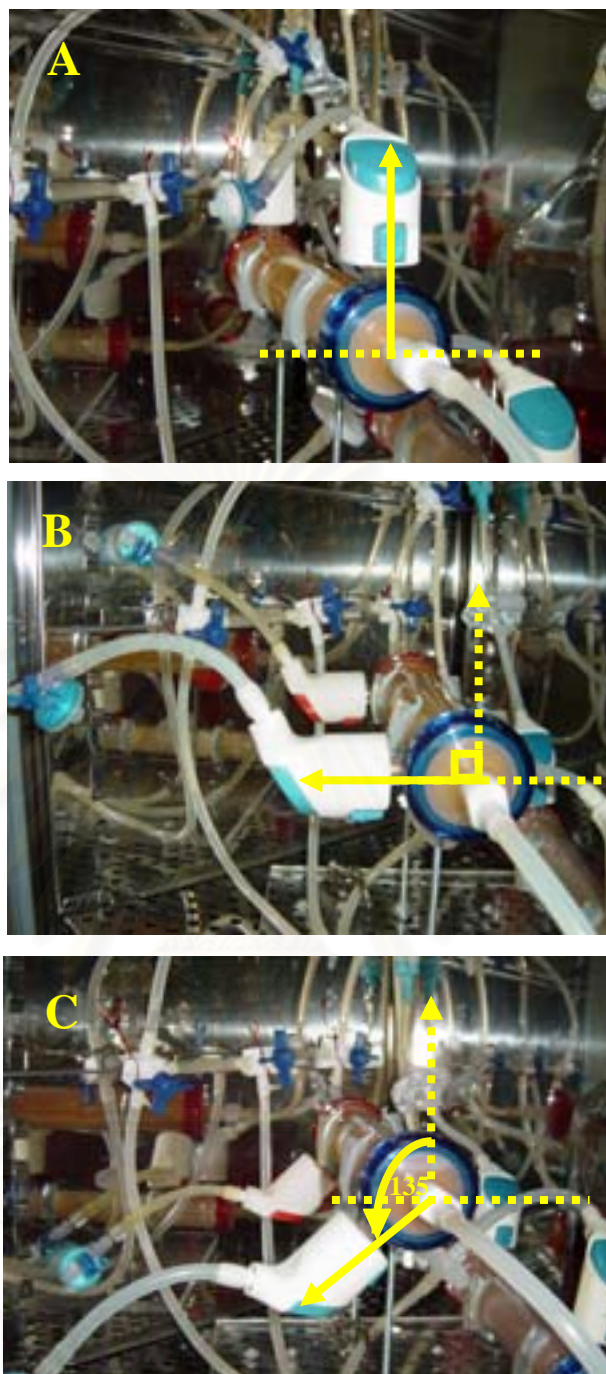


Fig. 10 The position of EC ports during the steady state of MAb-TSH production.

- (A) The vertical position
- (B) Angle of 90° from the vertical position
- (C) Angle of 135° from the vertical position

- For the bioreactor 1, cells were cultured in 5% serum supplement-medium throughout the culture period. Whereas bioreactor 2 and 3, cells were cultured by reducing the amount of FBS in basal medium from 5% to 2.5% at the beginning of the steady state of MAb-TSH production, and then reduced from 2.5% to 1% and 0% (vol/vol) respectively on every 10 days.
- The results of metabolite products in experiment 3.7.2.1 were used as a tool for monitoring the medium circulation rate, the position of EC ports, the replacement of medium reservoir, and the replacement of EC medium.

During the cultivation of experiment 3.7.1, 3.7.2.1 and 3.7.2.2, EC medium of the cell culture cartridge was replaced by connecting an empty syringe to one of the two EC ports. Then, the second syringe containing with 50 ml of 5% serum-supplemented medium was connected to the other. The injection of 5% serum-supplemented medium into the EC space of cell culture cartridge resulted in harvesting of cells and metabolite products. The injection must be done on the opposite port of the previous replacement. Additionally, before positioning the EC ports of cell culture cartridge as described in section 3.7.1, 3.7.2.1 and 3.7.2.2, the cell culture cartridge was turned backwards and forwards until cells were evenly distributed throughout the cartridge.

Samples from EC harvesting were monitored by cell numbers and cell viability as described in section 3.9.1. The remainders were centrifuged for 15 minutes at 3,000 rpm and the supernatant were kept frozen for determination of MAb-TSH concentration and purification process. Samples from IC medium were also monitored by determining the amount of glucose, lactate, ammonia, and concentration of MAb-TSH. The procedures were carried out as described in section 3.9 and 3.10. The consumption rate of glucose, the production rate of lactate and ammonia, and MAb-TSH concentration were calculated as described in Appendix B (Nayak and Herman, 1997). The results of metabolite products were then used as factors for changing the operation conditions of the operational mode 2 and 3 (Handa-Corrigan, Nikolay, Fletcher et al., 1995; Handa-Corrigan, Nikolay, Jeffery et al., 1992).

- The medium reservoir and EC medium must be replaced when one of the following conditions occurred: glucose concentration fell below 150 mg/dl, or lactate and ammonia concentration were above 150 mg/dl and 2.5 mM respectively.
- The medium circulation rate must be increased when both lactate concentration was higher than 150 mg/dl and ammonia concentration was higher than 2.5 mM.

3.8 Statistical analysis

All statistical analyses were performed using SPSS program. The analysis of variance for the completely randomized design was used to compare two types of experiments: experiment of EC ports positioning and experiment of reducing serum concentration in basal medium.

Experiment of EC ports positioning consisted of three treatments, which included positioning at the vertical position, at angle of 90° from the vertical position and at angle of 135° from the vertical position. Experiment of reducing serum concentration in basal medium consisted of four treatments, which included the culture in 5%, 2.5%, 1% and 0% serum concentration.

The evaluation of all experimental treatments was done by the determination of the amount of MAb-TSH in the EC harvesting medium. Statistic analysis was determined using a two-tail F test at p value < 0.05. A p value < 0.05 was considered significant. Least significant different (LSD) was used to identify significant difference between treatments.

3.9 Analytical methods

3.9.1 Cell numbers and cell viability determination

Cell numbers were determined using haemocytometer while cell viability was determined by using trypan blue dye exclusion. Cell suspension was diluted by basal medium. The dilution ratio is depended on the density of cell suspension. After diluted, mixed 20 µl of cell suspension with 20 µl of trypan blue solution, and then applied the solution to the counting area of the haemocytometer at the edge of cover slip. The cells in each of the four large corner squares were counted

for numbers of viable cells and dead cells. It was noticed that the viable cells were bright whereas the dead cells were blue and opaque.

3.9.2 Glucose determination

Glucose was determined by using commercial available kit. The reaction of glucose oxidase, a process of converting glucose to gluconic acid and hydrogen peroxide (H_2O_2). In the presence of H_2O_2 and o-dianisidine, peroxidase catalyzed the oxidative condensation of o-dianisidine to brown color. The intensity of the brown color measured at 450 nm was proportional to glucose concentration.

The glucose standard (100mg/dl) and samples were diluted twentyfold with distilled water. Then, 500 μ l of diluted glucose standard, diluted samples and distilled water were pipetted into standard tubes, sample tubes and blank tube respectively. Each tube was then added with 5 ml of enzyme-color reagent solution, incubated at room temperature for 45 minutes, and measured absorbance at 450 nm. In case of glucose concentration in samples exceeded 300 mg/dl, samples were diluted fourtyfold with distilled water and reassay.

3.9.3 Lactate determination

Lactate concentration was determined by using commercial available kit. The reaction of lactate oxidase, a process of converting lactate to pyruvate and hydrogen peroxide (H_2O_2). In the presence of H_2O_2 and chromogen precursor, peroxidase catalyzed the oxidative condensation of chromogen precursor to dark-blue color. The increase intensity of the dark-blue color measured at 540 nm was proportional to lactate concentration.

10 μ l of lactate standard (40 mg/dl), lactate control and samples were pipetted into standard tubes, control tubes and sample tubes respectively. Each tube was then added with 1 ml of lactate solution, incubated at room temperature for 10 minutes, and measured absorbance at 540 nm using lactate solution as blank. In case of lactate concentration in samples exceeded 120 mg/dl, samples were diluted twofold with distilled water and reassay.

3.9.4 Ammonia determination

Ammonia concentration was determined by using commercial available kit. The reaction was based on reductive amination of 2-oxoglutarate, using

glutamate dehydrogenase and reduced nicotinamide adenine dinucleotide phosphate (NADPH). The decrease in absorbance at 340 nm was due to the oxidation of NADPH to NADP which was proportional to the ammonia concentration.

100 μ l of distilled water, ammonia control, and samples were pipetted into blank cuvetts, control cuvetts and sample cuvetts respectively. Each cuvet was then added with 1 ml of ammonia solution, incubated at room temperature for 3 minutes, and measured absorbance at 340 nm. Then, added 10 μ l of glutamate dehydrogenase solution to each cuvet, mixed and incubated further for 5 minutes before measuring absorbance again at 340 nm. In case of ammonia concentration in samples exceeded 15 μ g/dl, samples were diluted twofold with distilled water and reassay.

3.9.5 Monoclonal antibody determination

3.9.5.1 Absorption of ultraviolet light

MAB-TSH concentration was determined by measuring protein concentration at 280 nm (Johnstone and Thorpe, 1987). When the obtained value was greater than 1.5, the sample was diluted in 0.15 M phosphate buffer saline, pH 7.2 until the reading fell between 0.4 and 1.5. The concentration of protein is then calculated by using $E^{1\%}_{280}$ as described in Appendix B. The extinction coefficient ($E^{1\%}_{280}$) was 13.6.

3.9.5.2 Enzyme linked immunosorbent assay (ELISA)

Assays were developed using technique described by Catty and Raykundalia (1989). 96-well micortiter plates were coated overnight with Goat anti-mouse immunoglobulins using 5 μ g/ml in 0.05 M carbonate buffer, pH 9.6 and 100 μ l per well. The plates were then washed 3 times with PBS buffer (0.1% Tween 80 in 0.15 M PBS, pH 7.4) and blocked with 3% BSA in PBS for 1 hr at 37°C. Then, follow by washing another three times with PBS buffer, and one time with 1% sucrose. Finally, all plates were dried for 3 hrs by vacuum at -50 °C before storing at 4°C.

A standard curve for determination of the amount of MAB-TSH were prepared by serial dilution of purified MAB-TSH from 1000 ng/ml to 500, 250, 125, 63, 31, 16, 8, 4, 2 ng/ml respectively. A standard curve was plotted between the absorbance at 450 nm and corresponding MAB-TSH concentrations as

shown in Appendix C. 100 μ l of samples and standards were pipetted to the plates and incubated at 37°C for 1 hr. The plates were then washed three times with saline buffer (0.05% Tween 20 in 0.9% NaCl). 100 μ l of 1:25000 dilution of peroxidase conjugated rabbit anti-mouse immunoglobulins was added, incubated at 37°C for 1 hr. After the final wash, 100 μ l of TMB solution in substrate buffer was added and the reaction mixtures were incubated at room temperature to develop the color for 20 minutes. 25 μ l of 2N H₂SO₄ was added to stop the reaction and the absorbance was measured at 450 nm.

The calculation of cell numbers, cell viability, GCR, LPR, APR and the concentration of glucose, lactate, ammonia and MAb-TSH were shown in Appendix B.

3.10 Monoclonal antibody purification

3.10.1 Protein A Sepharose affinity chromatography

Protein A Sepharose 4 fast flow was used for purification of MAb-TSH from the supernatant of cells cultured in mode 3 of three bioreactors that had been harvested every 2 weeks during the cultivation period. The column was equilibrated with 20 mM sodium phosphate buffer, pH 7.4. The supernatant was adjusted to pH 7.4 by adding 0.5M phosphate buffer, pH 7.4 and applied to the column. The column was washed with 20 mM sodium phosphate buffer, pH 7.4 until the absorbance at 280 nm was less than 0.02. MAb-TSH was then eluted from the column by 0.1 M citrate buffer, pH 4. The MAb-TSH-containing fractions which were detected by measuring at 280 nm were pooled and then dialyzed against 0.15 M phosphate buffer saline, pH 7.2. After dialysis, MAb-TSH concentration was determined as described in section 3.9.5.1.

3.10.2 Expanded - bed rProtein A affinity chromatography

MAb-TSH was purified from the whole culture supernatant by streamline 25 column containing 90 ml of rProtein A adsorbent. The column was operated by connecting to an automated liquid chromatography system (AKTA explorer). Prior to applying the sample, rProtein A adsorbent was expanded and equilibrated with 20 mM phosphate buffer, pH 7.4. The flow direction during expansion and equilibration was performed upward with the flow rate of 25 ml/min.

The culture supernatant was adjusted to pH 7.4 by adding 0.5 M phosphate buffer, pH 7.4 and then applied to the expanded-bed with the same upward flow direction. Residual cells, cell debris and other contaminants were washed out from the expanded-bed with 20 mM phosphate buffer, pH 7.4 while MAb-TSH was bounded to the absorbent. After the signal from UV monitor returned to baseline, the upward flow was stopped and the bed was allowed to settle. MAb-TSH was eluted with 0.1 M citrate buffer, pH 4. The flow direction was run downward at the flow rate of 10 ml/min. MAb-TSH-containing fractions which indicated by measuring at 280 nm were pooled and then dialysed against 0.15 M phosphate buffer saline, pH 7.2. After dialysis, MAb-TSH concentration was determined as described in section 3.9.5.1.

3.11 Denaturing polyacrylamide gel electrophoresis (SDS - PAGE)

MAb-TSH from each purification was analyzed by denaturing gel electrophoresis on a slab gel system according to the modified method described by Laemmli (1970). The slab gel system consisted of a stacking gel of 3%(W/V) acrylamide and separating gel with 10% (W/V) acrylamide. The preparation of both stacking and separating gel was described in Appendix A.

Samples at concentration 5 $\mu\text{g}/\mu\text{l}$ were mixed with 1:1 ratio of sample buffer containing 4% (w/v) SDS, 10%(v/v) glycerol, 10% (v/v) 2-mercaptoethanol, and small amount of bromophenol blue in 125 mM Tris-HCl, pH 6.8. Then, boiled for 5 minutes, and cooled in ice bath before loading 10 μl of samples into the gel. Electrophoresis was performed with 0.1% SDS in 25mM Tris-glycine, pH 8.3 as electrode buffer at constant voltage of 100 V. When the dye marker moved to approximately 1 cm above the bottom edge of the gel, the run was stopped. The gel was removed and stained for protein with 0.1% Brilliant blue R-250 in 50% methanol and 7% acetic acid for 30 minutes at room temperature with moderate shaking. Destaining was performed by immersing the gel overnight in a solution containing 25% methanol and 7% acetic acid. Destainer solution must be changed frequently until the background of the gel was clear and only blue-colored protein bands were observed.

Protein molecular weight markers containing Myosin (203 kDa), β - galactosidase (120 kDa), Bovine serum albumin (90 kDa), Ovalbumin (51.7 kDa), Carbonic anhydrase (34.1 kDa), Soybean trypsin inhibitor (28 kDa), Lysozyme

(20kDa) and Aprotinin (6.4 kDa) was also subjected to electrophoresis under the same conditions as sample proteins. The molecular weight of sample proteins was known by comparing the relative mobility (R_f) of sample proteins to the protein markers running in each gel. A plot of R_f versus the logarithm of molecular weights of the marker proteins was shown in Appendix D.



สถาบันวิทยบริการ
จุฬาลงกรณ์มหาวิทยาลัย

CHAPTER IV

RESULTS

4.1 Optimization and control strategy

4.1.1 The hollow fiber bioreactor with single flow direction

Two hollow fiber bioreactors with single flow direction were assembled and operated as described in section 3.4.1, 3.5 and 3.6. Approximately, 8×10^8 cells and 7×10^8 cells were inoculated in the bioreactor 1 and 2 respectively. After inoculation, both bioreactors were operated in mode 1 as described in section 3.7.1. The amount of MAb-TSH during the culture period was monitored by measuring the MAb-TSH concentration in the samples of IC medium and EC harvest using ELISA. The results are shown in Fig. 11.

MAb-TSH production of both bioreactors appeared in the saw-tooth profiles (Fig. 11A). Greater amount of MAb-TSH was consistently recovered from the downstream EC port. After inoculation, MAb-TSH production increased exponentially until day 53 in the bioreactor 1 and until day 47 in the bioreactor 2. Then, MAb-TSH production in both bioreactors were entered the steady state of MAb-TSH production. Fig. 11B illustrates the detection of MAb-TSH in the samples of IC medium from both bioreactors. The results demonstrated that the increase of MAbPR in the samples of IC medium was accompanied by the increase of amount of MAb-TSH produced in the samples of EC harvest.

The IC medium pump rates plotted against the concentration of glucose, lactate and ammonia in the samples taken from the IC medium of both bioreactors are shown in Fig. 12. In Fig. 12A, the amount of glucose of both bioreactors reduced continually and reached 62% on day 44. Then, little change was observed until the end of the experiment. In contrast as shown in Fig. 12B, the amount of lactate of both bioreactors had been above 1.5 g/L since day 44 and continued to increase until day 77. The amount of ammonia of both bioreactors shown in Fig. 12C was above 3 mM after 5 days of inoculation, and increased to approximately 4 mM until the end of the experiment.

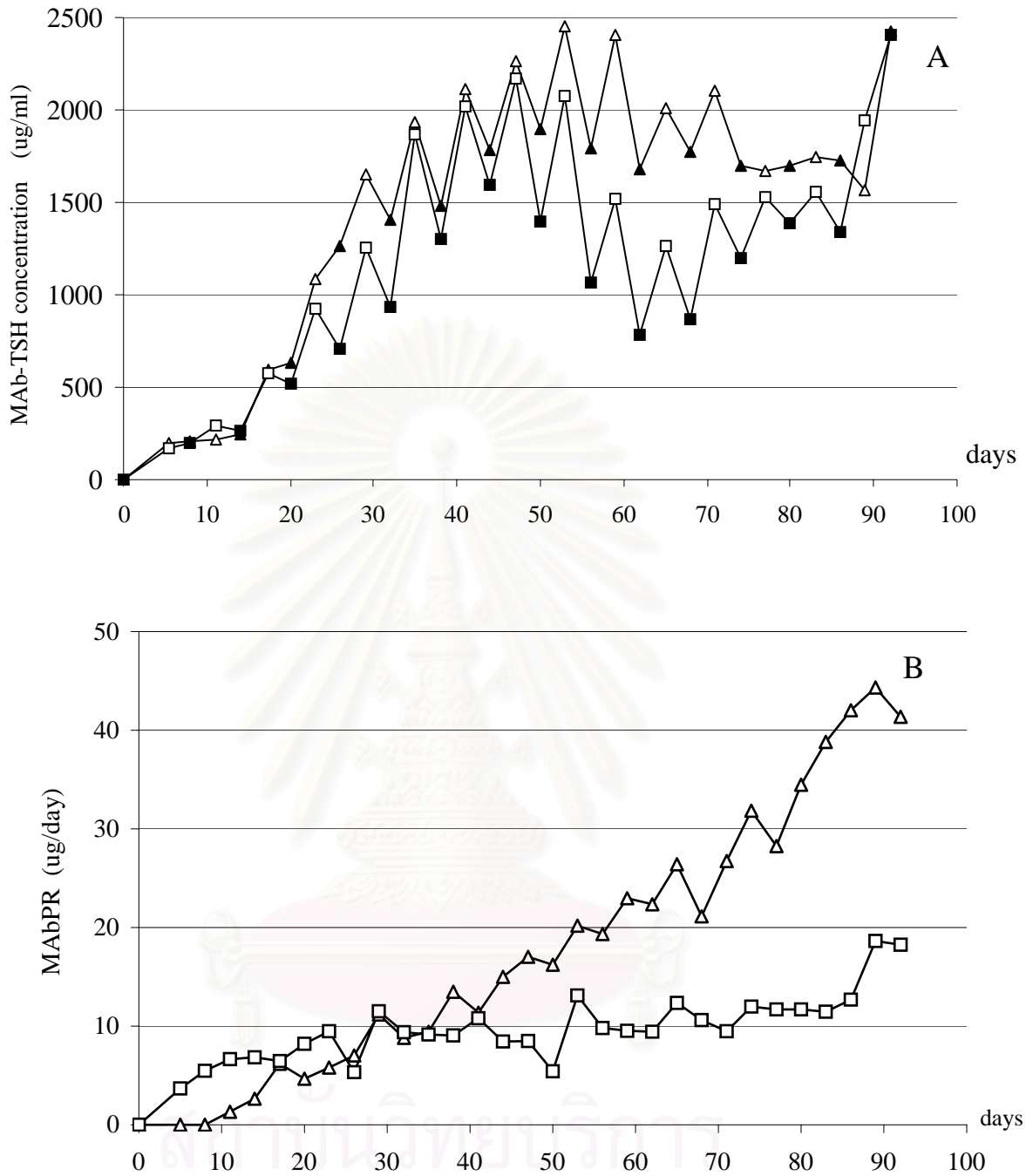


Fig. 11 MAb-TSH production in the hollow fiber bioreactors with single flow direction.

—△— bioreactor 1 —□— bioreactor 2

(A) MAb-TSH concentration in the samples of EC harvest from upstream and downstream port.

opened symbols (Δ , \square) harvested from downstream port

closed symbols (\blacktriangle , \blacksquare) harvested from upstream port

(B) MAb-TSH detection in the samples of IC medium

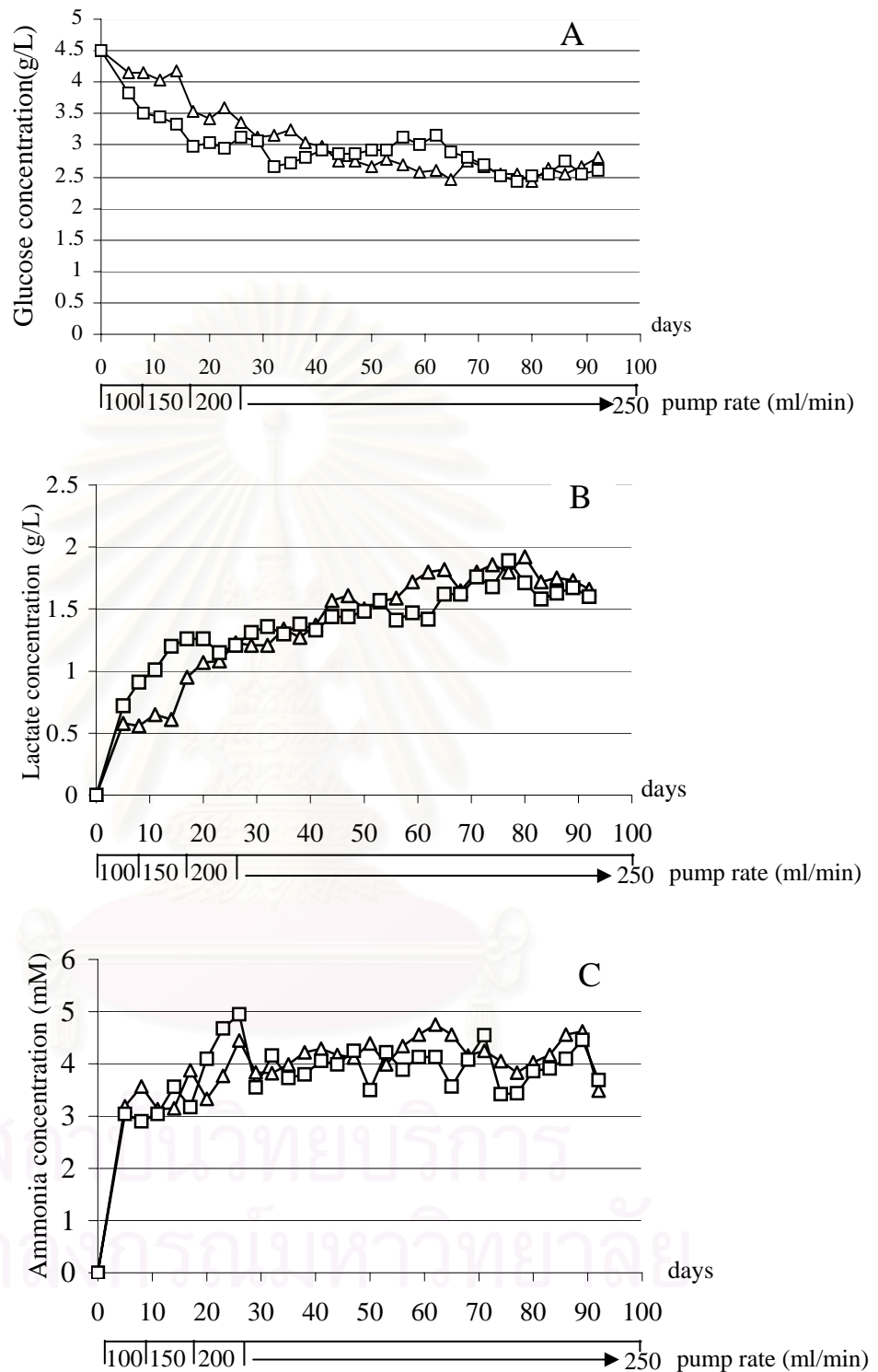


Fig. 12 IC pump rates plotted against the concentration of glucose (A), lactate (B) and ammonia (C) in the samples of IC medium of the hollow fiber bioreactors with single flow direction.

—△— bioreactor 1

—□— bioreactor 2

4.1.2 The hollow fiber bioreactor with reverse flow direction

The hollow fiber bioreactor with reverse flow direction were assembled in system B and C, and then pre-incubated as described in section 3.4.2 and 3.5 respectively. During pre-incubation of system C, the air was trapped in the IC space of system. Subsequently, the IC medium could not circulate through the IC space of cartridges. Although the medium circulation rate was increased 500 ml/min, the trapped air still occurred in the IC space of system. Therefore, the experiments of reverse flow operation was only performed by system B.

4.1.2.1 The hollow fiber bioreactor with operational mode 2

Two hollow fiber bioreactors with reverse flow direction were assembled and operated as described in section 3.4.2, 3.5 and 3.6. Approximately, 6×10^8 cells and 7×10^8 cells were inoculated in the bioreactor 1 and 2 respectively. After inoculation, both bioreactors were operated in mode 2 as described in section 3.7.2 and 3.7.2.1. The flow direction of both bioreactors was reversed every 24 hrs during day 5 to 35 and then reversed every 12 hrs until the last day of culture.

The results of metabolite products in section 4.1.1 illustrated that the amount of glucose was above 1.5g/L throughout the culture period. After day 44 while the medium pump of both bioreactors was set at the maximum flow rate, lactate and ammonia concentrations were above 1.5 g/L and 2.5 mM respectively.

Therefore, to keep the amount of lactate and ammonia lowered than that level, the EC medium and medium reservoir of both bioreactors in this experiment had been replaced every 2 days since day 43. The medium circulation rates were still set as described in section 3.7.1. MAb-TSH production in the hollow fiber bioreactors with reverse flow every 24 and 12 hrs is shown in Fig. 13.

Fig. 13A shows the MAb-TSH concentration in the samples of EC harvest of both bioreactors. After inoculation, MAb-TSH production increased exponentially until day 29 for the bioreactor 1 and until day 32 for the bioreactor 2. Then, MAb-TSH production of both bioreactors was entered the steady state of MAb-TSH production. The saw-tooth profiles of MAb-TSH production were not observed when the flow direction of both bioreactors was reversed every 24 hrs, but appeared when the follow direction was reversed to every 12 hrs. The detection of MAb-TSH in the samples of IC medium of both bioreactors are shown in Fig. 13B.

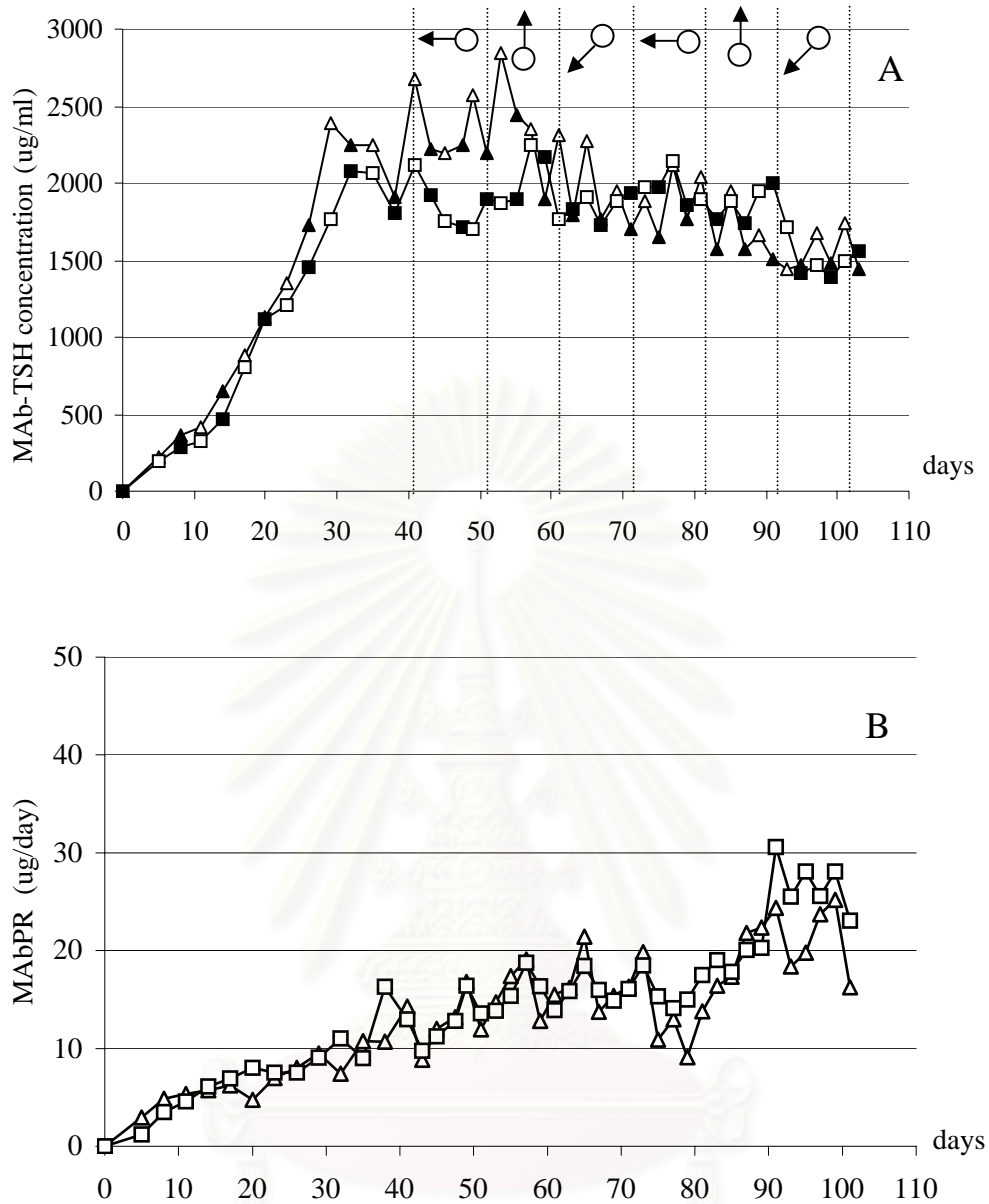


Fig. 13 MAb-TSH production in the hollow fiber bioreactors with reverse flow every 24 and 12 hrs.

—△— bioreactor 1 —□— bioreactor 2

(A) MAb-TSH concentration in the samples of EC harvest from upstream and downstream port.

opened symbols (△, □) harvested from downstream port

closed symbols (▲, ■) harvested from upstream port

position of EC ports ↑ the vertical position

←○ angle of 90° from the vertical position

↙○ angle of 135° from the vertical position

(B) MAb-TSH detection in the samples of IC medium

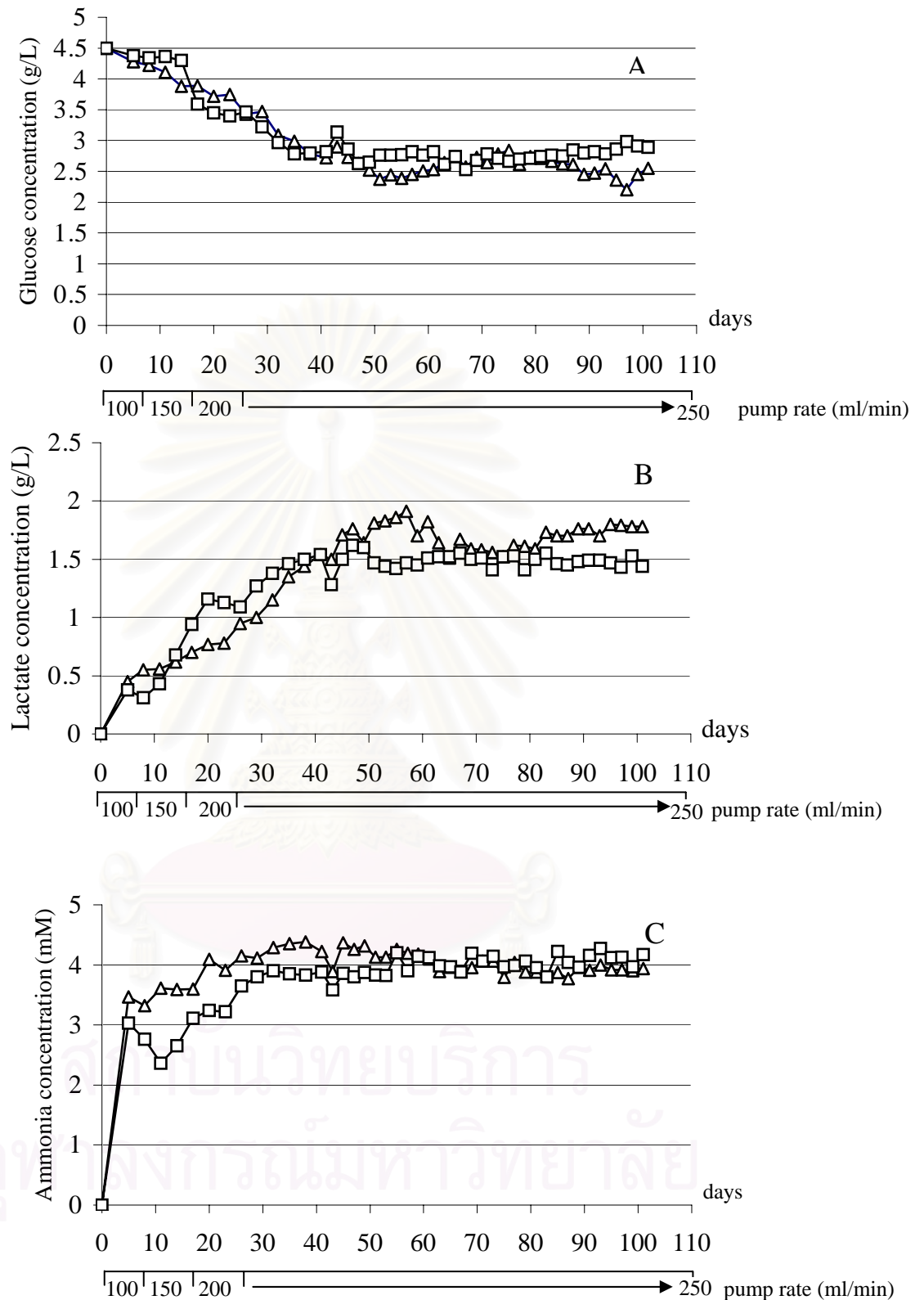


Fig.14 IC pump rates plotted against the concentration of glucose (A),lactate (B) and ammonia (C) in the IC medium of the hollow fiber bioreactors with reverse flow every 24 and 12 hrs.

—△— bioreactor 1

—□— bioreactor 2

It was found that the increase of MAbPR in the samples of IC medium was accompanied by the increase of the amount of MAb-TSH produced in the samples of EC harvest.

The IC pump rates plotted against the concentration of glucose, lactate and ammonia in the samples taken from the IC medium of both bioreactors are shown in Fig. 14. In Fig. 14A, the amount of glucose of both bioreactors was reduced to 58% on day 49 and then little changes were observed until the end of experiment. In contrast as shown in Fig. 14B, the amount of lactate of both bioreactors had been above 1.5 g/L since day 41 and continued to increase until day 57 for the bioreactor 1 and until day 47 for the bioreactor 2. Thereafter, little changes were observed from both bioreactors until the end of the experiments. In Fig. 14C, the amount of ammonia of both bioreactors was above 2.5 mM after 5 days of inoculation and then increased to 4 mM and little changes were observed until the end of the experiments.

The position of EC ports was investigated during day 43 to 101. The experimental treatments consisted of positioning at the vertical position, at angle of 90° from the vertical position and at angle of 135° from the vertical position. The response of three treatments was measured from the MAb-TSH concentration of EC harvesting. The ANOVA table for the position of EC ports is shown in Table 3.

Table 3 ANOVA table for the position of EC ports.

Source	Sum of squares	d _f	Mean squares	F	Sig.
position of EC ports	1060671	2	53033552	7.199	0.002
residual	4198893	57	73665		
total	5259564	59			

The p value for the test of significance for the position of EC ports was 0.002. Thus, it can be concluded that the position of EC ports affected the MAb-TSH concentrations. Table 4 shows the additional analysis of LSD at the 0.05 level.

Table 4 Multiple comparison of the position by LSD.

Position of EC ports (I)	Position of EC ports (J)	Mean difference (I - J)	Sig.
the vertical position	angle of 90° from the vertical position	-15.55	0.857
	angle of 135° from the vertical position	273.95	0.002
angle of 90° from the vertical position	the vertical position	15.55	0.857
	angle of 135° from the vertical position	289.50	0.001
angle of 135° from the vertical position	the vertical position	-273.95	0.002
	angle of 90° from the vertical position	-289.50	0.001

The statistics revealed that there was no significant difference between the position at vertical position and at angle of 90° from the vertical position (p value = 0.857). Conversely, the EC ports positioned at angle of 135° from the vertical position was found significant difference with positioned at vertical position (p value = 0.002) and positioned at angle of 90° from the vertical position (p value = 0.001). The mean difference of EC ports that positioned at angle of 90° from the vertical position was higher than harvested from the others.

4.1.2.2 The hollow fiber bioreactor with operational mode 3

Three hollow fiber bioreactors with reverse flow direction were assembled and operated as described in section 3.4.2, 3.5 and 3.6. Approximately, 4×10^8 cells, 5×10^8 and 6×10^8 cells were inoculated in the bioreactor 1, 2 and 3 respectively. After inoculation, three bioreactors were operated in mode 3 as described in section 3.7.2 and 3.7.2.2. The flow direction of three bioreactors was reversed every 12 hrs throughout the culture period. The EC ports of cell culture cartridge were positioned at angle of 90° from the vertical position and turned interchangeably between 90°clockwise and 90°anticlockwise direction every time after harvest. The medium circulation rates were still set as described in section 3.7.1.

Fig. 15A shows the MAb-TSH concentrations in the samples of EC harvest of three bioreactors. After inoculation, the MAb-TSH production increased exponentially until day 41 for the bioreactor 1 and until day 38 for the

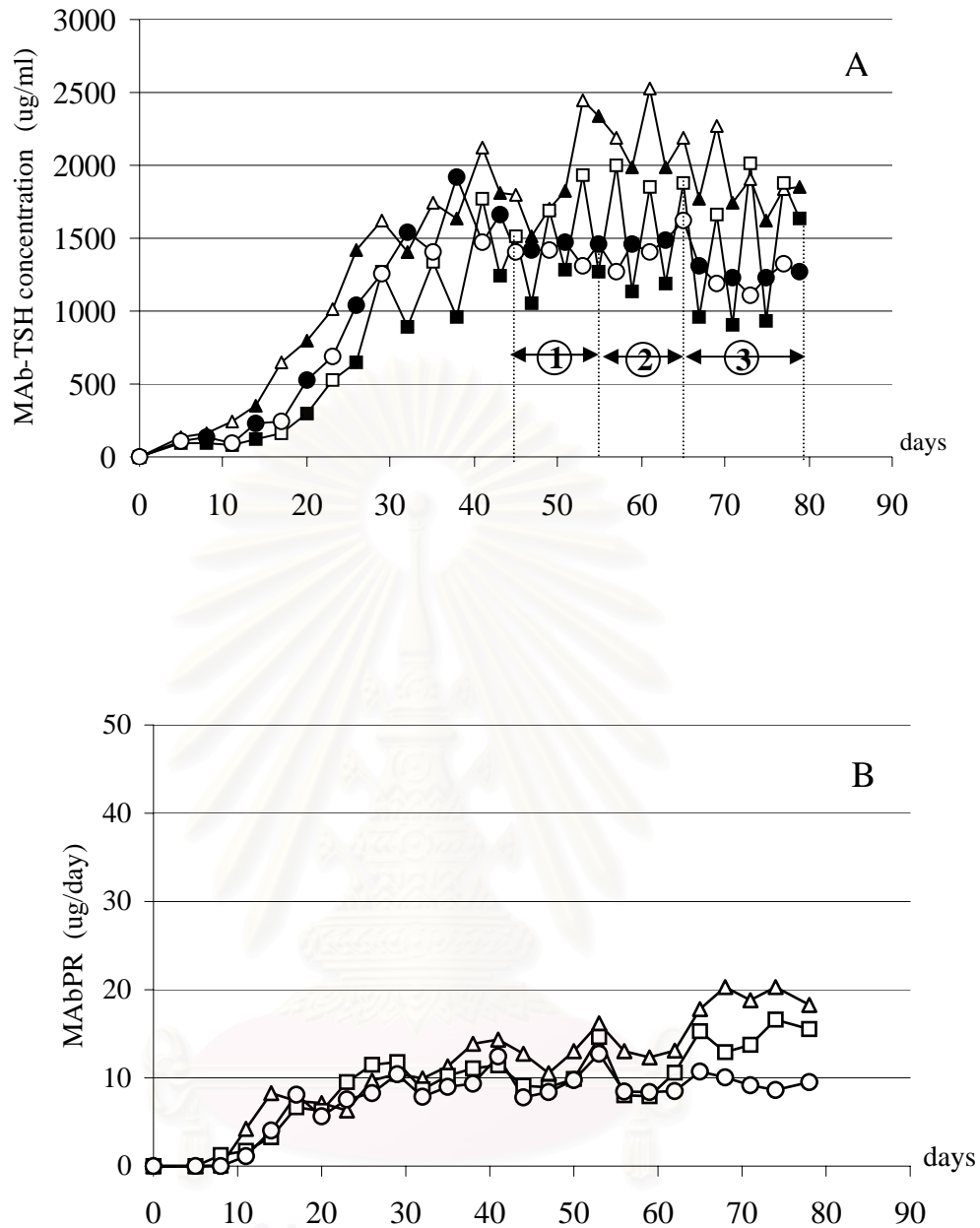


Fig. 15 MAb-TSH production in the hollow fiber bioreactors with reverse flow every 12 hrs.

—△— bioreactor 1 —□— bioreactor 2 —○— bioreactor 3

(A) MAb-TSH concentration in the samples of EC harvest from upstream and downstream port.

opened symbols (△, □, ○) harvested from downstream port

closed symbols (▲, ■, ●) harvested from upstream port

① culture in 2.5% FBS ② culture in 1% FBS ③ culture in 0% FBS

(B) MAb-TSH detection in the samples of IC medium

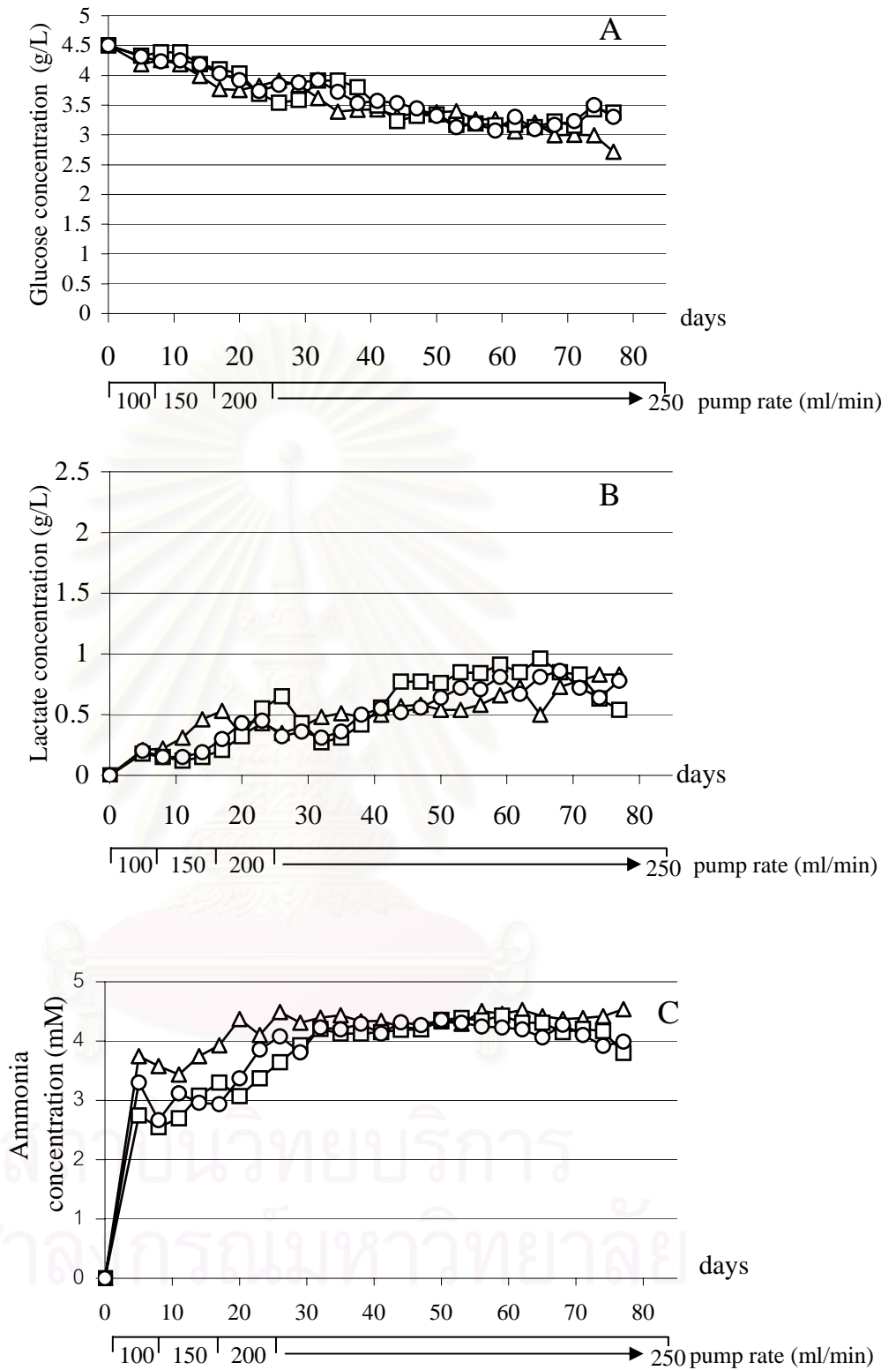


Fig. 16 IC pump rates plotted against the concentration of glucose (A) , lactate (B) and ammonia (C) in the IC medium of the hollow fiber bioreactors with reverse flow every 12 hrs.

—△— bioreactor 1 —□— bioreactor 2 —○— bioreactor 3

bioreactor 2 and 3. Thereafter, MAb-TSH production of three bioreactors entered the steady state. Fig. 15A demonstrated that the amount of MAb-TSH produced from the bioreactor 1 was higher than the others during the culture period. The saw-tooth profiles had been observed from three bioreactors since day 30. The detection of MAb-TSH in the samples of IC medium of three bioreactors is shown in Fig. 15B. It was noticed that the increase of MAbPR in the samples of IC medium was accompanied by the increase of MAb-TSH produced in the samples of EC harvest.

The IC pump rates plotted against the concentrations of glucose, lactate and ammonia in the samples taken from the IC medium of three bioreactors are shown in Fig. 16. In Fig. 16A, the amount of glucose of three bioreactors was reduced to 60% until the last day of culture. In contrast as shown in Fig. 16B, the amount of lactate of three bioreactors increased to a maximum value of 1.0 g/L. In Fig. 16C, the amount of ammonia of three bioreactors was above 2.5 mM after 5 days of inoculation and then increased to 4 mM and remained there until the end of the experiment.

The reduction of serum concentration was investigated in the bioreactor 2 and 3 during day 45 to 77. The experiment treatments consisted of the culture in 5%, 2.5%, 1% and 0% serum concentration respectively. The response of all experiments was measured from the MAb-TSH concentration of EC harvesting. The ANOVA table for the reduction of serum concentration is shown in Table 5.

Table 5 ANOVA table for the reduction of serum concentration in basal medium.

Source	Sum of squares	d _f	Mean squares	F	Sig.
serum concentration	4153902	3	1384634	11.879	0.000
residual	5828318	50	116566		
total	9982220	53			

The p value for the test of significance for the reduction of serum concentration in basal medium was 0.000. Therefore, it could be concluded that the reduction of serum concentration in basal medium affected the MAb-TSH concentrations. Table 6 showed the additional analysis of LSD at the 0.05 level.

Table 6 Multiple comparisons of the reduction of serum concentration by LSD.

Serum concentration (I)	Serum concentration (J)	Mean difference (I – J)	Sig.
0% FBS	1% FBS	-129	0.352
	2.5% FBS	-131	0.345
	5% FBS	-650	0.000
1% FBS	0% FBS	129	0.352
	2.5% FBS	-1.80	0.991
	5% FBS	-521	0.000
2.5% FBS	0% FBS	131	0.345
	1% FBS	1.80	0.991
	5% FBS	-519	0.000
5% FBS	0% FBS	650	0.000
	1% FBS	521	0.000
	2.5% FBS	519	0.000

The statistics revealed that the culture in 5% FBS was found significant differences with the culture in 0%, 1% and 2.5% FBS (p value = 0.000). Conversely, there were no significant differences between the culture in 0% and 1% FBS (p value = 0.352), between the culture in 0% and 2.5% FBS (p value = 0.345), and between the culture in 1% and 2.5% FBS (p value = 0.991). The mean difference of the culture in 5% FBS was higher than the cultures under serum reduction.

4.2 Comparative characterization of cells cultivation in different operational modes of the hollow fiber bioreactors

4.2.1 The metabolic activities

The metabolic activities of the duplicate runs in each operational mode as measured by GCR, LPR and APR were presented in Fig. 17. During the first 41 days, GCR (Fig. 17A) of the operational mode 1 and 2 increased to 1.71 g/day.

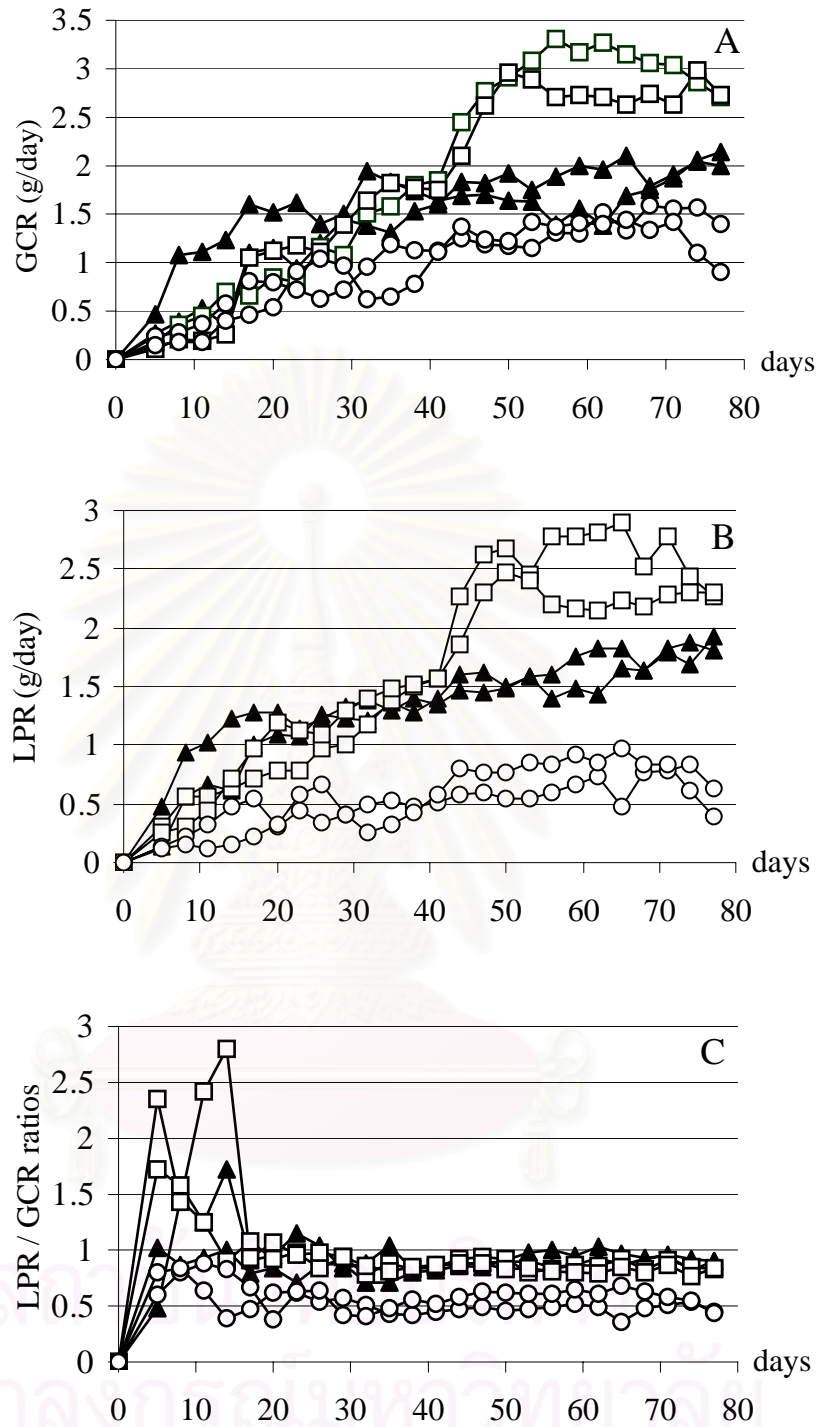


Fig. 17 Comparison of the GCR (A) ,LPR (B) , LPR/GCR ratios (C) and APR (D) of cells cultivation in different operational modes of the hollow fiber bioreactors.

▲ mode 1 ◻ mode 2 ◯ mode 3

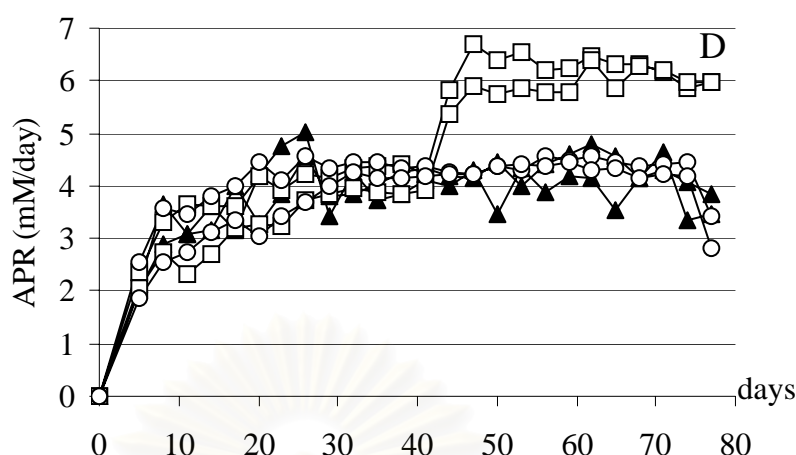


Fig. 17 Comparison of the GCR (A), LPR (B), LPR/GCR ratios (C) and APR (D) of cells cultivation in different operational modes of the hollow fiber bioreactors.

▲ mode 1 ◻ mode 2 ◯ mode 3

Thereafter, GCR of the operational mode 1 slowly increased to 2 g/day. Meanwhile, when the medium reservoir of the operational mode 2 was replaced every 2 days and the flow direction was reversed every 12 hrs, the GCR of operational mode 2 increased rapidly to 3 g/day on day 50 before approaching a steady state. Similarly, GCR of the operational mode 3 was identical to the operational mode 2 during the first 23 days and then slightly increased to a maximum value of 1.5 g/day. It was found that after day 23, GCR of the operational mode 3 was lower than the others.

LPR (Fig. 17B) of the three operational modes had the same profiles as GCR. During the first 41 days, LPR of the operational mode 1 and 2 increased to average value of 1.46 g/day. Thereafter, LPR of the operational mode 1 slowly increased to 2 g/day. Meanwhile, when the medium reservoir of the operational mode 2 was replaced every 2 days and the flow direction was reversed every 12 hrs, LPR was increased rapidly to 2.5 g/day on day 50 before approaching a steady state. Conversely, after 5 days of the batch culture, LPR of the operational mode 3 was lower than the LPR of the other operations. LPR of the operational mode 3 increased

very slowly and never exceeded its maximum value of 1 g/day during the culture period.

Data on LPR/GCR ratios for three operational modes are presented in Fig 17C. During the first 14 days, fluctuating profiles were observed for the operational mode 1 and 2. Then, the LPR/GCR ratios of both operational modes had an average value of 0.89 and remained there until the end of experiment. In contrast, the LPR/GCR ratios of the operational mode 3 increased to approximately 0.82 on day 8 and then decreased to approximately 0.53 and remained there until the end of experiment. It was found that after day 20, the average LPR/GCR ratios of the operational mode 1 and 2 were 1.5 times greater than the operational mode 3.

APR (Fig. 17D) of three operational modes was identical from the beginning through day 41. After 5 days of inoculation, APR of three operational modes increased rapidly to 2 mM and 4mM. However, after the medium reservoir of the operational mode 2 was replaced every 2 days and the flow direction was reversed every 12 hrs, APR increased rapidly and reached 6 g/day on day 45 before approaching a steady state. Conversely, APR of the operational mode 1 and 3 remained still at 4 mM throughout the rest of culture period.

4.2.2 MAb-TSH production and viability

MAb-TSH concentrations were determined by ELISA technique and viability of cells harvested throughout the culture period were shown in Fig. 18. The results in Fig.18A were presented by the highest MAb-TSH production run of each operational mode under 5%FBS culture media. The saw-tooth profile was observed from the operational mode 1 throughout the culture period while it was observed from the operational mode 2 and 3 only in the steady state of MAb-TSH production. The increasing state of MAb-TSH production of the operational mode 1 was 53 days whereas the increasing state of MAb-TSH production of the operational mode 2 and 3 were 41 days. Additionally, the amount of MAb-TSH produced from the operational mode 2 was higher than the other operations throughout the culture period. There was no difference in the amount of MAb-TSH produced from the operational mode 1 and 3 during the first 60 days. Thereafter, the amount of MAb-TSH produced from the operational mode 3, however, was increased above the operational mode 1 and corresponded to the operational mode 2.

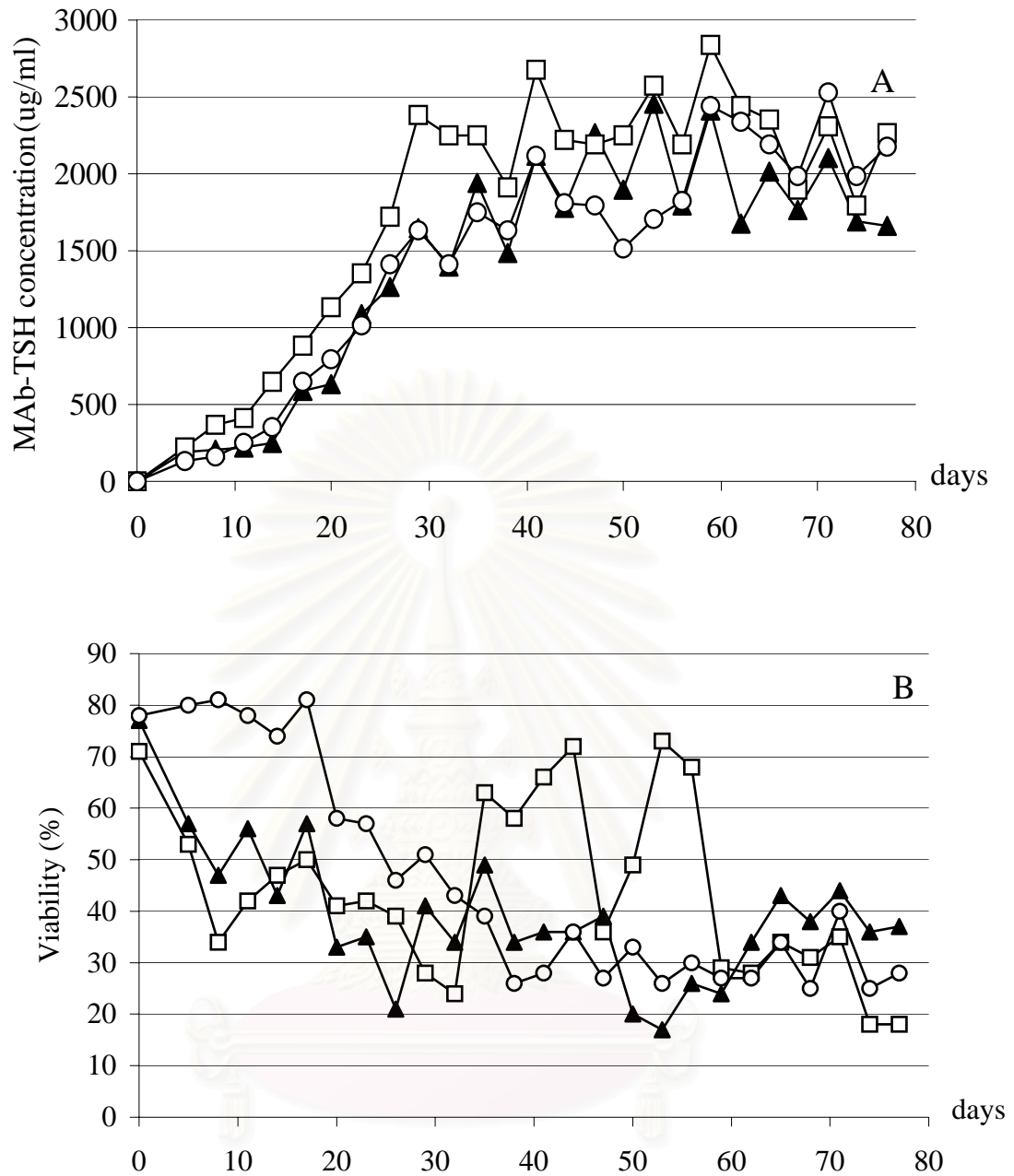


Fig. 18 Comparison of the MAb-TSH concentration (A) and viability (B) of samples harvested in different operational modes of the hollow fiber bioreactors.

▲ mode 1 □ mode 2 ○ mode 3

The viability of cells in different operational modes are shown in Fig. 18B. The trend of decreasing in the viability of cells was found in three operational modes. During the increasing state of MAb-TSH production, the viability of cells in the operational mode 1 and 2 decreased continually whereas the viability of cells in the operational mode 3 was constant during the first 10 days and then decreased continually with similar pattern to the others but at a higher rate. When the culture entered the steady state of MAb-TSH production, the viability of cells in three operational modes fluctuated between 20% and 40%. However, when the flow direction of the operational mode 2 was changed to reverse every 12 hrs, the viability of cells was increased above 60% and then decreased to the same value in 10 days later.

4.2.3 Purification of MAb-TSH from culture supernatant

MAb-TSH was purified from the culture supernatant as described in section 3.10.2. An example of elution profile of purified MAb-TSH by using expanded-bed rProtein A affinity chromatography and the yield of purified MAb-TSH under various culture conditions were shown in Fig. 19 and Table 7 respectively.

To estimate the efficiency of the hollow fiber bioreactors in different operational modes, the total amount of MAb-TSH production and the amount of MAb-TSH secreted of the operational mode 1 were compared to the operational mode 2 and 3 under the same conditions of 5% FBS culture media, culture period, and the position of EC ports as shown in Table 7.

During the increasing state of MAb-TSH production, the amount of MAb-TSH secreted of the operational mode 1 was approximately 2 and 3 times greater than that of the operational mode 2 and 3 respectively. However, the period of increasing state of the operational mode 1 was 12 days longer than the others.

During the steady state of MAb-TSH production, the total amount of MAb-TSH and the amount of MAb-TSH secreted of the operational mode 2 were generally higher than the others even if the EC ports were positioned at angle of 135° from the vertical position during day 62-71.

The position of EC ports was investigated in the operational mode 2 during day 42-103. The average amount of MAb-TSH secreted when the EC ports were positioned at the vertical position, at angle of 90° and at angle of 135° from the

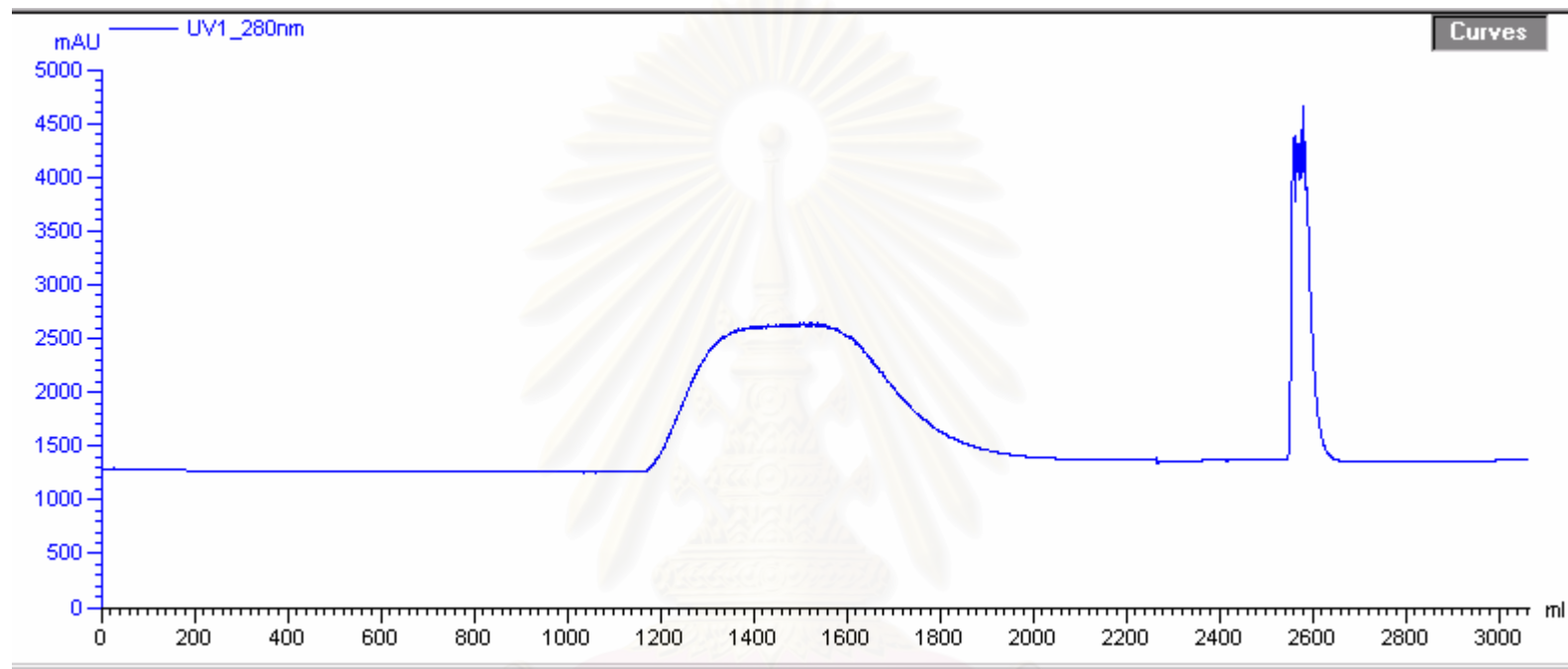


Fig. 19 Elution profile of the purified MAb-TSH by using expanded-bed rProtein A affinity chromatography.

The culture supernatant was collected from the hollow fiber bioreactor with single flow direction (bioreactor 2) during day 15-47. The first fraction detected residual cells, cell debris, and other contaminants that were washed out from the expanded-bed column. After the signal from UV monitor returned to baseline, the purified MAb-TSH pools was eluted with buffer, pH 4 as shown in the second fraction.

จุฬาลงกรณ์มหาวิทยาลัย

Table 7 Overview of the yield of purified MAb-TSH by expanded-bed rProteinA affinity chromatography.

Operational mode	The increasing state of MAb-TSH production						The steady state of MAb-TSH production						Total MAb (mg)
	Culture period (day)	FBS in culture (%)	Position of EC ports	Culture supernatant (ml)	MAb (mg)	MAb secreted (mg/ml)	Culture period (day)	FBS in culture (%)	Position of EC ports	Culture supernatant (ml)	MAb (mg)	MAb secreted (mg/ml)	
Mode 1 bioreactor 1	1 - 53	5	90° from the vertical position	745	725	0.97	54 - 92	5	90° from the vertical position	400	465	1.16	1,190
bioreactor 2	1 - 47	5		540	519	0.96	48 - 92	5		560	662	1.18	
Mode 2 bioreactor 1	1 - 41	5	90° from the vertical position	450	242	0.54	42 - 51	5	90° from the vertical position the vertical position	180	235	1.30	1,564
52 - 61							5	174		260	1.49		
62 - 71							5	135° from the vertical position		176	207	1.17	
72 - 81							5	90° from the vertical position the vertical position		180	231	1.28	
82 - 93							5	135° from the vertical position		220	219	0.99	
94 - 103	5	176	170	0.97									
bioreactor 2	1 - 41	5	90° from the vertical position	485	228	0.47	42 - 51	5	90° from the vertical position the vertical position	190	259	1.36	1,665
52 - 61							5	187		276	1.48		
62 - 71							5	135° from the vertical position		184	249	1.35	
72 - 81							5	90° from the vertical position the vertical position		188	256	1.36	
82 - 93							5	226		201	0.89		
94 - 103	5	184	196	1.06									
Mode 3 bioreactor 1	1 - 41	5	90° from the vertical position	485	118	0.24	42 - 53	5	90° from the vertical position	217	241	1.11	713
54 - 63							5	182		151	0.83		
64 - 78							5	314		203	0.65		
bioreactor 2	1 - 41	5	90° from the vertical position	497	136	0.27	42 - 53	2.5	90° from the vertical position	220	124	0.56	624
54 - 63							1	176		145	0.82		
64 - 78							0	314		219	0.70		
bioreactor 3	1 - 41	5	90° from the vertical position	468	140	0.30	42 - 53	2.5	90° from the vertical position	215	173	0.80	668
54 - 63							1	185		162	0.88		
64 - 78							0	290		193	0.67		

vertical position was 1.21, 1.33 and 1.14 mg/ml respectively. As a result of this calculation, it can be concluded that the secreted MAb-TSH obtained from the position at angle of 90° from the vertical position was higher than the others and corresponded to the results from statistical analysis.

The reduction of serum concentration in basal medium was examined in the operational mode 3 during day 42-78. For the same culture period, the MAb-TSH concentration of bioreactor 1 (5% FBS culture media) was compared to that of the other two bioreactors where FBS was reduced every 10 days from 5% to 2.5%, 1% and 0% (vol/vol) respectively.

During day 42-53 when FBS in bioreactor 2 and 3 was reduced to 2.5%, the average amount of MAb-TSH secreted from these two bioreactors were reduced to approximately 61% of the amount from bioreactor 1 where FBS was maintained at 5%. However, there was not much difference in the amount of MAb-TSH secreted between the bioreactor 1 and other two bioreactors when FBS was reduced to 1% during day 54 - 63 and then reduced to 0% during day 64 - 78.

Additionally, the reduction of FBS from 2.5% to 1% and 0% in bioreactor 2 and 3 had little effect on the amount of MAb-TSH secreted. The average amount of MAb-TSH secreted increased when FBS was reduced from 2.5% to 1%, and then decreased when FBS was reduced from 1% to 0%

4.2.4 SDS-PAGE analysis of the purified MAb-TSH

The purified MAb-TSH by expanded-bed rProteinA and ProteinA sepharose affinity chromatography were characterized using SDS-PAGE. SDS-PAGE allowed characterization of MAb-TSH by reducing disulfide bonds of intact IgG molecules to various molecular weights of the heavy and light chains. The protein stain and molecular weight calibration curve of the purified MAb-TSH under various culture conditions were shown in Appendix D.

In SDS-PAGE investigation, the supernatant of cells cultured in 5% serum-supplemented medium (lane 3 of Fig. 20, 22, 24, 26, 28, 30, 32, 34 and 36) appeared to contain 3 major bands. Two bands at molecular weight approximately 57 kDa and 29 kDa appeared at the same position as a single heavy and light chain band of mouse IgG reference standard respectively (lane 1 of Fig. 20, 22, 24, 26, 28, 30, 32, 34 and 36). The other was a major band of contaminating protein that was

conformed to the major band of FBS (lane 8 of Fig. 26, and lane 10 of Fig. 20, 32, 34 and 36).

The lighter contaminating protein band was observed from the supernatant of cell cultured in 2.5% and 1% serum-supplemented medium (lane 5 and 7 of Fig. 28 and 30) before disappeared from the supernatant of cell cultured in 0% serum-supplemented medium (lane 9 of Fig. 28 and 30). As a result of these experiments, it can be concluded that the major contaminating protein band was the protein from FBS.

Electrophoretograms of the purified MAb-TSH under various conditions of culture showed two different bands of the single heavy and light chain at the same molecular weight range of mouse IgG reference standard (Fig. 20, 22, 24, 26, 28, 30, 32, 34, and 36). The single heavy and light chain band indicated the purity of the MAb-TSH preparation. From the experiments, there were only two bands of heavy and light chain. Therefore, it could be concluded that there was no contaminating protein from the culture supernatant visible either purified by expanded-bed rProteinA or Protein A sepharose affinity chromatography.

CHAPTER V

DISCUSSION

5.1 Assembly of hollow fiber bioreactor

The present study described the production of MAb-TSH in the simple hollow fiber bioreactor. The bioreactor was assembled from commercially available components and used inexpensive hollow fiber dialyser as the cell culture and gas exchange cartridge. The fiber material of both cartridges is cellulose which has 35 kDa MWCO. Cellulose is a hydrophilic membrane material that has been widely recognized as an effective polymer for low protein adsorption and low cell adhesion. Therefore, the cell culture cartridge with cellulose fibers could reduce the problem of protein adsorption such as growth factor proteins, cells and MAb-TSH.

The cell culture cartridge was operated in the closed shell mode. The basal medium was introduced to the tube side or IC space of cartridge and flowed through the downstream end of the tube. In order to investigate the effects of pressure gradient and starting flow in the closed shell operation, the EC medium of cell culture cartridge was collected from the alternate upstream and downstream EC ports throughout the culture period. Then, the amount of MAb-TSH was determined by ELISA technique.

The results in Fig. 11A showed that when the hollow fiber bioreactor was operated by feeding medium flow to the cell culture cartridge with single flow direction (operational mode 1), the greater amount of MAb-TSH was consistently obtained from the downstream EC port throughout the culture period as indicated in the saw tooth profiles. This should be the effect of pressure gradient and starting flow that caused MAb-TSH to be entrained and accumulated at the downstream end of cartridge

To further test for the importance of MWCO of fibers in the aspect of productivities, the samples from EC harvest and IC medium were assayed for MAb-TSH concentration. The results from Fig. 11B, 13B and 15B are shown the leakage of MAb-TSH product from the EC space to the IC space for the 35 kDa MWCO of fiber. Furthermore, the increase of monoclonal antibody production rate in the samples of IC medium was accompanied by the increase of MAb-TSH concentration in the samples of EC space. This was occurred despite the fact that the size of IgG

(156,000 daltons) is much larger than the MWCO of the fibers (35,000 daltons). Detection of MAb-TSH leakage in the IC medium resulted from the concentration gradients established between the EC and IC space.

The gas exchange cartridge was operated in the crossflow mode. The bioreactor was gassed by pumping the gas mixture (5% CO₂ in air) resided in the CO₂ incubator to the EC space via the downstream EC port of gas exchange cartridge, then flowed across the fiber bed and permeated to the circulating basal medium. The upstream EC port of gas exchange cartridge was also attached by a tubing clip, a component located next to a hydrophobic filter that was used to control pressure in the EC space. The pressure in the EC space can be controlled at higher level by compressing the silicone tube with a tubing clip.

The pressure in the EC space of gas exchange cartridge must be carefully maintained at all time. The pressure in the EC space must have enough to stay in level above the tube side pressure so that the gas mixture could permeate to the circulating basal medium and the basal medium could not diffuse into the EC space to cause the contamination. However, the EC space should not have too much pressure since the pressure would resist and sometimes stop the pumping of basal medium from the medium reservoir into the gas exchange cartridge.

Another criteria to observe the appropriate pressure in the EC space of gas exchange cartridge is the dryness of fiber bed texture. If the pressure in the EC space was too high, resulting in blocking the basal medium from flowing into the tube side of gas exchange cartridge, the fiber bed texture will be too dry.

5.2 Cells cultivation in different operational modes

In order to reduce the heterogeneous nature of cell culture cartridge, two operational modes with reverse flow direction were performed. Fig. 13A and 15A show MAb-TSH production in the hollow fiber with reverse flow every 24 and 12 hrs and the hollow fiber bioreactor with reverse flow every 12 hrs respectively. It was found that the greater amount of MAb-TSH was still obtained from the downstream EC port of both operational modes during the steady state of MAb-TSH production. This can be concluded that the heterogeneous nature can be reduced but cannot be entirely eliminated by both operational modes.

An additional metabolite assays were performed to monitor and evaluate the three operational modes. Moreover, the LPR/GCR ratio was also used to estimate the

efficiency of oxygen usage. The results presented in Fig. 17C showed that the LPR/GCR ratio of the operational mode 1 and 2 were not different throughout the culture period. These results give evidence that the operational mode 2 could not deliver more oxygen to the cells than the operational mode 1. However, when the flow direction of operational mode 2 was changed to reverse every 12 hrs, the viability was increased above 60% (Fig. 18B). This result indicates that when oxygen and nutrients are delivered to the cells more frequently, further improvement of the viability can be occurred.

Comparing to the operational mode 1 and 2, the operational mode 3 resulted in the lower LPR/GCR ratio (Fig. 17C). This means that more oxygen can be delivered to the cells as a result of more efficient glucose usage. In addition, the bioreactors with operational mode 3 had higher cell viability (>60%) than the others during the increasing state of MAb-TSH production (Fig. 18B). It can be concluded that the reverse flow every 12 hrs brought more oxygen delivery to the cells and increased the efficiency of nutritious usage that led to the higher cell viability.

However, when comparing the amount of MAb-TSH produced in 3 operational modes, the bioreactor operated in mode 3 returned almost the same amount of MAb-TSH as the amount received from mode 1 despite the fact that mode 3 has higher cell viability (Fig. 18A). The result indicates that the MAb-TSH production is not conformed to the amount of viable cells. This may be the reason that cells tend to use the cellular demand for ATP to support nucleic acid and protein synthesis for cell division rather than MAb-TSH synthesis.

As the experiment proceeded, the duration of replacing medium reservoir in the operational mode 2 was reduced in order to control the level of lactate and ammonia during culture. In Fig. 17, it shows that the shorter period of replacing medium reservoir caused rapid increase of GCR, LPR, and APR. The rapid increase of GCR indicated the higher rate of glycolysis that was due to an increase of glucose concentration in bioreactor. Likewise, the rapid increase in APR indicated the higher rate of glutamine catabolism as a consequence of an increase of glutamine concentration.

The higher rate of glycolysis and glutamine catabolism caused a large fraction of NADH generated while the efficiency of oxygen usage was not increased as shown by the unchanging LPR/GCR ratio (Fig. 17C). The usage of NADH as electron carrier in oxidative phosphorylation is limited by the level of oxygen, which

is available in the system. Therefore, in order to reduce the large fraction of NADH formed in glycolysis and TCA cycle, NADH oxidation was performed via the reaction of changing from pyruvate to lactate instead, which was the reasons of having rapid increase in LPR.

Another aspect observed in this experiment was the rapidly increased in ammonia concentrations. The results in Fig. 12C, 14C and 16C illustrate the rapid increase in ammonia concentrations from 0 to 3 mM within 5 days after inoculation. However, from the experiment during this 5-day period, the growth rate and cell density were still low. Therefore, it can be concluded that the increase in ammonia concentration was not the main consequence of glutamine utilization that occurred in the mitochondria. It was noticed from the experiment that the presence of ammonia concentrations at approximately 4 mM had no effect on cell growth and MAb-TSH production during the culture.

5.3 Impact of gravity sedimentation on MAb-TSH concentration

The effect of EC space gravity sedimentation on MAb-TSH concentration was studied by positioning the EC ports during the steady state of MAb-TSH production. The statistics in Table 4 revealed that the lower amount of MAb-TSH was obtained when the EC ports were positioned at angle of 135° from the vertical position. This may be the reason that the position at 135° from the vertical position caused the cells to settle at the EC harvest ports and caused more cells to be removed from the bioreactor during harvest. Subsequently, the lower cell density would be remained in the EC space after harvest and then led to the lower productivity.

When comparing between the position at the vertical position and at angle of 90° from the vertical position, there was no significant difference between these two positions. However, observing from the experiments, it is recommended that the EC ports positioned at angle of 90° from the vertical position was more suitable for operating the cell culture cartridge after harvest since cells were distributed and settled in wider area than the vertical position.

5.4 Adaptation to low serum - supplemented medium

These experiments were executed during the steady state of MAb-TSH production to ensure that the effect of serum concentration on cell growth was

eliminated. The statistics in Table 6 revealed that there were significant differences in MAb-TSH concentrations between the culture with 5% serum (control run) and the culture with serum reduction. The amount of MAb-TSH obtained from the culture with constant 5% serum were higher than the cultures with 2.5%, 1% and 0% serum concentration. However, there were no significant differences in the amount of MAb-TSH when the serum concentration was reduced from 2.5% to 1% and eventually to 0% during the culture. The different results were due to the reason that the reduction of serum concentration from 5% to 2.5% in the bioreactor 2 and 3 was prematurely done before entering their steady conditions. As the result, cell growth rate was limited and consequently led to the lower cell density and MAb-TSH production.

To overcome the loss in MAb-TSH production of this study during adaptation to low serum level, the reduction of serum concentration should be done when the culture was at the steady state. Additionally, serum reduction in this cell line resulted in lower cell growth but did not greatly affect cell metabolism and MAb-TSH production.

5.5 Evaluation of the hollow fiber bioreactor as an alternative for MAb-TSH production.

In order to evaluate the efficiency of the hollow fiber bioreactor, the average amount of MAb-TSH produced from the duplicate runs under optimal condition was compared against the amount of MAb-TSH routinely produced from ascites fluid at Radioisotope Laboratory section, National Institute of Health as shown in Table 8.

Table 8 Comparison of total MAb-TSH production in hollow fiber bioreactor and in murine ascites.

System	Time-consuming (days)	Volume of supernatant or ascites fluid (ml)	Total MAb (mg)
hollow fiber bioreactor *	67	833	750
18 mice**	22	28	34

* the average amount of MAb-TSH produced from the duplicate runs.

** the amount of MAb-TSH produced at Radioisotope Laboratory section, National Institute of Health.

Hybridoma TSH II were grown as ascites tumors in 18 BALB/C mice. Mice were primed with 0.5 ml pristane intraperitoneally 7 days before injection of 10^7 hybridoma cells per mouse. When ascites formation was obviously noticed, ascites fluid was collected from the peritoneal cavity.

From this comparison it was found that the hollow fiber bioreactor could generate 750 mg of MAb-TSH in 67 days. The results confirmed that the hollow fiber bioreactor in this study could be utilized as an alternative system to substitute the use of mice in small-scale production.

However, time spent in labor and production costs were greater for operation with the hollow fiber bioreactor. The great expenses are due to the facts that many of the cost items are spent on the equipment investment such as CO₂ incubator, CO₂ tank, peristaltic pump and glass bottle (5 L), and also have to be spent on the consumable materials during cultivation. Table 9 shows the material costs of producing MAb-TSH in hollow fiber bioreactor under optimal conditions.



สถาบันวิทยบริการ
จุฬาลงกรณ์มหาวิทยาลัย

Table 9 Material costs of producing MAb-TSH in hollow fiber bioreactor under optimal conditions.

System	Time-consuming (days)	Materials	Quantity	Costs* (bahts)
Hollow fiber bioreactor	67	CO ₂ gas	1 tank	380
		Hollow fiber cartridge	2	2,000
		Tubing	4.5 meters	2,550
		Valves and connectors	17	27,000
		Filters	16	4,500
		Syringes	50	850
		Needles	25	38
		Gloves	1 box	123
		Tissue paper	2 packs	73
		Aluminum foil	1 box	67
		RPM I medium	74 L	7,301
		FBS	55 ml	825
		TOTAL		

* 2002 costs

สถาบันวิทยบริการ
จุฬาลงกรณ์มหาวิทยาลัย

CHAPTER VI

CONCLUSION

The hollow fiber bioreactor presented in this study could produce high concentrated products. The amount of MAb-TSH produced in excess of 1 mg/ml could substantially reduced downstream processing costs. Furthermore, the expensive FBS was supplied only in the EC medium and could be reduced without any effect on MAb-TSH production. The reduction of FBS helped to decrease production costs. Therefore, the hollow fiber bioreactor in this study is considered as a cost-effective alternative system to replace the use of mice in small-scale commercial production.

For the purpose of producing high yield of MAb-TSH against thyroid stimulating hormone, the optimal culture conditions are suggested as follows:

1. Reverse flow direction is used to operate the hollow fiber bioreactor. By this operation, the heterogeneous nature of bioreactor can be reduced by periodically alternating the direction of media flow before feeding to the cell culture cartridge.
2. A total cell viability of 10^8 cells are inoculated into the EC space of cell culture cartridge.
3. After inoculation, a 5-day batch with one direction of media flow is operated. Then, followed by the 24-hours circulating media flow alternated clockwise and anticlockwise throughout the culture period. In case that viability of cells is less than 10%, the frequency of reversing direction must be changed from 24 to 12 hrs.
4. The medium reservoir and EC medium must be replaced when one of the following conditions occurred: glucose concentration fell below 150 mg/dl, or lactate and ammonia concentration are above 150 mg/dl and 2.5 mM respectively. The medium circulation rate must be increased when both lactate concentration is higher than 150 mg/dl and ammonia is higher than 2.5 mM.
5. After harvest, the cell culture cartridge is turned backwards and forwards until cells are evenly distributed throughout the cartridge. Then, the EC ports

of cell culture cartridge are positioned at angle of 90° from the vertical position and turned interchangeably between 90° clockwise direction and 90° anticlockwise direction every time after harvest. This is due to evenly distribute and settle the cells in wider area and increase the yield of MAb-TSH from harvest.

6. When the culture is at the steady state, the reduction of FBS can be done without any effects on MAb-TSH production and cell metabolism.

Suggestion:

During production of MAb in the hollow fiber bioreactor, the medium circulation rate, the replacement of medium reservoir, and the harvest of product are based on metabolite products that can be predicted by using linear regression equation. For this strategy, routine metabolic assays of glucose, lactate, ammonia and MAb are carried out throughout the culture period. Then, follow by calculating the consumption rate of glucose, the production rate of lactate and ammonia, and MAb concentration, and then consider the linear relationship between the MAb concentration and GCR, LPR and APR, and between GCR and LPR.

If the statistics reveal the linear relationship, further metabolic assay of lactate and ammonia will be not necessary for subsequent runs whereas MAb or glucose assay should be carried out throughout the cultivation and then use the regression equations for prediction the amount of metabolite products and, therefore, help operate and monitor the hollow fiber bioreactor.

REFERENCES

- Adema, E., and Sinskey, A. J. 1987. An analysis of intra-versus extracapillary growth in a hollow fiber reactor. Biotechnol. Prog. 3: 74-79.
- Altshuler, G. L., Dziewulski, D. M., Soweck, J. A., and Belfoot, G. 1986. Continuous hybridoma growth and monoclonal antibody production in hollow fiber reactors-seperators. Biotechnol. Bioeng. 28: 646-658.
- Baker, R.W. 2000. Membrane technology and applications. New York: Mc Graw-Hill.
- Brotherton, J. D., and Chau, P. C. 1995. Protein-free human-human hybridoma cultures in an intercalated-spiral alternated-dead-ended hollow fiber bioreactor. Biotechnol. Bioeng. 47: 384-400.
- Brotherton, J. D., and Chau, P. C. 1996. Modeling of axial-flow hollow fiber cell culture bioreactors. Biotechnol. Prog. 12: 575-590.
- Capiaumont, J., Legrand, C., Carbonell, D., Dousset, B., Belleville, F., and Nabet, P. 1995. Methods for reducing the ammonia in hybridoma cell cultures. J. Biotechnol. 39: 49-58.
- Catty, D., and Raykundalia, C. 1989. ELISA and related enzyme immunoassays. In D. Catty (ed.), Antibodies volume II: a practical approach, pp. 97-154. New York: Oxford IRL press.
- Chen, K., Liu, Q., Xie, L., Sharp, A., and Wang, D. I. C. 2001. Engineering of mammalian cell line for reduction of lactate formation and high monoclonal antibody production. Biotechnol. Bioeng. 72: 55-61.
- Cherlet, M., and Marc, A. 1998. Intracellular pH monitoring as a tool for the study of hybridoma cell behavior in batch and continuous bioreactor cultures. Biotechnol. Prog. 14: 626-638.
- Chresand, T. J., Gillies, R. J., and Dale, B. E. 1988. Optimum fiber spacing in a hollow fiber bioreactor. Biotechnol. Bioeng. 32: 983-992.
- Flickinger, M. C., Goebel, N. K., Bibila, T., and Boyce-Jacino, S. 1992. Evidence for posttranscriptional stimulation of monoclonal antibody secretion by L-glutamine during slow hybridoma growth. J. Biotechnol. 22: 201-226.

- Glacken, M. W., Adema, E., and Sinsky, A. J. 1988. Mathematical descriptions of hybridoma culture kinetics: I. Initial metabolic rates. Biotechnol. Bioeng. 32: 491-506.
- Glacken, M. W., Fleischaker, R. J., and Sinsky, A. J. 1986. Reduction of waste product excretion via nutrient control: possible strategies for maximizing product and cell yields on serum in cultures of mammalian cells. Biotechnol. Bioeng. 28: 1376-1389.
- Gorter, A., Van De Griend, R. J., Van Eendenburg, J. D. H., Haasnoot, W. H. B., and Fleuren, G. J. 1993. Production of bi-specific monoclonal antibodies in a hollow-fibre bioreactor. J. Immunol. Methods 161: 145-150.
- Gramer, M. J., and Poeschl, D. M. 1998. Screening tool for hollow fiber bioreactor process development. Biotechnol. Prog. 14: 203-209.
- Gramer, M. J., Poeschl, D. M., Conroy, M. J., and Hammer, B. E. 1999. Effect of harvesting protocol on performance of a hollow fiber bioreactor. Biotechnol. Bioeng. 65: 334-340.
- Griffiths, B. 1991. Products from animal cells. In M. Butler (ed.), Mammalian cell biotechnology: a practical approach, pp. 207-229. New York: Oxford university press.
- Griffiths, B. 2001. Scale up of suspension and anchorage-dependent animal cells. Mol. Biotech. 17: 225-238.
- Heifetz, A. H., Braatz, R. A., Wolfe, R. M., Barry, R. M., Miller, D. A., and Solomon, B. A. 1989. Monoclonal antibody production in hollow fiber bioreactor using serum-free medium. Biotechniques 7: 192-199.
- Handa-Corrigan, A., Nikolay, S., Fletcher, D., Mistry, S., Young, A., and Ferguson, C. 1995. Monoclonal antibody production in hollow-fiber bioreactors: process control and validation strategies for manufacturing industry. Enzyme Microb. Technol. 17: 225-230.
- Handa-Corrigan, A., Nikolay, S., Jeffery, D., Heffernan, B., and Young, A. 1992. Controlling and predicting monoclonal antibody production in hollow fiber bioreactors. Enzyme Microb. Technol. 14: 58-63.
- Hu, W., and Dodge, T. C. 1985. Cultivation of mammalian cells in bioreactors. Biotechnol. Prog. 1: 209-215.

- Jackson, L. R., Trudel, L. J., Fox, J. G., and Lipman, N. S. 1996. Evaluation of hollow fiber bioreactor as an alternative to murine ascites production for small scale monoclonal antibody production. J. Immunol. Methods 189: 217-231.
- Jeong, H., and Wang, S. S. 1995. Role of glutamine in hybridoma cell culture: effects on cell growth, antibody production, and cell metabolism. Enzyme Microb. Technol. 17: 47-55.
- Johnstone, A., and Thorpe, R. 1987. Immunochemistry in practice. Cambridge: Cambridge university press.
- Kelsey, L. J., Pillarella, M. R., and Zydney, A. L. 1990. Theoretical analysis of convective flow profiles in a hollow-fiber membrane bioreactor. Chem. Engng. Sci. 45: 3211-3220.
- Klerx, J. P. A. M., Verplanke, C. J., Blonk, C. G., and Twaalfhoven, L. C. 1988. *In vitro* production of monoclonal antibodies under serum-free conditions using a compact and inexpensive hollow fiber cell culture unit. J. Immunol. Methods 111: 179-188.
- Kohler, G., and Milstein, C. 1975. Continuous culture of fused cells secreting antibody of predefined specificity. Nature 256: 495-497.
- Kromenaker, S. J., and Srienc, F. 1994. Effect of lactic acid on the kinetic of growth and antibody production in murine hybridoma: secretion patterns during the cell cycle, J. Biotechnol. 34: 13-34.
- Kurokawa, H., Park, Y. S., Lijima, S., and Kobayashi, T. 1994. Growth characteristics in fed-batch culture of hybridoma cells with control of glucose and glutamine concentration. Biotechnol. Bioeng. 44: 95-103.
- Laemmli, U.K. 1970 Cleavage of structure protein during assembly of head of bacteriophage-T4. Nature 227: 680-685.
- Lowrey, D., Murphy, S., and Goffe, R. A. 1994. A comparison of monoclonal antibody productivity in different hollow fiber bioreactors. J. Biotechnol. 36: 35-38.
- Luan, Y. T., Mutharasan, R., and Magee, W. E. 1987. Factors governing lactic acid formation in long term cultivation of hybridoma cells. Biotechnology letters 9: 751-756.

- Mancuso, A., Sharfstein, S. T., Tucker, S. N., Clark, D. S., and Blanch, H. W. 1994. Examination of primary metabolic pathways in a murine hybridoma with carbon-13 nuclear magnetic resonance spectroscopy. Biotechnol. Bioeng. 44: 565-585.
- Mancuso, A., Sharfstein, S. T., Fernandez, E. J., Clark, D. S., and Blanch, H. W. 1998. Effect of extracellular glutamine concentration on primary and secondary metabolism of a murine hybridoma: an *in vivo* ¹³C nuclear magnetic resonance study. Biotechnol. Bioeng. 57: 172-186.
- Martinelle, K., and Haggstrom, L. 1993. Mechanisms of ammonium ion toxicity in animal cells: Transport across cell membranes. J. Biotechnol. 30: 339-350.
- Mcqueen, A., and Bailey, J. E. 1990. Effect of ammonium ion and extracellular pH on hybridoma cell metabolism and antibody production. Biotechnol. Bioeng. 35: 1067-1077.
- Miller, W. M., Wilke, C. R., and Blanch, H.W. 1987. Effects of dissolved oxygen concentration on hybridoma growth and metabolism in continuous culture. J. Cell Physiol. 132: 524-530.
- Miller, W. M., Wilke, C.R., and Blanch, H. W. 1989a. Transient responses of hybridoma cells to nutrient additions in continuous culture: II. Glucose pulse and step changes. Biotechnol. Bioeng. 33: 477-486.
- Miller, W. M., Wilke, C. R., and Blanch, H. W. 1989b. Transient responses of hybridoma cells to nutrient additions in continuous culture: II. Glutamine pulse and step changes. Biotechnol. Bioeng. 33: 487-499.
- Nayak, R. C., and Herman, I. M. 1997. Measurement of glucose consumption by hybridoma cells growing in hollow fiber cartridge bioreactors: use of blood glucose self-monitoring devices. J. Immunol. Methods 205: 109-114.
- Nelson, P. N., Reynolds, G. M., Waldran, E. E., Ward, E., Giannopoulos, K., and Murray, P. G. 2000. Monoclonal antibodies. J. Clin. Pathol.:Mol. Pathol. 53: 111-117.
- Nune, S. P., and Peinemann., eds. 2001. Membrane technology in the chemical industry. Weinheim: Wiley-VCH.
- Omasa, T., Higashiyama, K., Shioya, S., and Suga, K. 1992. Effects of lactate concentration on hybridoma culture in lactate-controlled fed-batch operation. Biotechnol. Bioeng. 39: 556-564.

- Ozturk, S. S., and Palsson, B. O. 1990. Effects of dissolved oxygen on hybridoma cell growth, metabolism, and antibody production kinetics in continuous culture. Biotechnol. Prog. 6: 437-446.
- Ozturk, S. S., Riley, M. R., and Palsson, B. O. 1992. Effects of ammonia and lactate on hybridoma growth, metabolism, and antibody production. Biotechnol. Bioeng. 39: 418-431.
- Patkar, A. Y., Bowen, B. D., and Piret, J. M. 1993. Protein adsorption in polysulfone hollow fiber bioreactor used of serum free medium mammalian cell culture. Biotechnol. Bioeng. 42: 1099-1106.
- Piret, J. M., and Cooney, C. L. 1990. Mammalian cell and protein distributions in ultrafiltration hollow fiber bioreactors. Biotechnol. Bioeng. 36: 902-910.
- Piret, J. M., Devens, D. A., and Cooney, C. L. 1991. Nutrient and metabolic gradients in mammalian cell hollow fiber bioreactors. Can. J. Chem. Eng. 69: 421-428.
- Ramirez, O., and Mutharasan, R. 1990. Cell cycle and growth phase-dependent variations in size distribution, antibody productivity, and oxygen demand in hybridoma cultures. Biotechnol. Bioeng. 36: 839-848.
- Riley, M. R., Muzzio, F. J., and Reyes, S. C. 1997. Effect of oxygen limitations on monoclonal antibody production by immobilized hybridoma cells Biotechnol. Prog. 13: 301-310.
- Sanfeliu, A., Cairo, J. J., Casas, C., Sola, C., and Godia, F. 1996. Analysis of nutritional factors and physical conditions affecting growth and monoclonal antibody production of the hybridoma KB-26.5 cell line. Biotechnol. Prog. 12: 209-216.
- Scott, A. M., Geleick, D., Rubira, M., Clarke, K., Nice, E. C., Smyth, F. E., Stockert, E., Richards, E. C., Carr, F. J., Harris, W. J., Armour, K. L., Rood, J., Kypridis, A., Kronina, V., Murphy, R., Lee, F-T., Liu, Z., Kitamura, K., Ritter, G., Laughton, K., Hoffman, E., Burgess, A. W., and Old, L. J. 2000. Construction, production, and characterization of humanized anti-lewis y monoclonal antibody 3S193 for targeted immunotherapy of solid tumor. Cancer Res. 60: 3254-3261.
- Sharfstein, S. T., Tucker, S. N., Mancuso, A., Blanch, H. W., and Clark, D. S. 1994. Quantitative *in vivo* nuclear magnetic resonance studies of hybridoma metabolism. Biotechnol. Bioeng. 43: 1059-1074.

- Shi, Y., Ryu, D. D. Y., and Park, S. H. 1993. Monoclonal antibody productivity and the metabolic pattern of perfusion cultures under varying oxygen tensions. Biotechnol. Bioeng. 42: 430-439.
- Shi, Y., Sardonini, C. A., and Goffe, R. A. 1998. The use of oxygen carriers for increasing the production of monoclonal antibodies from hollow fibre bioreactors. Res. Immunol. 149: 576-587.
- Stryer, L., 1995. Biochemistry. 4nd ed. New York: W.H. Freeman and Company.
- Tharakan, J. P., and Chau, P. C. 1986a. Operation and pressure distribution of immobilized cell hollow fiber bioreactors. Biotechnol. Bioeng. 28: 1064-1071.
- Tharakan, J. P., and Chau, P. C. 1986b. A radial flow hollow fiber bioreactor for the large scale culture of mammalian cells. Biotechnol. Bioeng. 18: 329-342.
- Tildon, J.T., and Zielke, H.R. 1988. Glutamine: An energy source for mammalian tissues. In E. Kvamme (ed.), Glutamine and glutamate in mammals, pp. 167-182. CRC Press.
- Vetterlein, D. 1989. Monoclonal antibodies: production, purification and technology. Adv. Clin. Chem. 27: 303-354.
- Xie, L., and Wang, D. T. C. 1994. Fed-batch cultivation of animal cells using different medium design concepts and feeding strategies. Biotechnol. Bioeng. 43: 1175-1189.
- Zhang, S., Honda-Corrigan, and Spier, R. E. 1993. A comparison of oxygenation methods for high-density perfusion cultures of animal cells. Biotechnol. Bioeng. 41: 685-692.



APPENDICES

สถาบันวิทยบริการ
จุฬาลงกรณ์มหาวิทยาลัย

APPENDIX A

Reagent and buffer preparations

1. Preparation for cell culture

Basal medium

RPM I medium powder for	10 L
D-glucose	25 g
L-glutamine	2.92 g
Sodium pyruvate	1.10 g
NaHCO ₃	20 g

Dissolved mixture and adjusted pH to 7.4 with 6 M HCl or 6 M NaOH and then adjusted volume to 10 L with distilled water. Immediately filtered through 0.2 µm filter into sterilized bottles with screw cap.

Serum-supplemented medium (5% vol/vol in basal medium)

Added 50 ml fetal bovine serum in 950 ml basal medium.

Trypan blue (0.1% in 0.15 M PBS , pH 7.2)

Added 0.1 g trypan blue in 100 ml 0.15 M PBS, pH 7.2.

2. Preparation for ELISA assays

2.1 0.05 M carbonate buffer, pH 9.6

Sodium carbonate / bicarbonate buffer, pH 9.6

Na ₂ CO ₃	1.59 g (0.015 M)
NaHCO ₃	2.93 g (0.035 M)

Adjusted volume to 1 L with distilled water.

2.2 PBS buffer

0.15 M Phosphate buffer saline (PBS), pH 7.4 with tween 80

KH ₂ PO ₄	0.21 g
Na ₂ HPO ₄	0.72 g
NaCl	7.45 g
Tween 80	1 g

Adjusted pH to 7.4 with 1 M HCl or 1 M NaOH and adjusted volume to 1 L with distilled water.

2.3 Blocking buffer

0.15 M Phosphate buffer saline (PBS) , pH 7.4 with 3% BSA

KH_2PO_4	0.21 g
Na_2HPO_4	0.72 g
NaCl	7.45 g
BSA	30 g

Adjusted pH to 7.4 with 1 M HCl or 1 M NaOH and adjusted volume to 1 L with distilled water.

2.4 1% Sucrose solution

Sucrose	10 g
---------	------

Adjusted volume to 1 L with distilled water.

2.5 Diluting/incubation buffer

0.1 M Phosphate buffer saline, pH 7.4 with 0.05% Tween 20

KH_2PO_4	0.20 g
Na_2HPO_4	1.11 g
NaCl	8.00 g
KCl	0.20 g

Adjusted pH to 7.4 with 1 M HCl or 1 M NaOH and adjusted volume to 1 L with distilled water.

2.6 Saline buffer

0.9% NaCl with 0.05% Tween 20

NaCl	9.0 g
Tween 20	0.5 ml

Adjusted volume to 1 L with distilled water.

2.7 Peroxidase substrate

Solution A, pH 5.0 (pH range 5.0-6.0)

Na_2HPO_4	14.32 g
Citric acid. H_2O	10.36 g
H_2O_2 (30%)	500 μl

Adjusted volume to 1 L with distilled water.

Solution B, pH 2.4

Citric acid. H_2O	10.36 g
-----------------------------------	---------

Added 250 mg TMB in 40 ml DMSO and adjusted volume to 1 L with distilled water.

2.8 2N H₂SO₄

H ₂ SO ₄	55.5 ml
--------------------------------	---------

Adjusted volume to 1 L with distilled water.

3 Preparation for monoclonal antibody purification

0.5 M Phosphate buffer, pH 7.4

Na ₂ HPO ₄	57.1 g
----------------------------------	--------

NaH ₂ PO ₄ .H ₂ O	13.53 g
----------------------------------------------------	---------

Adjusted pH to 7.4 with 1 M HCl or 1 M NaOH and adjusted volume to 1 L with distilled water.

20 mM Phosphate buffer, pH 7.4

0.5 M Phosphate buffer, pH 7.4	40 ml
--------------------------------	-------

Adjusted volume to 1 L with distilled water.

0.1 M Citrate buffer, pH 4

0.1 M Citric acid.H ₂ O	(21.01 g/L)
------------------------------------	-------------

0.1 M Sodium citrate	(29.41 g/L)
----------------------	-------------

Added sodium citrate solution into citric acid solution until pH equaled to 4.

0.15 M Phosphate buffer saline (PBS), pH 7.2

KH ₂ PO ₄	0.20 g
---------------------------------	--------

Na ₂ HPO ₄	1.15 g
----------------------------------	--------

NaCl	8.00 g
------	--------

KCl	0.20 g
-----	--------

Adjusted pH to 7.2 with 1 M HCl or 1 M NaOH and adjusted volume to 1 L with distilled water.

0.1 M Glycine-HCl buffer, pH 2

Glycine	7.5 g
---------	-------

Adjusted pH to 2 with 1 M HCl and adjusted volume to 1 L with distilled water.

1M Tris-HCl buffer, pH 9.0

Tris (hydroxymethyl)-aminomethane	12.1 g
-----------------------------------	--------

Adjusted pH to 9 with 1 M NaOH and adjusted volume to 100 ml with distilled water.

4. Preparation for denaturing polyacrylamide gel electrophoresis (SDS-PAGE)

4.1 Stock reagents

30% Acrylamide, 0.8% Bis-acrylamide

Acrylamide 30 g

N,N'-Methylene-bis-acrylamide 0.80 g

Adjusted volume to 100 ml with distilled water.

0.75 M Tris-HCl buffer, pH 8.8

Tris (hydroxymethyl)-aminomethane 22.71 g

Adjusted pH to 8.8 with 1 M HCl and adjusted volume to 250 ml with distilled water.

0.25 M Tris-HCl buffer, pH 6.8

Tris (hydroxymethyl)-aminomethane 7.57 g

Adjusted pH to 6.8 with 1 M HCl and adjusted volume to 250 ml with distilled water.

Electrode buffer (25 mM Tris, 192 mM glycine, 0.1% SDS)

Tris (hydroxymethyl)-aminomethane 3.03 g

Glycine 14.40 g

SDS 1 g

Dissolved in distilled water to 1L without pH adjustment (final pH should be 8.3).

Sample buffer

0.25 M Tris-HCl buffer, pH 6.8 12.50 g

SDS 1 g

Glycerol 5 ml

2-Mercaptoethanol 2.5 ml

Bromophenol blue 0.013 g

Adjusted volume to 25 ml with distilled water.

Stainer

Coomassie brilliant blue R 250 1 g

Methanol 500 ml

Acetic acid 70 ml

Adjusted volume to 1 L with distilled water.

Destainer

Methanol 500 ml

Acetic acid 140 ml

Adjusted volume to 2 L with distilled water.

4.2 Preparation of SDS-PAGE

Reagent	Stacking gel (3%)	Separation gel (10%)
0.75 M Tris-HCl, pH 8.8 (ml)	-	7.5
0.25 M Tris-HCl, pH 6.8 (ml)	5	-
30% Acrylamide, 0.8% Bis (ml)	1	5
10% SDS (μ l)	100	150
distilled water (ml)	3.38	1.58
TEMED (μ l)	20	20
1% Ammonium persulfate (μ l)	500	750
final volume (ml)	10	15

APPENDIX B

Calculation

1. Glucose concentration

$$\text{Glucose (mg/dl)} = \frac{\text{Read absorbance at 450 nm of TEST} \times 100}{\text{Read absorbance at 450 nm of STANDARD glucose(100 mg/dl)}}$$

If TEST result is greater than 300 mg/dL, repeat assay using a 40-fold rather than 20-fold dilution of sample and multiply result by 2.

2. Lactate concentration

$$\text{Lactate (mg/dl)} = \frac{\text{Read absorbance at 540 nm of TEST} \times 100}{\text{Read absorbance at 540 nm of STANDARD lactate (40 mg/dl)}}$$

If lactate level exceeds 120 mg/dl, dilute 1 part sample with 1 part water and reassay. Multiply result by 2 to compensate for dilution.

3. Ammonia concentration

$$\text{Ammonia } (\mu\text{g/ml}) = (\Delta A \text{ TEST} - \Delta A \text{ BLANK}) \times 30.3$$

$$\text{Factor } 30.3 = \frac{1.11 \times 17}{6.22 \times 0.1}$$

1.11 = volume of liquid in cuvet

17 = weight (μg) of 1 μmole of ammonia

6.22 = millimolar absorptivity of NADPH at 340 nm

0.1 = volume (ml) of specimen

ΔA = INITIAL absorbance at 340 nm – FINAL absorbance at 340 nm

If ammonia concentration in the sample exceeds 15 $\mu\text{g/ml}$, diluted 1 part sample with 1 part ammonia-free water and multiply result by 2.

4. Monoclonal antibody determination by absorption of ultraviolet light

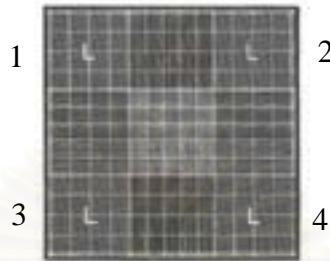
$$\text{MAb concentration (mg/ml)} = \frac{\text{Read absorbance at 280 nm of sample} \times 10 \text{ mg/ml}}{\text{Extinction coefficient at 280 nm ; } E_{280}^{1\%}}$$

Measurement the UV absorbance using 1 cm quartz cells. The sample should be diluted with buffer until the reading falls between 0.1 and 1.5 and multiply result by dilution factor.

Extinction coefficient at 280; $E_{280}^{1\%} = 13.6$

($E_{280}^{1\%}$; the absorbance of a 1% solution of IgG in a 1 cm light path.)

5. Cell number and cell viability



$$\text{Cell numbers (cells/ml)} = \left[\frac{\text{Number of cells in the four large corner squares (area 1 to 4 as shown in the diagram)}}{4} \right] \times 10^4 \times \text{dilution factor}$$

$$\text{Cell viability (\%)} = \frac{\text{Number of living cells} \times 100}{\text{Total number of cells}}$$

6. Glucose consumption rate

$$\text{Glucose consumption rate (mg/day)} = \frac{\left[(V_f \times G_f) + (V_r \times G_r) \right] - (V_t \times G_c)}{\text{days}}$$

V_f = liters of fresh medium introduced at the time of the previous glucose reading

V_r = liters of unreplaced medium residing in the reservoir, circuit and cartridge at the time of the previous glucose reading

V_t = liters of total amount of medium at the time of the previous glucose reading

G_f = glucose concentration of fresh medium (mg/L)

G_r = glucose concentration of medium at the time of the previous reading (mg/L)

G_c = glucose concentration of medium at the current measurement (mg/L)

7. Lactate production rate

$$\text{Lactate production rate (mg/day)} = \frac{(V_t \times L_c) - [(V_f \times L_f) + (V_r \times L_r)]}{\text{days}}$$

V_f = liters of fresh medium introduced at the time of last measurement

V_r = liters of unreplaced medium residing in the reservoir, circuit and cartridge at the time of the previous measurement

V_t = liters of total amount of medium at the last measurement

L_f = lactic acid concentration of fresh medium (mg/L)

L_r = lactic acid concentration of medium at the time of the last measurement (mg/L)

L_c = current lactic acid concentration in medium (mg/L)

8. Ammonia production rate

$$\text{Ammonia production rate (mmole/day)} = \frac{(V_t \times A_c) - [(V_f \times A_f) + (V_r \times A_r)]}{\text{days}}$$

V_f = liters of fresh medium introduced at the time of last measurement

V_r = liters of unreplaced medium residing in the reservoir, circuit and cartridge at the time of the previous measurement

V_t = liters of total amount of medium at the last measurement

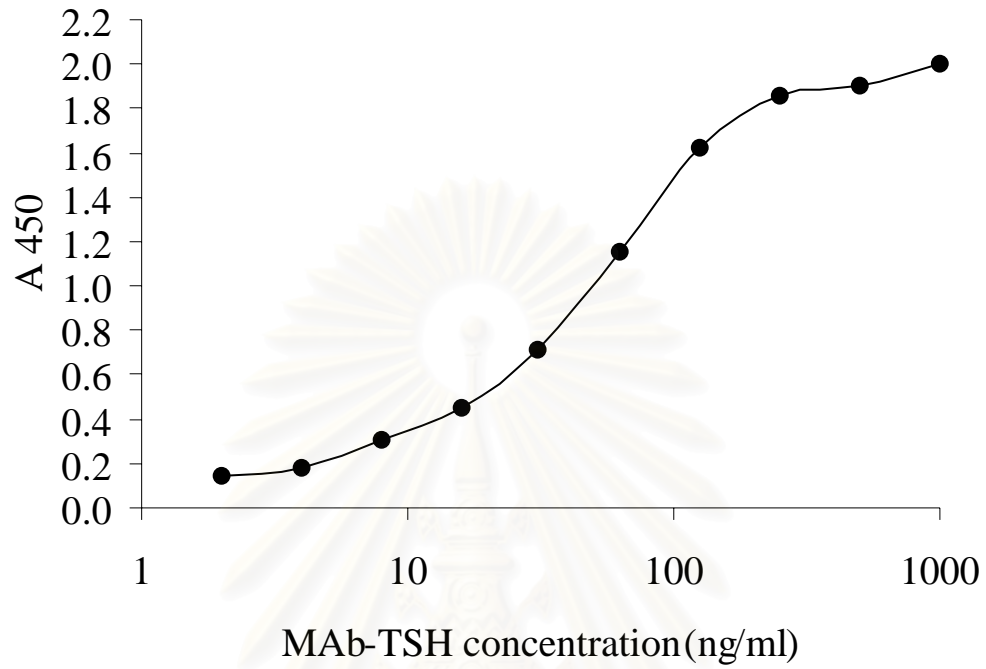
A_f = ammonia concentration of fresh medium (mM)

A_r = ammonia concentration of medium at the time of the last measurement (mM)

A_c = current ammonia concentration in medium (mM)

9. Relative mobility

$$\text{Relative mobility (Rf)} = \frac{\text{The mobility of protein band (cm)}}{\text{The mobility of dye marker (cm)}}$$

APPENDIX C**Standard curve of monoclonal antibody determination by ELISA**

สถาบันวิทยบริการ
จุฬาลงกรณ์มหาวิทยาลัย



APPENDIX D

The protein stain and molecular weight calibration curve of the purified MAb-TSH under various culture conditions.

สถาบันวิทยบริการ
จุฬาลงกรณ์มหาวิทยาลัย

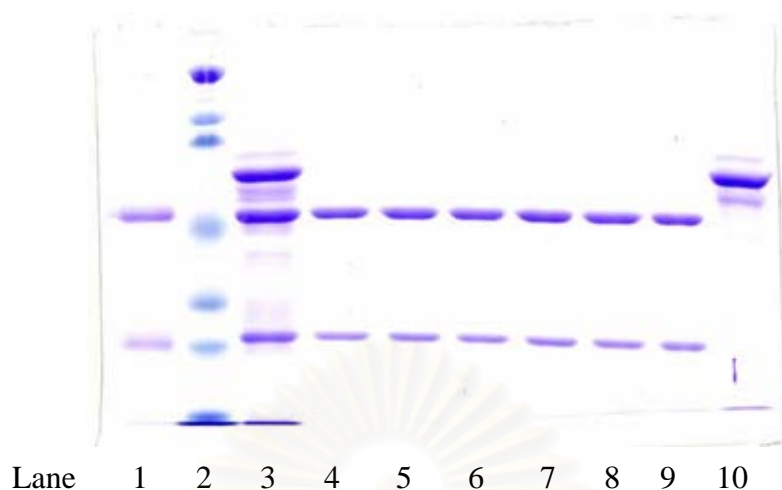


Fig. 20 SDS-PAGE gel of MAb-TSH purified from the supernatant of cells cultured in mode 1 using expanded-bed affinity chromatography.

Lane 1 = Mouse IgG reference standard (2.5 µg)

Lane 2 = Standard protein marker (28-203 kDa; loaded 10 µl)

Lane 3 = The supernatant of cells cultured in 5% serum-supplemented medium (fivefold dilution; loaded 10 µl)

Lane 4 = MAb-TSH purified from the supernatant of bioreactor 1 during day 1-15 (2.5 µg)

Lane 5 = MAb-TSH purified from the supernatant of bioreactor 1 during day 16-53 (2.5 µg)

Lane 6 = MAb-TSH purified from the supernatant of bioreactor 1 during day 54 -92 (2.5 µg)

Lane 7 = MAb-TSH purified from the supernatant of bioreactor 2 during day 1-15 (2.5 µg)

Lane 8 = MAb-TSH purified from the supernatant of bioreactor 2 during day 16-47 (2.5 µg)

Lane 9 = MAb-TSH purified from the supernatant of bioreactor 2 during day 48-92 (2.5 µg)

Lane 10 = FBS (a hundredfold dilution; loaded 10 µl)

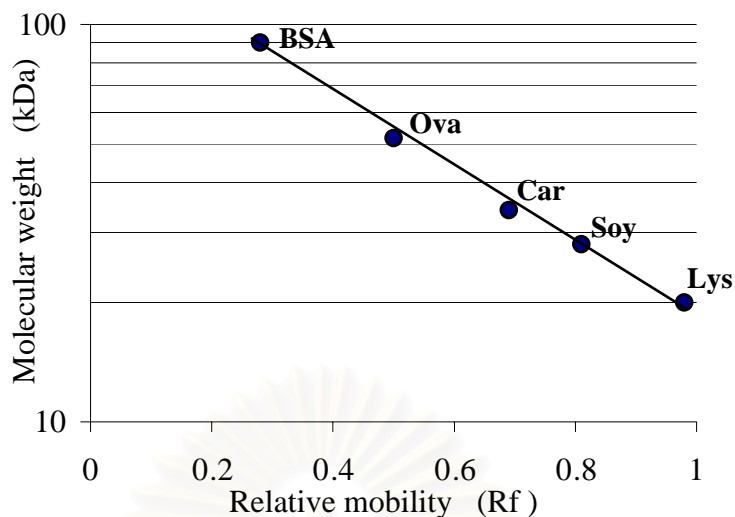


Fig. 21 Molecular weight calibration curve obtained from SDS-PAGE gel of Fig. 20.

Table 10 Molecular weight and relative mobility of protein bands appeared in SDS-PAGE gel of Fig. 20.

Protein	Molecular weight (kDa)	Relative mobility (Rf)
BSA	90	0.28
Ovalbumin	51.7	0.50
Carbonic anhydrase	34.1	0.69
Soybean trypsin inhibitor	28	0.81
Lysozyme	20	0.98
Mouse IgG reference standard	58	0.47
	29	0.79
The supernatant of cells cultured in 5% serum-supplemented medium	73	0.37
	57.5	0.48
	30	0.78
MAB-TSH purified from the supernatant of bioreactor 1 during day 1-15	58	0.47
	29	0.79
MAB-TSH purified from the supernatant of bioreactor 1 during day 16-53	57.5	0.48
	29	0.79
MAB-TSH purified from the supernatant of bioreactor 1 during day 54 -92	57.5	0.48
	29	0.79
MAB-TSH purified from the supernatant of bioreactor 2 during day 1-15	57	0.49
	28	0.81
MAB-TSH purified from the supernatant of bioreactor 2 during day 16-47	53.5	0.51
	27	0.83
MAB-TSH purified from the supernatant of bioreactor 2 during day 48-92	53.5	0.51
	27	0.83
FBS	67.5	0.41

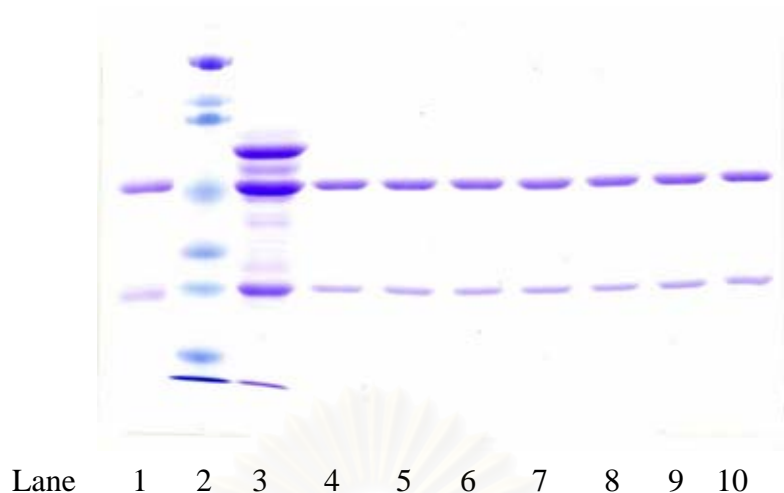


Fig. 22 SDS-PAGE gel of MAb-TSH purified from the supernatant of cells cultured in mode 2 of bioreactor 1 using expanded-bed affinity chromatography.

Lane 1 = Mouse IgG reference standard (2.5 µg)

Lane 2 = Standard protein marker (28-203 kDa; loaded 10 µl)

Lane 3 = The supernatant of cell cultured in 5% serum-supplemented medium (fivefold dilution; loaded 10 µl)

Lane 4 = MAb-TSH purified from the supernatant during day 1-41 (2.5 µg)

Lane 5 = MAb-TSH purified from the supernatant during day 42-51 (2.5 µg)

Lane 6 = MAb-TSH purified from the supernatant during day 52-61 (2.5 µg)

Lane 7 = MAb-TSH purified from the supernatant during day 62-71 (2.5 µg)

Lane 8 = MAb-TSH purified from the supernatant during day 72-81 (2.5 µg)

Lane 9 = MAb-TSH purified from the supernatant during day 82-93 (2.5 µg)

Lane 10 = MAb-TSH purified from the supernatant during day 94-103 (2.5 µg)

สภานิติบัญญัติ
จุฬาลงกรณ์มหาวิทยาลัย

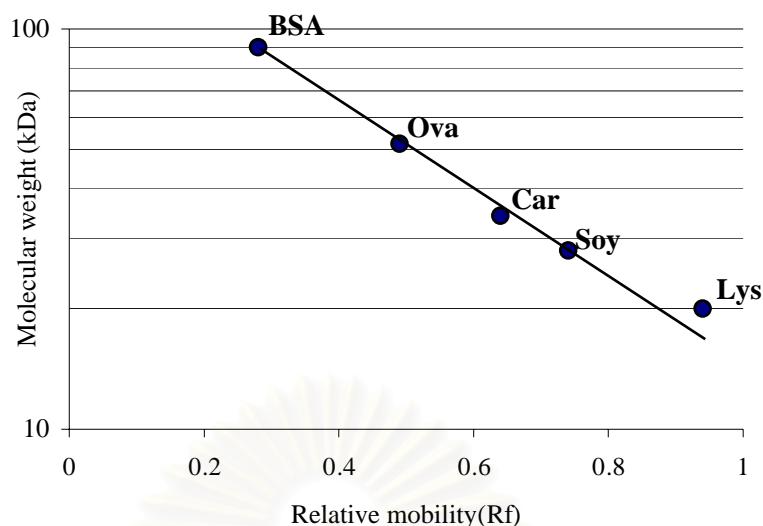


Fig. 23 Molecular weight calibration curve obtained from SDS-PAGE gel of Fig. 22.

Table 11 Molecular weight and relative mobility of protein bands appeared in SDS-PAGE gel of Fig. 22.

Protein	Molecular weight (kDa)	Relative mobility (Rf)
BSA	90	0.28
Ovalbumin	51.7	0.49
Carbonic anhydrase	34.1	0.64
Soybean trypsin inhibitor	28	0.74
Lysozyme	20	0.94
Mouse IgG reference standard	54	0.48
	25	0.78
The supernatant of cells cultured in 5%serum-supplemented medium	73	0.36
	55	0.47
	25.5	0.74
MAB-TSH purified from the supernatant during day 1-41	60	0.43
	30	0.71
MAB-TSH purified from the supernatant during day 42-51	60	0.43
	30	0.71
MAB-TSH purified from the supernatant during day 52-61	60	0.43
	30	0.71
MAB-TSH purified from the supernatant during day 62-71	60	0.43
	30	0.71
MAB-TSH purified from the supernatant during day 72-81	59.5	0.44
	29	0.73
MAB-TSH purified from the supernatant during day 82-93	60	0.43
	29.5	0.72
MAB-TSH purified from the supernatant during day 94-103	63	0.42
	29.5	0.72

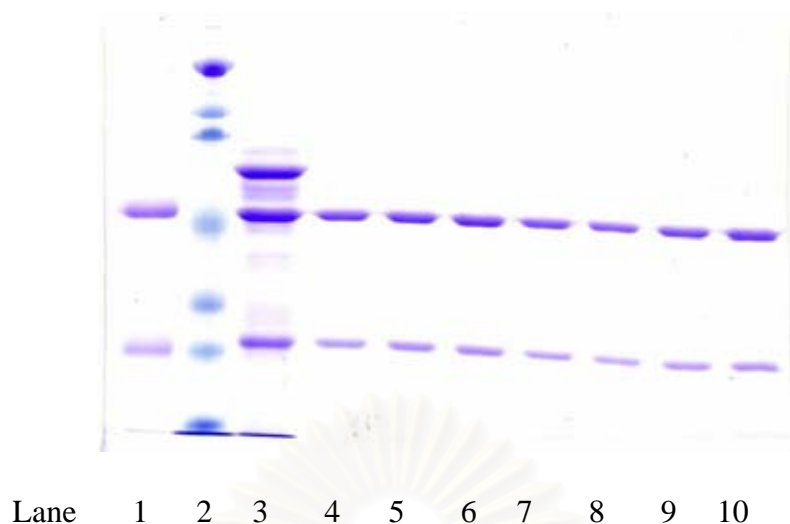


Fig. 24 SDS-PAGE gel of MAb-TSH purified from the supernatant of cells cultured in mode 2 of bioreactor 2 using expanded-bed affinity chromatography.

Lane 1 = Mouse IgG reference standard (2.5 µg)

Lane 2 = Standard protein marker (28-203 kDa; loaded 10 µl)

Lane 3 = The supernatant of cell cultured in 5% serum-supplemented medium (fivefold dilution; loaded 10 µl)

Lane 4 = MAb-TSH purified from the supernatant during day 1-41 (2.5 µg)

Lane 5 = MAb-TSH purified from the supernatant during day 42-51 (2.5 µg)

Lane 6 = MAb-TSH purified from the supernatant during day 52-61 (2.5 µg)

Lane 7 = MAb-TSH purified from the supernatant during day 62-71 (2.5 µg)

Lane 8 = MAb-TSH purified from the supernatant during day 72-81 (2.5 µg)

Lane 9 = MAb-TSH purified from the supernatant during day 82-93 (2.5 µg)

Lane 10 = MAb-TSH purified from the supernatant during day 94-103 (2.5 µg)

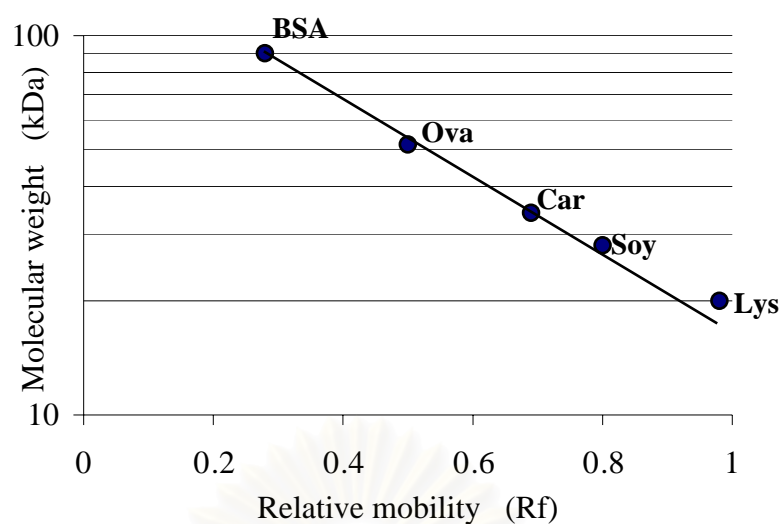


Fig. 25 Molecular weight calibration curve obtained from SDS-PAGE gel of Fig. 24.

Table 12 Molecular weight and relative mobility of protein bands appeared in SDS-PAGE gel of Fig. 24.

Protein	Molecular weight (kDa)	Relative mobility (Rf)
BSA	90	0.28
Ovalbumin	51.7	0.50
Carbonic anhydrase	34.1	0.69
Soybean trypsin inhibitor	28	0.80
Lysozyme	20	0.98
Mouse IgG reference standard	58	0.47
	27.5	0.81
The supernatant of cells cultured in 5% serum-supplemented medium	74	0.37
	60	0.46
	29.5	0.78
MAb-TSH purified from the supernatant during day 1-41	57.5	0.48
	29.5	0.78
MAb-TSH purified from the supernatant during day 42-51	57.5	0.48
	29.5	0.78
MAb-TSH purified from the supernatant during day 52-61	58	0.47
	29.5	0.78
MAb-TSH purified from the supernatant during day 62-71	58	0.47
	29.5	0.78
MAb-TSH purified from the supernatant during day 72-81	57.5	0.48
	27.5	0.81
MAb-TSH purified from the supernatant during day 82-93	56	0.49
	27.5	0.81
MAb-TSH purified from the supernatant during day 94-103	53.5	0.51
	25.5	0.84

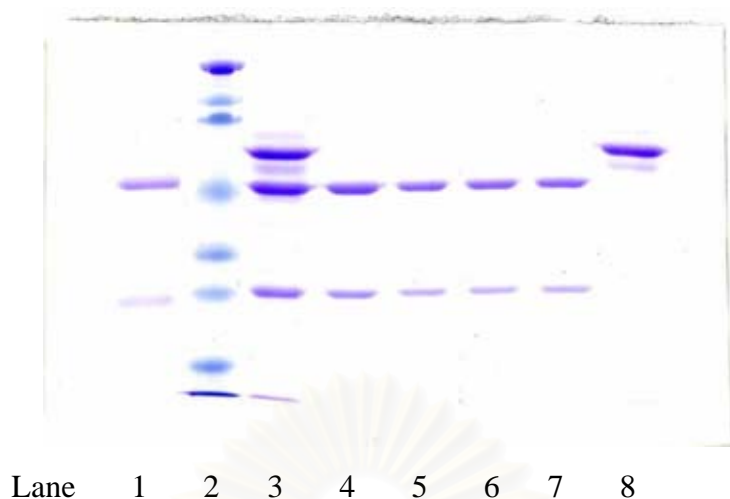


Fig. 26 SDS-PAGE gel of MAb-TSH purified from the supernatant of cells cultured in mode 3 of bioreactor 1 using expanded-bed affinity chromatography.

Lane 1 = Mouse IgG reference standard (2.5 µg)

Lane 2 = Standard protein marker (28-203 kDa; loaded 10 µl)

Lane 3 = The supernatant of cells cultured in 5% serum-supplemented medium (fivefold dilution; loaded 10 µl)

Lane 4 = MAb-TSH purified from the supernatant during day 1-41 (2.5 µg)

Lane 5 = MAb-TSH purified from the supernatant during day 42-53 (2.5 µg)

Lane 6 = MAb-TSH purified from the supernatant during day 54-63 (2.5 µg)

Lane 7 = MAb-TSH purified from the supernatant during day 64-78 (2.5 µg)

Lane 8 = FBS (a hundredfold dilution; loaded 10 µl)

สถาบันวิทยบริการ
จุฬาลงกรณ์มหาวิทยาลัย

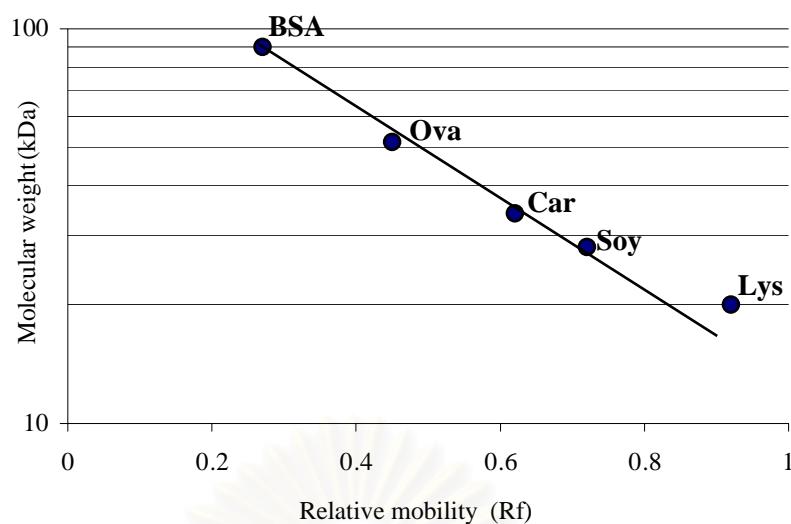


Fig. 27 Molecular weight calibration curve obtained from SDS-PAGE gel of Fig. 26.

Table 13 Molecular weight and relative mobility of protein bands appeared in SDS-PAGE gel of Fig. 26.

Protein	Molecular weight (kDa)	Relative mobility (Rf)
BSA	90	0.27
Ovalbumin	51.7	0.45
Carbonic anhydrase	34.1	0.62
Soybean trypsin inhibitor	28	0.72
Lysozyme	20	0.92
Mouse IgG reference standard	57	0.44
	26.5	0.74
The supernatant of cells cultured in 5% serum-supplemented medium	73	0.35
	56	0.45
	28	0.72
MAB-TSH purified from the supernatant during day 1-41	59	0.43
	28.5	0.71
MAB-TSH purified from the supernatant during day 42-53	59	0.43
	28.5	0.71
MAB-TSH purified from the supernatant during day 54-63	60	0.42
	30	0.69
MAB-TSH purified from the supernatant during day 64-78	60	0.42
	29.5	0.70
FBS	71	0.33

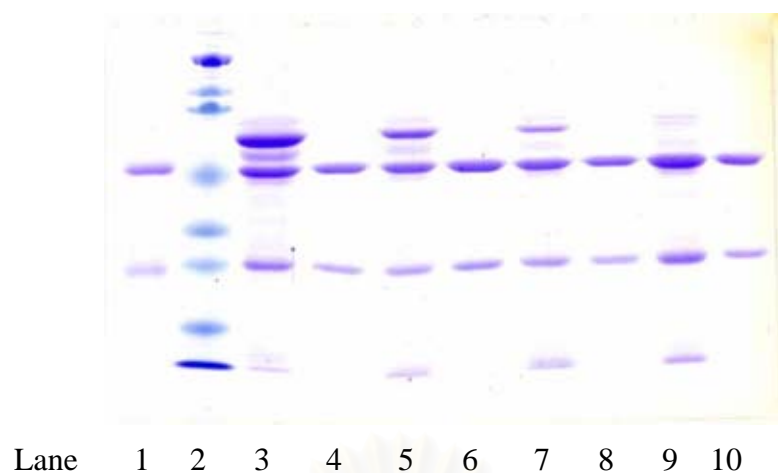


Fig. 28 SDS-PAGE gel of MAb-TSH purified from the supernatant of cells cultured in mode 3 of bioreactor 2 using expanded-bed affinity chromatography.

Lane 1 = Mouse IgG reference standard (2.5 µg)

Lane 2 = Standard protein marker (28-203 kDa; loaded 10 µl)

Lane 3 = The supernatant of cell cultured in 5% serum-supplemented medium (fivefold dilution; loaded 10 µl)

Lane 4 = MAb-TSH purified from the supernatant during day 1-41 (2.5 µg)

Lane 5 = the supernatant of cells cultured in 2.5% serum-supplemented medium (fivefold dilution; loaded 10 µl)

Lane 6 = MAb-TSH purified from the supernatant during day 42-53 (2.5 µg)

Lane 7 = the supernatant of cells cultured in 1% serum-supplemented medium (fivefold dilution; loaded 10 µl)

Lane 8 = MAb-TSH purified from the supernatant during day 54-63 (2.5 µg)

Lane 9 = the supernatant of cells cultured in 0% serum-supplemented medium (fivefold dilution; loaded 10 µl)

Lane 10 = MAb-TSH purified from the supernatant during day 64-78 (2.5 µg)

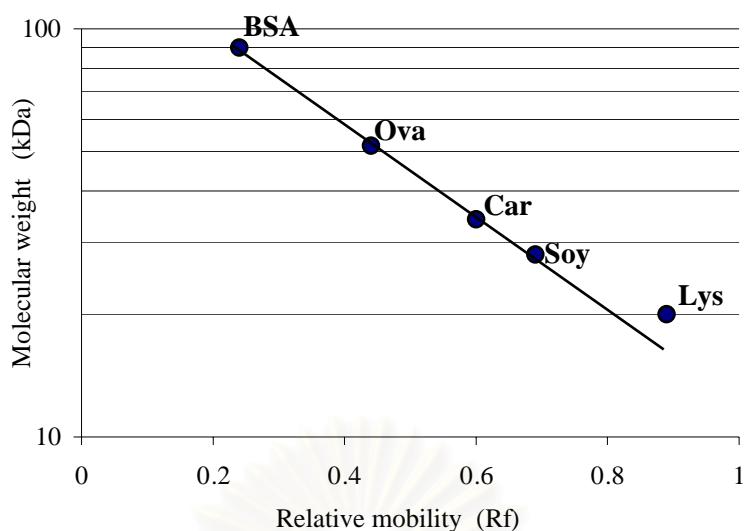


Fig. 29 Molecular weight calibration curve obtained from SDS-PAGE gel of Fig. 28.

Table 14 Molecular weight and relative mobility of protein bands appeared in SDS-PAGE gel of Fig. 28.

Protein	Molecular weight (kDa)	Relative mobility (Rf)
BSA	90	0.24
Ovalbumin	51.7	0.44
Carbonic anhydrase	34.1	0.60
Soybean trypsin inhibitor	28	0.69
Lysozyme	20	0.89
Mouse IgG reference standard	56	0.42
	25.5	0.73
The supernatant of cells cultured in 5%serum-supplemented medium	71	0.33
	56	0.42
	28	0.69
MAb-TSH purified from the supernatant during day 1- 41	60	0.39
	29	0.68
The supernatant of cells cultured in 2.5%serum-supplemented medium	76	0.30
	59	0.40
	27.5	0.70
MAb-TSH purified from the supernatant during day 42-53	58	0.41
	22.5	0.78
The supernatant of cells cultured in 1%serum-supplemented medium	74	0.31
	56	0.42
	26.5	0.71
MAb-TSH purified from the supernatant during day 54-63	58	0.41
	27.5	0.70
The supernatant of cells cultured in 0%serum-supplemented medium	58	0.41
	27.5	0.70
MAb-TSH purified from the supernatant during day 64-78	59	0.40
	27.5	0.70

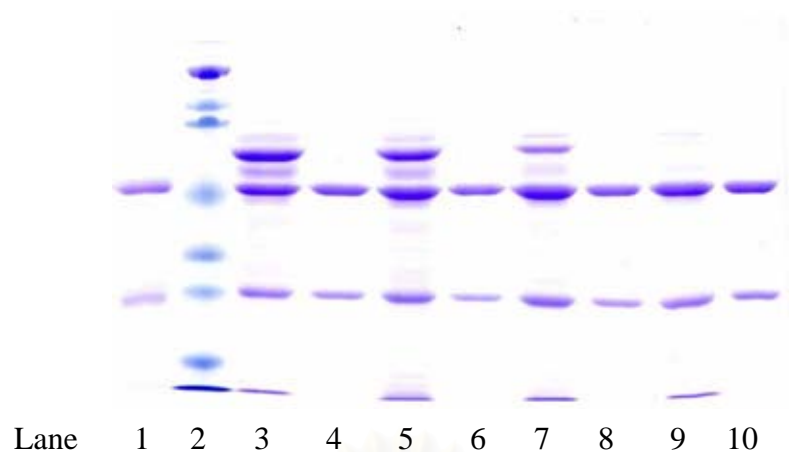


Fig. 30 SDS-PAGE gel of MAb-TSH purified from the supernatant of cells cultured in mode 3 of bioreactor 3 using expanded-bed affinity chromatography.

Lane 1 = Mouse IgG reference standard (2.5 μ g)

Lane 2 = Standard protein marker (28-203 kDa; loaded 10 μ l)

Lane 3 = Supernatant of cells cultured in 5% serum-supplemented medium (fivefold dilution; loaded 10 μ l)

Lane 4 = MAb-TSH purified from the supernatant during day 1-41 (2.5 μ g)

Lane 5 = Supernatant of cells cultured in 2.5% serum-supplemented medium (fivefold dilution; loaded 10 μ l)

Lane 6 = MAb-TSH purified from the supernatant during day 42-53 (2.5 μ g)

Lane 7 = Supernatant of cells cultured in 1% serum-supplemented medium (fivefold dilution; loaded 10 μ l)

Lane 8 = MAb-TSH purified from the supernatant during day 54 -63 (2.5 μ g)

Lane 9 = Supernatant of cells cultured in 0% serum-supplemented medium (fivefold dilution; loaded 10 μ l)

Lane 10 = MAb-TSH purified from the supernatant during day 64-78 (2.5 μ g)

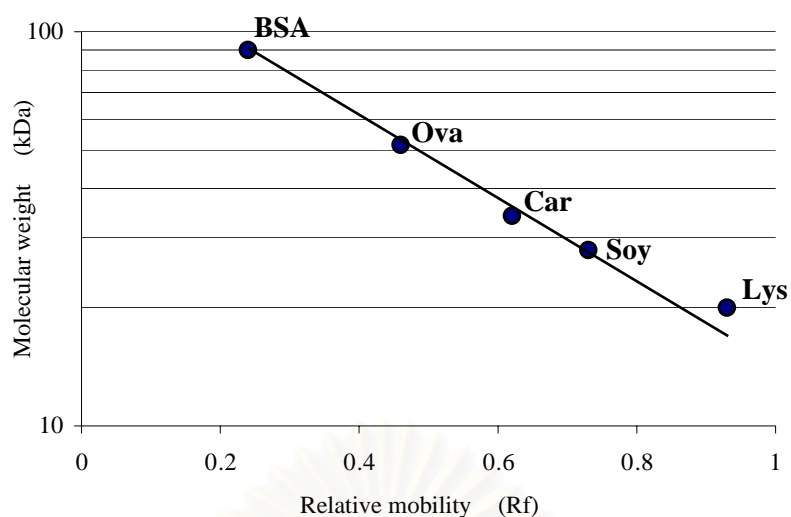


Fig. 31 Molecular weight calibration curve obtained from SDS-PAGE gel of Fig. 30.

Table 15 Molecular weight and relative mobility of protein bands appeared in SDS-PAGE gel of Fig. 30.

Protein	Molecular weight (kDa)	Relative mobility (Rf)
BSA	90	0.24
Ovalbumin	51.7	0.46
Carbonic anhydrase	34.1	0.62
Soybean trypsin inhibitor	28	0.73
Lysozyme	20	0.93
Mouse IgG reference standard	56.5	0.43
	27.5	0.74
Supernatant of cells cultured in 5%serum-supplemented medium	73	0.32
	56.5	0.43
	29	0.72
MAB-TSH purified from the supernatant during day 1- 41	56.5	0.43
	29	0.72
Supernatant of cells cultured in 2.5%serum-supplemented medium	72	0.33
	55	0.44
	28	0.73
MAB-TSH purified from the supernatant during day 42-53	55	0.44
	28	0.73
Supernatant of cells cultured in 1%serum-supplemented medium	73	0.32
	55	0.44
	28	0.73
MAB-TSH purified from the supernatant during day 54-63	55	0.44
	28	0.73
Supernatant of cells cultured in 0%serum-supplemented medium	55	0.44
	27.5	0.74
MAB-TSH purified from the supernatant during day 64-78	55	0.44
	28	0.73

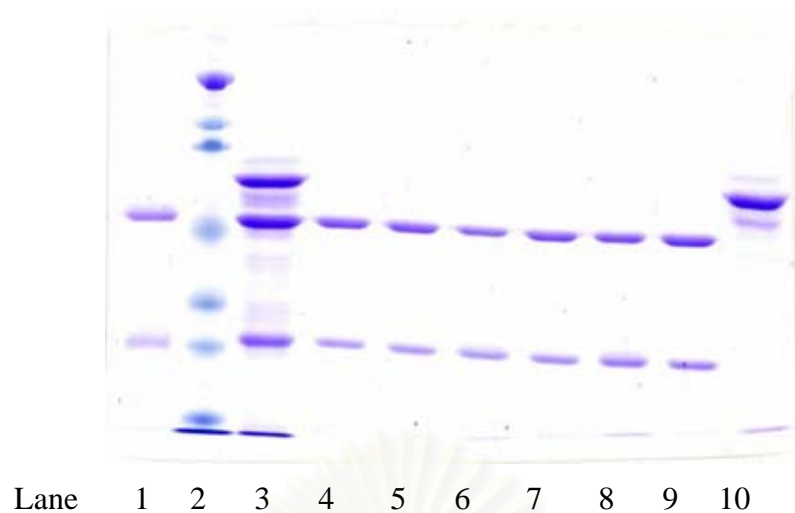


Fig. 32 SDS-PAGE gel of MAb-TSH purified from the supernatant of cells cultured in mode 3 of bioreactor 1 using Protein A sepharose affinity chromatography.

Lane 1 = Mouse IgG reference standard (2.5 µg)

Lane 2 = Standard protein marker (28-203 kDa; loaded 10 µl)

Lane 3 = Supernatant of cell cultured in 5% serum-supplemented medium (fivefold dilution; loaded 10 µl)

Lane 4 = MAb-TSH purified from the supernatant on day 5 (2.5 µg)

Lane 5 = MAb-TSH purified from the supernatant on day 20 (2.5 µg)

Lane 6 = MAb-TSH purified from the supernatant on day 35 (2.5 µg)

Lane 7 = MAb-TSH purified from the supernatant on day 51 (2.5 µg)

Lane 8 = MAb-TSH purified from the supernatant on day 65 (2.5 µg)

Lane 9 = MAb-TSH purified from the supernatant on day 77 (2.5 µg)

Lane 10 = FBS (a hundredfold dilution; loaded 10 µl)

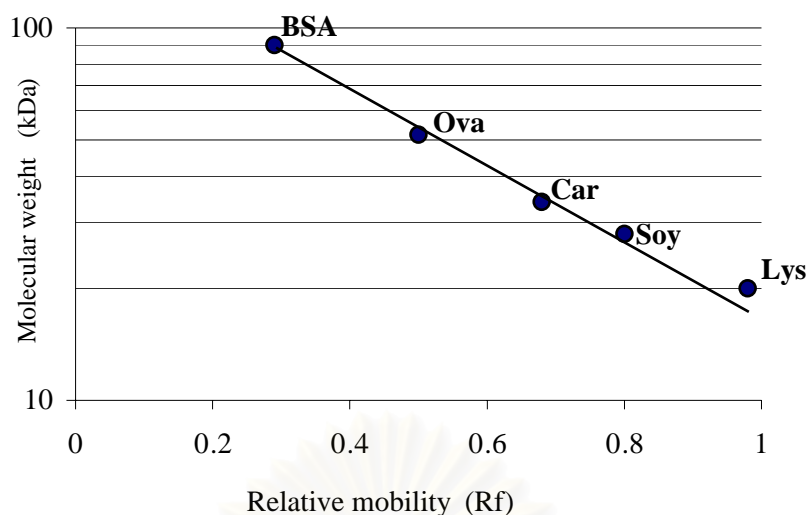


Fig. 33 Molecular weight calibration curve obtained from SDS-PAGE gel of Fig. 32.

Table 16 Molecular weight and relative mobility of protein bands appeared in SDS-PAGE gel of Fig. 32.

Protein	Molecular weight (kDa)	Relative mobility (Rf)
BSA	90	0.29
Ovalbumin	51.7	0.50
Carbonic anhydrase	34.1	0.68
Soybean trypsin inhibitor	28	0.80
Lysozyme	20	0.98
Mouse IgG reference standard	59	0.48
	29.5	0.79
Supernatant of cells cultured in 5%serum-supplemented medium	75	0.37
	59	0.48
	30.5	0.77
MAB-TSH purified from the supernatant on day 5	63	0.45
	30.5	0.77
MAB-TSH purified from the supernatant on day 20	63	0.45
	30.5	0.77
MAB-TSH purified from the supernatant on day 35	58	0.49
	29.5	0.79
MAB-TSH purified from the supernatant on day 51	56.5	0.50
	28	0.80
MAB-TSH purified from the supernatant on day 65	56.5	0.50
	28	0.80
MAB-TSH purified from the supernatant on day 77	55	0.51
	26.5	0.83
FBS	72	0.39

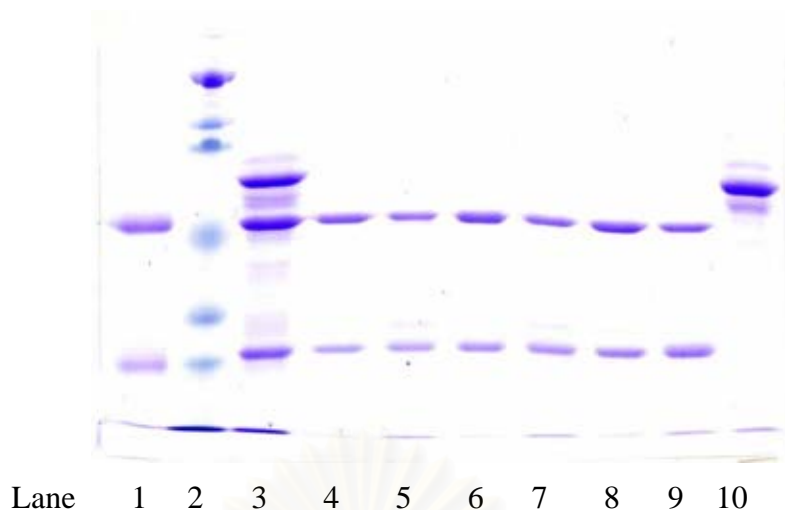


Fig. 34 SDS-PAGE gel of MAb-TSH purified from the supernatant of cells cultured in mode 3 of bioreactor 2 using Protein A sepharose affinity chromatography.

Lane 1 = Mouse IgG reference standard (2.5 µg)

Lane 2 = Standard protein marker (28-203 kDa; loaded 10 µl)

Lane 3 = Supernatant of cell cultured in 5% serum-supplemented medium (fivefold dilution; loaded 10 µl)

Lane 4 = MAb-TSH purified from the supernatant on day 5 (2.5 µg)

Lane 5 = MAb-TSH purified from the supernatant on day 20 (2.5 µg)

Lane 6 = MAb-TSH purified from the supernatant on day 35 (2.5 µg)

Lane 7 = MAb-TSH purified from the supernatant on day 51 (2.5 µg)

Lane 8 = MAb-TSH purified from the supernatant on day 65 (2.5 µg)

Lane 9 = MAb-TSH purified from the supernatant on day 77 (2.5 µg)

Lane 10 = FBS (a hundredfold dilution; loaded 10 µl)

จุฬาลงกรณ์มหาวิทยาลัย

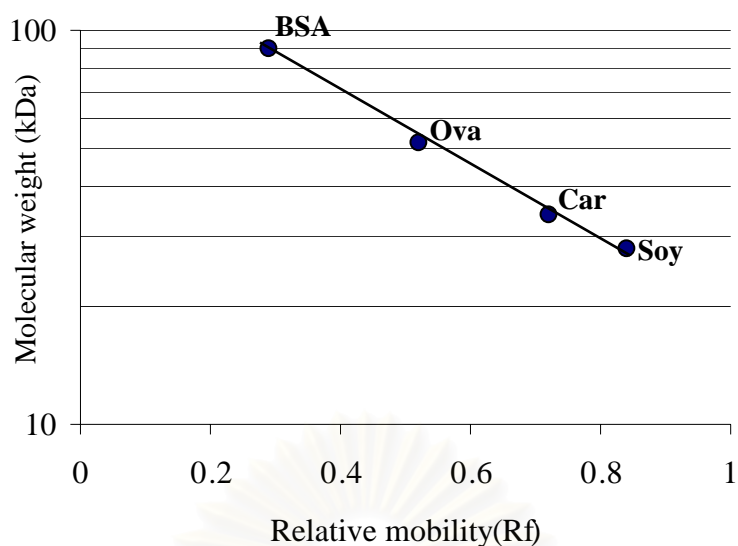


Fig. 35 Molecular weight calibration curve obtained from SDS-PAGE gel of Fig. 34.

Table 17 Molecular weight and relative mobility of protein bands appeared in SDS-PAGE gel of Fig. 34.

Protein	Molecular weight (kDa)	Relative mobility (Rf)
BSA	90	0.29
Ovalbumin	51.7	0.52
Carbonic anhydrase	34.1	0.72
Soybean trypsin inhibitor	28	0.84
Mouse IgG reference standard	57	0.50
	28	0.84
Supernatant of cells cultured in 5%serum-supplemented medium	74	0.38
	58.5	0.49
	29	0.82
MAB-TSH purified from the supernatant on day 5	62	0.46
	30	0.80
MAB-TSH purified from the supernatant on day 20	62	0.46
	31.5	0.78
MAB-TSH purified from the supernatant on day 35	62	0.46
	31.5	0.78
MAB-TSH purified from the supernatant on day 51	62	0.46
	31.5	0.78
MAB-TSH purified from the supernatant on day 65	59.5	0.48
	30	0.80
MAB-TSH purified from the supernatant on day 77	59.5	0.48
	30	0.80
FBS	72	0.39

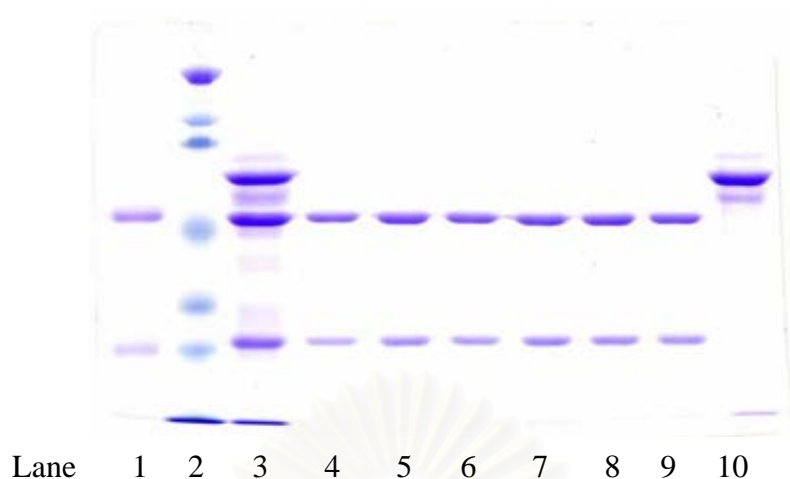


Fig. 36 SDS-PAGE gel of MAb-TSH purified from the supernatant of cells cultured in mode 3 of bioreactor 3 using Protein A sepharose affinity chromatography.

Lane 1 = Mouse IgG reference standard (2.5 µg)

Lane 2 = Standard protein marker (28-203 kDa; loaded 10 µl)

Lane 3 = Supernatant of cell cultured in 5% serum-supplemented medium (fivefold dilution; loaded 10 µl)

Lane 4 = MAb-TSH purified from the supernatant on day 5 (2.5 µg)

Lane 5 = MAb-TSH purified from the supernatant on day 20 (2.5 µg)

Lane 6 = MAb-TSH purified from the supernatant on day 35 (2.5 µg)

Lane 7 = MAb-TSH purified from the supernatant on day 51 (2.5 µg)

Lane 8 = MAb-TSH purified from the supernatant on day 65 (2.5 µg)

Lane 9 = MAb-TSH purified from the supernatant on day 77 (2.5 µg)

Lane 10 = FBS (a hundredfold dilution; loaded 10 µl)

จุฬาลงกรณ์มหาวิทยาลัย

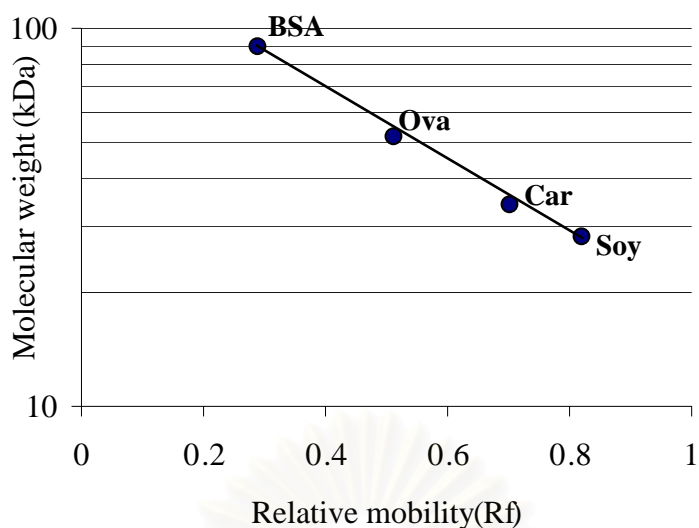


Fig. 37 Molecular weight calibration curve obtained from SDS-PAGE gel of Fig. 36.

Table 18 Molecular weight and relative mobility of the protein bands appeared in SDS-PAGE gel of Fig. 36.

Protein	Molecular weight (kDa)	Relative mobility (Rf)
BSA	90	0.29
Ovalbumin	51.7	0.51
Carbonic anhydrase	34.1	0.70
Soybean trypsin inhibitor	28	0.82
Mouse IgG reference standard	58	0.48
	28	0.80
Supernatant of cells cultured in 5%serum-supplemented medium	73	0.38
	58	0.48
	28	0.80
MAB-TSH purified from the supernatant on day 5	58	0.48
	28	0.80
MAB-TSH purified from the supernatant on day 20	59	0.47
	28.5	0.79
MAB-TSH purified from the supernatant on day 35	57	0.49
	28.5	0.79
MAB-TSH purified from the supernatant on day 51	57	0.49
	28	0.80
MAB-TSH purified from the supernatant on day 65	57	0.49
	28	0.80
MAB-TSH purified from the supernatant on day 77	55	0.50
	27.5	0.81
FBS	71.5	0.39

BIOGRAPHY

Name: Jaranee Phoungphosop
Date of Birth: 21 January 1973
Place of Birth: Phuket, Thailand
Institutions Attended: Chiang Mai University, 1991-1995
Bachelor of Science (Biochem and Biochemical
Technology)
Chulalongkorn University, 2000-2003
Master of Science (Biotechnology)
Present Position: Medical Scientist
National Institute of Health
Department of Medical Sciences
Ministry of Public Health



สถาบันวิทยบริการ
จุฬาลงกรณ์มหาวิทยาลัย